CCSP Synthesis and Assessment Report 3.1

Climate Models: An Assessment of Strengths and Limitations for User Applications

Reviewers' Draft

February 7, 2007

Chapter I - Introduction

Climate Modeling continues to be one of the great scientific success stories of the past 50 years. The way to understand the behavior of the climate system, with its many processes and process feedbacks, is by creating mathematical models to run simulations of climate. It is impossible to build a physical analog, a small version of the Earth system with all of its complexity, in the laboratory. Climate modeling and forecasting grew out of the desire to predict weather. As researchers extended the capabilities of models from predicting weather to simulating climate, they raised and studied questions related to atmospheric physics and chemistry, and the contribution to the climate system of oceans, land, and ice; these became important to the realism of climate system models (Joint Scientific Committee, 1973). Modeling and simulation are the ultimate tests of our understanding of climate as an integrated system, embodying to the extent possible all our knowledge of processes and their interactions. From a classical physics perspective, if we consider that decadal to century-scale changes in the Earth's energy budget are just a few per cent of the mean value, the Earth's climate can be thought of as a highly non-linear, chaotic, weakly forced system with several hundred to several thousands degrees of freedom.

This report will focus primarily on the most advanced physical climate models that were used for the most recent international Coupled Model Intercomparison Project's (CMIP) coordinated experiments (Meehl, et al., 2006), sponsored by the World Climate Research Programme (WCRP). These coupled Atmosphere-Ocean General Circulation Models (AOGCMs) incorporate detailed representations of the atmosphere, land surface, oceans, and sea ice. Where practical, we will emphasize and highlight the results from the three US modeling projects that participated in the CMIP experiments. Additionally, this report examines the use of Regional Climate Models used for obtaining higher resolution details from AOGCM simulations over smaller regions. Nevertheless, it must be noted that there are other types of climate models being developed and applied to climate simulation. More complete Earth systems models build carbon cycle and ecosystems processes on top of the AOGCMs, but are employed more for studies of future climate

change and paleoclimatology, neither of which is relevant to this report. Another class of models used extensively, particularly when computer resources are limited, are Earth-system Models of Intermediate Complexity (EMICs). Although these models have many more assumptions and simplifications than is found in the CMIP models (Claussen et al., 2002), they are particularly useful in obtaining broad estimates of future climate change scenarios that can be further refined with AOGCM experiments.

Brief History of Climate Model Development

Atmospheric General Circulation Model (AGCM) development began in earnest during the 1950s. Joseph Smagorinsky started a program in 1955 that ultimately became one of the most vigorous and longest lived GCM development programs in the world at the Geophysical Fluid Dynamics Laboratory at Princeton University. The University of California at Los Angeles Department of Meteorology began producing increasingly sophisticated AGCMs beginning in 1961 under the leadership of Yale Mintz and Akio Arakawa. This program greatly influenced others, especially in the 1960s and 1970s, leading to modeling programs found today at NASA laboratories and several universities. At Lawrence Livermore National Laboratory, Cecil E. Leith developed an AGCM in the early and mid-1960s that was conceived during sabbatical visits to the Massachusetts Institute of Technology's Meteorology Department. The U.S. National Center for Atmospheric Research (NCAR) initiated an AGCM effort in 1964 under Akira Kasahara and Warren Washington. Leith later moved to NCAR and oversaw the development of the Community Climate Model, a predecessor to the present Community Atmospheric Model that is the atmospheric component of the Community Climate System Model. In England, the UK Meteorological Office began building an AGCM in the early 1960s; this office evolved into the Hadley Centre for Climate Prediction and Research.

Additions to the original atmospheric general circulation models used for weather analysis and prediction were needed to improve simulations and forecasts. The early weather models focused on dynamics but did not properly represent the atmosphere's energy budget, which is needed for proper climate simulations models. Furthermore, the

climate system encompasses elements of the Earth system other than the atmosphere. Thus, ocean, terrestrial, and ice models have been coupled with atmospheric models. The first of these were ocean models. The GFDL researchers were one of the first to coupled crude ocean models to the GFDL atmospheric model in the late 1960s. GFDL pioneers Cox and Bryan extended ocean modeling to full ocean general circulation models (OGCMs) using a formulation that is still in use today.

Climate models began to be used in research on carbon dioxide and climate in the mid-1970s. Two important studies, the Study of Critical Environmental Problems and the Study of Man's Impact on Climate, both endorsed the use of GCM-based climate models to study the possibility of anthropogenic climate change. Beginning in the late 1980s, several national and international organizations were formed with the purpose of assessing and expanding scientific research related to global climate change. These developments spurred interest in developing and improving climate models. The work of the Intergovernmental Panel on Climate Change (IPCC), beginning in 1987, had as a primary focus of Working Group 1 scientific inquiry into atmospheric processes governing climate change. The IPCC's 1990 Scientific Assessment (Houghton et al., 1990) stated, "Improved prediction of climate change depends on the development of climate models, which is the objective of the climate modeling programme of the World Climate Research Programme (WCRP)." The United States Global Change Research Program (USGCRP), established in 1989, designated Climate Modeling and Prediction as one of the four high-priority integrating themes of the program (CEES, 1991). The combination of steadily increasing computer power and research spurred by the WCRP and USGCRP has led to a steady improvement in the completeness, accuracy and resolution of AOGCMS used for climate simulation and prediction. A classic figure from the Third IPCC Working Group I Scientific Assessment of Climate Change in 2001 depicts this evolution in Figure 1, below.

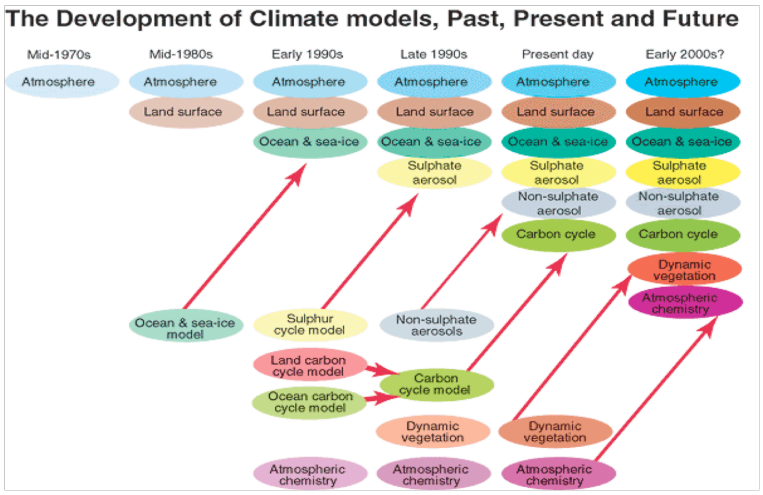

Fig.1 Historical development of climate models (From IPCC, 2001)

Climate model construction

State-of-the-science climate models are constructed using expert judgments to satisfy many constraints and requirements. The overarching consideration is the determination of the most important climate features that must be accurately simulated. Typically, the basic requirement is that model must correctly simulate features that are important to humans, particularly surface variables, such as temperature, precipitation, windiness, and storminess. Although this may sound straightforward, a good climate model must correctly simulate, or at least properly represent, all of the complex interactions in the coupled atmosphere–ocean–land surface–cryosphere system that are manifested as the climate variables of interest. It must correctly produce the climate statistics, including means, extremes and measures of variability, observed at the surface over averaging times of 20 to 30 years. Further, it must correctly simulate the changes in those statistics that result from small changes in the Earth's energy budget that result from natural and human actions.

Climate processes operate on time scales ranging from several hours to millennia, and spatial scales ranging from a few centimeters to thousands of kilometers. Principles of

scale analysis, dynamical simulation, and numerical analysis are used to make intelligent compromises and approximations to simplify the system sufficiently to make it tractable to formulate mathematical representations of the processes and their interactions. These mathematical models are then translated into computer codes, which are executed on some of the most powerful computers in the world. Even with all of this power, more compromises are made so that climate simulations can be completed in a timely manner so that they can be analyzed by scientists. This is one reason why climate models have shown steady improvement over time as computer power has increased.

The remaining sections of this report describe more details about climate model development, evaluation and applications. Chapter II describes more detail about the development and construction of models and how they are employed for climate research. Chapter III discusses the Regional Climate Models and their use in "downscaling" global model results to specific geographic regions, particularly North America. The concept of model climate sensitivity, which is the response of a model's surface temperature to a specified change in the energy budget at the top of the model's atmosphere, is described in Chapter IV. A survey of how well important climate features are simulated by modern models is found in Chapter V, while Chapter VI depicts the near-term development priorities for future model development. Finally, Chapter VII illustrates a few examples of how climate model simulations are used for practical applications.

Chapter II - Description of Global Climate System Models

Atmospheric General Circulation Models

Atmospheric general circulation models (AGCMs) are numerical codes that calculate the state variables of the atmosphere and their time evolution. They are formulated by using geophysical fluid dynamics theory and physical laws of exchanges of the mass and energy. A component of an AGCM that deals with the movement of air is customarily referred to as the model dynamics. The component that calculates the sources and sinks of energy and mass is referred to as the model physics. A third component of an AGCM is the boundary conditions.

Mathematical formulation of all current AGCMs uses primitive equations with hydrostatic balance assumption. This assumption filters out sound waves that do not carry meteorological information but require very small time steps of integration. With this assumption, buoyancy force is balanced by gravity. Current AGCMs therefore do not calculate vertical accelerations of air movement. On horizontal scales of several tens of kilometers, this is a very good approximation. On smaller scales, such as in cumulus convections, this approximation may not be valid.

Although AGCMs use the same primitive dynamical equations, they use different numerical algorithms. Computational approach of the model dynamics can be grouped into four categories: spectral method, finite difference method, semi-Lagrangian method, and finite volume method. The majority of the climate models use the first two approaches. Several AGCMs in the United States are starting to use the finite volume method because it is better suited for transport calculation. Even with the same numerical approach, AGCMs differ in spatial resolutions and configuration of model grids. Some models have few layers above the troposphere while others could have as many layers above the troposphere as in it. AGCMs all use transformed equations to treat the Earth's surface as a constant coordinate surface so that the specification of boundary conditions can be simplified. Numerical algorithms of all AGCMs preserve the basic conservation of

mass and energy of the atmospheres. Typical AGCMs have spatial resolution of 200 kilometers in the horizontal and 20 levels below the altitude of 15 km. Held and Suarez (1994) designed a set of idealized cases to test AGCM dynamical equations and computational algorithms. But because numerical errors often depend on flow patterns, there are no simple ways to assess the accuracy of numerical discretization of AGCMs. Table 1 lists the specifications of numerical approaches and resolutions of some AGCMs.

All AGCMs calculate radiative transfer, clouds, cumulus convection, turbulence and subgrid scale mixing. The radiative transfer code computes the absorption and emission of electric magnetic waves by air molecules and atmospheric particles. Since most atmospheric gases absorb and emit radiations at discrete spectral lines, but the computational costs are too high to calculate the radiative transfer for all these lines, AGCMs use band models to approximate groups of spectral lines. Different models have different specifications of wavelength bands. They all have separate radiation codes to treat solar radiation and terrestrial radiation. The radiation calculation includes the effects of water vapor, carbon dioxide, ozone, and clouds. Some models also include aerosols and trace gases such as methane and CFCs. Validation of the AGCM radiation codes is often done offline against line-by-line model calculations.

For cloud calculations, AGCMs all treat ice and liquid water as part of the atmospheric state variables. Some models also separate cloud habitats into ice crystals, snow, graupel, cloud water, and rain water. Empirical relationships are used to calculate conversions between different habitat types. The representation of these processes on the scale of model grids is particularly difficult. It relies heavily on empirical formulations because of the lack of sub-grid scale information. This includes the calculation of cloud amount, which greatly affects radiative transfer and model sensitivity. Current models use one of the following two methods to calculate cloud amount: statistical distribution of thermodynamic and hydrological variables within a grid box, or prognostic cloud amount calculation. The statistical method may use simple model diagnostics, such as relative humidity, or more sophisticated calculations with higher order of moments of moisture

contents. A sample of cloud schemes used in AGCMs is listed in Table 1. None of the current AGCMs calculates size-resolved cloud particles and non-spherical habitats.

Cumulus convections, which are important in the atmosphere but cannot be explicitly resolved at GCM scale, are calculated using convective parameterization algorithms or schemes. These schemes originate from one of the three methods: cumulus mass flux scheme of Arakawa and Schubert (1974), moist adjustment by Manabe (1968), and moisture closure by Kuo (1974). At the present time, the majority of AGCMs use variants of the Arakawa-Schubert formulations. In this method, cumulus mass fluxes are calculated by using a simple entraining-detraining model. A quasi-equilibrium assumption is used to obtain the mass fluxes. Most current schemes do not account for the differences of convection between organized mesoscale systems and simple plumes. They have to empirically specify the initiation condition of convection, the turbulent mixing rate of updrafts and downdrafts with the environments, and the phase changes of water vapor within the convective systems. Some models also include a separate calculation of shallow convection with different assumptions from those for deep convections. Most models do not separately calculate the area and vertical velocity of convection. Cloud amount and cloud habitat in cumulus are therefore based on empirical observational relationships. Convection schemes used in AGCMs are listed in Table 1.

All AGCMs compute turbulent transport of momentum, moisture, and energy in the atmospheric boundary layer (ABL) near the surface. Similarity theory is used to calculate the vertical distribution of turbulent fluxes and state variables in a thin air layer of tens of meters adjacent to the surface. Above that, turbulent fluxes are calculated based on covariances and closure assumptions, which differ among AGCMs. Some models use high order closures in which the fluxes or second order moments are prognostically calculated. Other models calculate the fluxes diagnostically. Turbulent ABL fluxes heavily depend on surface conditions such as roughness, soil moisture, and vegetation. Besides explicit calculation of boundary layer turbulence, all models use additional diffusion schemes to either calculate impact of local static or shear instabilities and

gravity wave breaking, or to damp artificial numerical modes introduced in the discretization of the model. Table 1 lists turbulent schemes in AGCMs.

Table 1. Description of physical parameterization schemes in a sample of AGCMs.

	Resolution	Convection	ABL	Stratiform Clouds	Convective Clouds	Cloud Microphysics
CAM3	T85L26 (1.4^ox1.4^o) Spectral	Mass Flux *[Hack* 1994; *Zhang and McFarlane*, 1995]	1st order non-local [*Holtslag and Boville*, 1993]	Diagnostic (RH based) [*Kiehl et al.*, 1996]	Diagnostic [*Rasch and Kristjansson*, 1998]	*Rasch and Kristjánsson* [1998]
GFDL	2.5^ox2.0^oL24 Finite Difference	Mass flux (RAS) [*Moorthi and Suarez*, 1992]	Cloud entrainments [*Lock et al.*, 2000; *GFDL GAMDT*, 2004]	Prognostic [*Tiedtke*, 1993; *GFDL GAMDT*, 2004]	Prognostic [*Tiedtke*, 1993; *GFDL GAMDT*, 2004]	*Rotstayn* [1997], *GFDL GAMDT* [2004]
GISS	4^ox5^o L12 Finite Difference	Mass flux [*Del Genio and Yao*, 1993]	2nd order [*Cheng et al.*, 2002]	Diagnostic (RH based) [*Del Genio et al*., 2004]	Diagnostic [*Del Genio et al.*, 2004]	*Del Genio et al.* [2004]
GSFC	2.5^ox2^o L40 Finite Volume	Mass flux (RAS) [*Moorthi and Suarez*, 1992]	2.5 order [*Helfand and Labraga*, 1988]	Diagnostic (RH based) [*Del Genio et al*., 2004]	Diagnostic [*Del Genio et al.*, 1996]	*Del Genio et al.* [1996], *Sud and Walker* [1999]
HadAM4	3.75^ox2.5^oL30 Finite Difference	Mass flux [*Gregory and Rowntree*, 1990; *Gregory and Allen*, 1991]	1st order with cloud entrainment [*Lock et al.*, 2000; *Martin et al.*, 2000]	Diagnostic statistical [*Smith*, 1990; *Pope et al.*].	Diagnostic [*Gregory and Rowntree*, 1990]	*Wilson and Ballard* [1999]
ECHAM5	T63L31 (1.9^ox1.9^o) Spectral	Mass flux [*Tiedtke*, 1989;	1st order, [*Brinkop and Roeckner,*	Prognostic statistical [*Tompkins*,	Diagnostic [*Roeckner et al.,* 1996]	*Lohmann and Roeckner* [1996]

		Nordeng, 1994]	1995]	2002],		
LMD	3.75°x2.5°L19 Finite Difference	*Emanuel* [1991]	1st order [*Li*, 1999]	Statistical [*Le Treut and Li*, 1991]	Statistical [*Bony and Emanuel,* 2001]	*Le Treut and Li* [1991]

1

2

3 ***Ocean General Circulation Models***

4

5 **General overview**: The ocean component of the current generation of climate models
6 can be placed into one of two general categories. All the models are fully four
7 dimensional primitive equation models and are coupled to the atmosphere and ice models
8 through the exchange of fluxes of heat, temperature, and momentum at the boundary
9 between components. The categories, described next, distinguish the models' differences
10 in their definition of their fundamental quantities. Table 1 gives a brief summary of the
11 major differences between the models described in the next paragraphs.

12

13 The first category of ocean model, referred to a z-level (i.e. explicit depths are used to
14 define the model's vertical grid) ocean general circulation model, includes models based
15 on the early efforts of Bryan and Cox (1967) and Bryan (1969a, b). GFDL has two such
16 ocean models (OM3.0 and OM3.1) that are components of the CM2.0 and CM2.1 climate
17 models (Griffies et al., 2005). The two GFDL ocean models (OM3.0 and OM3.1) differ
18 in the choice of some parameterizations and numerical schemes to advance the simulation
19 forward in time. The specifics can be found in the referenced paper. NCAR's CCSM3
20 climate model uses the Parallel Ocean Model v. 1.4.3, a similarly constructed Z-level
21 model (Smith and Gent, 2002). The models are similar in that the fundamental physical
22 quantities advancing in time are the same. These quantities are velocity, potential
23 temperature, salinity, sea surface height, ideal age (time since an ocean parcel was at the
24 surface), and any number of specific passive tracers that maybe included for a given
25 simulation. The two modeling efforts define their resolution at about the same order: 1
26 degree or 110 km for most of the Earth and about 1/3 of a degree at the equator. Physical

processes that include changes on scales smaller than the models' resolution (for example, eddy scales and smaller) are parameterized. Such schemes include using Gent and McWilliams (1990) (GM) method to incorporate mesoscale eddy mixing of tracer fields. The K-profile parameterization (KPP) (Large et al., 1994) method is used in both models for simulating the vertical mixing of the ocean.

The differences between the GFDL and NCAR models are found in the numerical schemes and their horizontal and vertical grid layout. The vertical structure of the GFDL models is defined as 50 separate levels, while the NCAR model has 40 levels. The NCAR model's horizontal grid has its north pole displaced onto a land coordinate (a so-called stretched grid) and the GFLD models use a grid that has three poles (Murray, 1996). This type of grid can be thought of as having two separate grids with the Arctic region on one grid and the rest of the global as a regular Mercator-like grid. There is an explicit treatment of the bottom boundary and overflow regions in the GFDL models (Beckman and Doscher, 1997) to improve the down-slope flow of water. Such treatment of the overflows should improve the representation of deep ocean waters (Roberts and Wood, 1997), but significant improvement in the bottom flow is not seen in the GFDL model implementation (Griffies et al., 2005). The GFDL models also include tidal mixing to improve the realism of the flow on continental shelves. The NCAR ocean model includes anisotropic horizontal viscosity, unique among the models (Large et al., 2001; Smith and McWilliams, 2003).

The second category of ocean models discussed in this review includes those developed by NASA-GISS. These models, while similar in some aspects of their numerics, differ significantly from the models that are included in the first category that is necessary to consider them separately. There are two different ocean models that are used in the GISS simulations: the "Russell Ocean" (GISS-ModelE-R and GISS-AOM: Russell et al., 1995, Russell et al., 2000) and the "HYCOM Ocean" (GISS-ModelE-H: Sun and Bleck, 2001; Bleck 2002; Sun and Hansen, 2003; **Hy**brid **C**oordinate **O**cean **M**odel).

The fundamental (prognostic) variables for the E-R and AOM simulations are potential enthalpy (rather than potential temperature), salt, mass, vertical gradients of potential enthalpy and salt, in addition to velocity. Because the heat content and uptake of heat by the ocean are important aspects in furthering our understanding of the climate system, these models use potential enthalpy, rather than temperature as one of its prognostic variables. This allows for direct accounting of the ocean's specific heat content. At this time, these models are run at a resolution much lower than the models of the first category, a 4 by 5 degree grid (GISS-ER) or 4 by 3 (GISS-AOM) in the horizontal with 16 layers in the vertical. The grid is a regular grid, with the pole velocity treated as a single rotating vector or filtering. The vertical coordinate is defined in units of mass/unit area (while in category 1, the unit is meters). The number of layers at a horizontal grid location is invariant in time and a horizontal location may have fewer than 16 layers. The amount of mass allocated to each layer may vary with time. There is a fixed ratio of mass of one layer to the layer below it at a location. There are 12 straits explicitly defined to handle the flows that are important in climate research, such as the flow that passes Gibraltar. These models include the K-profile mixing scheme (Large et al., 1994) and the E-R version incorporates the GM eddy parameterization while the AOM version does not.

The HYCOM ocean model's (GISS-EH) fundamental variables include temperature, salinity, layer thickness, velocity, and isopycnal or diapycnal mass fluxes. The horizontal grid is different from the others described. It is 2 grids, with one a Mercator grid to 60°N with a resolution of 2 degrees and it is patched (i.e. boundary values exchanged at each time step) to a North Pole grid defined as 1° at 60°N to 0.5° at the North Pole. The vertical grid is a complex or "hybrid" with a z-level grid (units meters) to represent the mixed upper ocean and layers below represented as density layers (*Bleck* 2002). There is no explicit scheme to account for eddies and the vertical mixing is handled through the method of *Kraus and Turner* (1967).

The analyses of the simulations, in most cases, are performed on the model fields that are interpolated to a common grid. This interpolation may introduce small inaccuracies

(*AchutaRao et al.,* 2006) in the results of analyses of a model, but is not considered significant. For example, no more than 3% of heat content change can be associated with regridding errors at the end of a simulation.

Most of the international models are of the first category: Hadley Center (UK), Meteo-France, CSIRO (Australia), and MIROC (Japan). All of the models represent major advances over the previous versions of the ocean models (IPCC TAR).

Model	Resolution Long x Lat L = Levels	Diabatic mixing	Adiabatic mixing	Primary variables	Other Comments
NCAR: CCSM3 POP	320x395 L40	KPP	GM	Velocity, T, S, SSH, ideal age	z-level vertical coordinate
NOAA: GFDL: CM2: OM3	360x200 L50	KPP	GM	Velocity, T, S, SSH, ideal age	z-level vertical coordinate
NASA: GISS: AOM	90x60 L16	KPP	none	Potential Enthalpy, velocity, salt, mass	z* vertical coordinate
NASA: GISS: ER	72x46 L16	KPP	GM	See AOM	See AOM
NASA: GISS EH:	180x90	Kraus-Turner	No special treatment	T, S, SSH, mass flux, velocity	Isopycnal vertical coordinate

Parameterization

Ocean Mixing: At the interface of the atmosphere and the ocean, the sea surface temperature plays a critical role in the climate problem. Processes that control mixing in the ocean are complicated and take place on small scales (order of centimeters) in the

turbulent regime near the surface (the mixed layer). Within the stratified, adiabatic interior of the ocean, mixing is influenced by the exchange of water on scales on the order of meters to kilometers (Figure 1). The current ocean components of climate models are at resolutions that are greater than either of these scales. The mixing of the ocean contributes to the ocean's stratification and heat uptake. This stratification, in turn, affects the circulation patterns on temporal scales of decades and longer. It is also generally felt (Schopf et al., 2003) that the mixing schemes in the ocean modeling components contribute significantly to the uncertainty in the estimates of the ocean's contribution to the predictions of climate change.

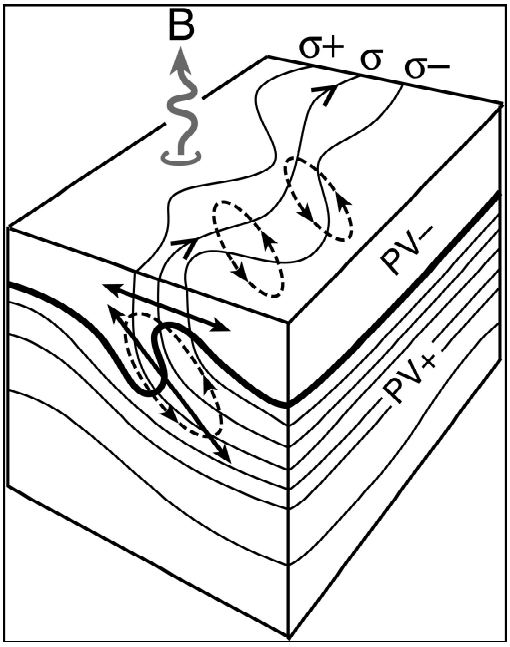

??? Figure 1: Schematic showing the interaction of a mixed layer (low Potential Vorticity: PV) with the stratified interior (high PV) in a strong frontal region with outcropping isopycnal surfaces, , undergoing cooling, B. Eddies forming along the front play a central role in controlling horizontal fluxes through the mixed layer and quasi-adiabatic exchange between the mixed layer and the interior. This process is poorly observed, understood and modeled and must be parameterized in large-scale models.

Fig. from a US CLIVAR white paper: P. Schopf, M.Gregg, R. Ferrari, D. Haidvogel, R. Hallberg, W. Large, J. Ledwell, J. Marshall, J. McWilliams, R. Schmitt, E. Skyllingstad, K. Speer, K. Winters, *Coupling Process and Model Studies of Ocean Mixing to Improve Climate Models - A Pilot Climate Process Modeling and Science Team*, 2003

For turbulent mixing of the upper ocean at the boundary with the atmosphere, the current generation of climate models (resolutions on the order of degrees) parameterizes the processes primarily through the use of several different approaches. The first can be referred to as a bulk formula type of parameterization such as the Kraus and Turner (1967) scheme. The second type are the second order turbulence closure schemes similar to those of Mellor and Yamada (1982) scheme and the third, the most computer intensive schemes, the K-profile parameterization (KPP) which incorporates a non-local eddy diffusivity (K) structure (Large, et al., 1994) in the determination of the mixing parameter. Large, et al. (1994) also provides a more complete comparison of these mixing schemes. While not all international state-of-the-art climate models use the KPP scheme, most of the major US climate models (GISS-ER, GISS-AOM, GFDL models, and the NCAR CCSM) incorporate a version of the scheme. The only one that doesn't is the GISS-EH that uses the Kraus-Turner scheme. Li et al. (2001) showed that in the tropical Pacific, the use of the KPP scheme for handling the mixed layer of the upper ocean reduced the error in the simulation as compared to observations over a simulation that used a more simplified method (Pacanowski and Philander, 1981).

The adiabatic mixing, related to the interactions of eddy motions, is handled through the incorporation of the methods of Gent and McWilliams (1990) and Griffies (1998). The GFDL, NCAR, and GISS-EH/ER models incorporate such a scheme while the GISS-AOM model does not. Eddies will generally mix the ocean on constant density surface. The GM method incorporates various separate parameters that include the scale of the process to be considered and a parameter related to the ability of a parcel to move up and down. For any model the parameters are set so that coefficient related to diffusivity is high in the boundary currents and low in the interior of the ocean (Griffies et al., 2006). The ocean's flow is effected by the eddies, leading to adjustments in how much heat is moved through the oceans, and thus impacts the climate characteristics of the ocean.

To accurately represent ocean mixing at scales important to climate, other processes may need to be represented explicitly or parameterized in the model. These include incorporation of tidal mixing and more accurate representation of interactions with the

ocean's bottom. Of the recent generation of U.S. climate models, only the GFDL models include the numerics to handle tidal mixing (Lee et al., 2005). The limited study of *Lee et al.* [2005] shows that the tidal mixing enhanced the ventilation of the surface waters and increased the formation of deep water in the Labrador Sea by homogenizing the salinity distribution but did not have a major effect on the overturning circulation in the CM2 series of models. It is still an open discussion on the importance of tidal mixing in ocean in relationship other larger scale changes occurring in the ocean related to climate. The current generation of GFDL models are also the only ones that explicitly treat the bottom boundary and sill overflows (Beckman and Dosher, 1997).

Other parameterizations: Another aspect of the model that is available to climate modelers when running the simulations is the explicit treatment for handling the penetration of sunlight (and thus, affecting chlorophyll distributions) into the upper ocean (e.g.. Paulson and Simpson, 1977: Morel and Antoine, 1994: Ohlmann, 2003). All of the US models include such capability. The inclusion of river input (which, in turn, effects ocean mixing locally) in the ocean component is also handled by most of the models in a variety of ways. The models' low resolution results in the smaller seas of the Earth being isolated from the large ocean basins. This requires that there be a method to exchange water between an isolated sea and the ocean to simulate which in nature involves a channel or strait. The various modeling groups have chosen different methods to handle the mixing of the water between these seas and the larger ocean basins. The influences of river input or the mixing of water from isolated seas have not been rigorously analyzed in these climate models.

Evaluation of AGCMs and ocean GCMs: Both the atmosphere and ocean components of climate models are separately evaluated, in addition to the evaluation of coupled ocean-atmosphere GCMs discussed in Chapter V below. Separate evaluation of atmosphere and ocean GCMs allows these individual components to be tested more thoroughly than coupled simulations alone would allow. It requires specification (as input to the computer models) of boundary conditions at the air-sea interface. AGCM stand-alone simulations

require ocean surface temperatures and sea ice distributions to be specified in advance. Typically, they are specified to match observations of the recent decades, and the AGCM simulation is then evaluated by comparison with observations of the atmosphere from the same time period. This method has been institutionalized in the Atmospheric Model Intercomparison Project (AMIP, see Gates et al., 1998) and related projects. Although there remains much room for improvement in the AMIP-style simulations (e.g., Gleckler et al., 2005), the analogous ocean GCM experiments with specified sea surface boundary conditions are at present less systematic and generally exhibit more uncertainty in model performance.

Land Surface Models

The interaction of the Earth's surface with the atmosphere is an integral aspect of the climate system. At the interface, there are exchanges (fluxes) of mass and energy, notably heat, water vapor, and momentum. Feedbacks between the atmosphere and the surface affecting these fluxes have important effects on the climate system (Seneviratne et al., 2006). Modeling the processes over land is particularly challenging because the land surface is very heterogeneous and biological mechanisms in plants are important. It has been demonstrated that climate model simulations are very sensitive to the choice of land parameterizations (Irannejad et al., 2003).

In the earliest global climate models, the land surface modeling occurred in large measure to provide a lower boundary to the atmosphere that was consistent with energy, momentum and moisture balances (e.g., Manabe 1969). The land surface was represented by a balance among incoming and outgoing energy fluxes and a "bucket" that received precipitation from the atmosphere and evaporated moisture into the atmosphere, with a portion of the bucket's water draining away from the model as a type of runoff. There was little attention given to the detailed set of biological, chemical and physical processes linked together in the terrestrial portion of the climate system. From this simple starting point, land surface modeling for climate simulation has increased markedly in sophistication, with increasing realism and inclusiveness of terrestrial surface and subsurface processes.

Although these developments have increased the physical basis of land modeling, the greater complexity has at times contributed to greater differences between climate models (Gates et al., 1995). However, the advent of systematic programs comparing land models, such as the Project for Intercomparison of Land Surface Parameterization Schemes (PILPS; Henderson-Sellers et al., 1995; Henderson-Sellers, 2006) has gradually led to greater agreement among land models (Overgaard et al. 2006), in part because more observations have been used to constrain their behavior. This section reviews the developments that have led to contemporary simulation of land processes in climate models.

Fig. LS-1 shows schematically the types of physical processes included in typical land models. It is noteworthy that the schematic in Fig. LS-1 describes a land model used for both weather forecasting and climate simulation, an indication of the increasing sophistication demanded by both. The figure also hints at important biophysical and biogeochemical processes that have gradually been added to land models used for climate simulation (and continue to be added), such as biophysical controls on transpiration and carbon uptake.

Vegetation Some of the most extensive increases in complexity and sophistication have occurred with vegetation modeling in land models. An early generation of land models (Wilson et al., 1987; Sellers et al., 1986) introduced biophysical controls on plant transpiration by adding a vegetation canopy over the surface, thereby implementing vegetative control on the terrestrial water cycle. These models included exchanges of energy and moisture between the surface, canopy and atmosphere, along with momentum loss to the surface. Further developments included improved plant physiology that allowed simulation of carbon dioxide fluxes (e.g., Bonan 1995; Sellers et al., 1996), which lets the model treat the flow of water and carbon dioxide as an optimization problem balancing carbon uptake for photosynthesis against water loss through transpiration. Improvements also included implementation of model parameters that could be calibrated with satellite observation (Sellers et al., 1996), thereby allowing global-scale calibration.

Continued development has included more realistic parameterization of roots (Arora and Boer, 2003; Kleidon, 2004) and adding multiple canopy layers (e.g., Gu et al., 1999; Baldocchi and Harley, 1995; Wilson et al., 2003). However, the latter has not been used in climate models as the added complexity of multi-canopy models renders unambiguous calibration very difficult. An important ongoing advance is the incorporation of biological processes that produce carbon sources and sinks through vegetation growth and decay and cycling of carbon in the soil (e.g., Li et al., 2006), although considerable work is needed to determine observed magnitudes of carbon uptake and depletion.

Soils The spatial distribution of soils, at least for the contiguous U.S. appears to be fairly well mapped (Miller and White 1998). Most land models include only inorganic soils, generally composed of mixtures of loam, sand and clay. However, high-latitude regions may have extensive zones of organic soils (peat bogs), and some models have included organic soils topped by mosses, which has led to decreased soil heat flux and increased surface sensible and latent heat fluxes (Berringer et al., 2001).

Snow and ice Climate models initially treated snow as a single layer that could grow through snow fall or deplete though melt (e.g., Dickinson et al., 1993). More recent land models for climate simulation include sub-grid distributions of snow depth (Liston, 2004) and blowing of snow (Essery and Pomeroy, 2004). Snow models now may use multiple layers to represent fluxes through the snow (Oleson et al., 2004). Effort has also gone into including and improving effects of soil freezing and thawing (Koren et al., 1999; Boone et al., 2000; Warrach et al., 2001; Li and Koike, 2003; Boisserie et al., 2006) though permafrost modeling is more limited (Malevsky-Malevich et al., 1999; Yamaguchi et al., 2005).

Hydrology The initial focus of land models was vertical coupling of the surface with the overlying atmosphere. However, horizontal water flow through river routing has been available in some models for some time (e.g., Sausen et al., 1994; Hagemann and Dümenil, 1998), with spatial resolution of routing in climate models increasing in more recent versions (Ducharne et al., 2003). However, freezing soil poses additional challenges for modeling runoff (Pitman et al., 1999), with more recent work showing some skill in representing its effects (Luo et al., 2003; Rawlins et al., 2003; Niu and Yang, 2006).

Work is also underway to couple ground-water models into land models (e.g., Gutowski et al., 2002; York et al., 2002; Liang et al., 2003; Maxwell and Miller, 2005; Yeh and Eltahir, 2005). Ground water potentially introduces longer time scales of interaction in the climate system in places where it has contact with vegetation roots or emerges through the surface.

Scale considerations Land models encompass spatial scales ranging from the size of the model grid box down to biophysical and turbulence processes operating on scales the size of leaves. Explicit representation of all these scales in a climate model is beyond the scope of current computing systems as well as observing systems that would be needed to provide adequate model calibration for global and regional climate. As indicated above, land models have been developed to increase the sophistication of their climate-system simulation without becoming so complex as to be intractable. Thus, for example, typical land models in climate simulation do not represent individual leaves but the collective behavior of a canopy of leaves, and multiple canopy layers are generally represented by a single, effective canopy.

Although model fluxes are primarily in the vertical direction, they do not represent a single point but behavior in a grid box that may be many tens or hundreds of kilometers across. Initially, these grid boxes were treated as homogeneous units, but starting with the pioneering work of Avissar and Pielke (1989), many land models have tiled a grid box with patches of different land-use and vegetation types. Although these patches may not interact directly with their neighbors, they are linked by their coupling to the grid box's atmospheric column. This coupling does not allow possible small-scale circulations that might occur because of differences in surface-atmosphere energy exchanges between patches (Segal and Arritt, 1992; Segal et al., 1997), but under most conditions, the imprint of such spatial heterogeneity on the overlying atmospheric column appears to be limited to a few meters above the surface (e.g., Gutowski et al.,1998).

Vertical fluxes linking the surface, canopy and near-surface atmosphere generally assume some form of down-gradient diffusion, though counter-gradient fluxes can exist in this region much like in the overlying atmospheric boundary layer, so there has been some attempt to replace diffusion with more advanced, Lagrangian random-walk approaches (Gu et al., 1999; Baldocchi and Harley, 1995; Wilson et al., 2003).

Digital Elevation Models Topographic variation within a grid box is usually ignored in land modeling. However, implementing detailed river-routing schemes will require accurate digital elevation models (e.g., Hirano et al., 2003; Saraf et al., 2005). In addition,

some soil water schemes also include effects of land slope on water distribution (Choi et al., 2007) and surface radiative fluxes (Zhang et al., 2006).

Validation Validation of land models, especially globally, remains a problem, due to lack of measurements for relevant quantities such as soil moisture and energy, momentum, moisture and carbon fluxes. PILPS (Henderson-Seller et al., 1995) has provided opportunity to make detailed comparisons of multiple models with observations at point locations around the world with differing climates, thus providing some constraint on the behavior of land models. Global participation in PILPS has led to a greater understanding of differences among schemes and improvements. The latest generation of land surface models exhibit relatively smaller differences (Henderson-Sellers et al., 2003) compared to previous generations. River routing can provide a diagnosis versus observations of the spatially distributed behavior of a land model (Kattsov et al., 2000). Remote sensing has been useful for calibration of models developed to exploit it, but it has not generally been used for model validation. The development of regional observing networks that aspire to give Earth-system observations, such as some of the mesonets in the United States, offers promise of spatially distributed networks of important fields for land models with observations resolving some of the spatial variability of land behavior.

Future Land modeling has developed in other disciplines roughly concurrently with the advances implemented in climate models. Applications are wide ranging and include detailed models used for water resource planning (Andersson et al. 2006), managing ecosystems (e.g., Tenhunen et al., 1999), estimating crop yields (e.g., Jones and Kiniry, 1986; Hoogenboom et al.; 1992), simulating ice sheet behavior (Peltier, 2004), and projecting land-use, such as for transportation planning (e.g., Schweitzer; 2006). As suggested by this list, there are widely disparate applications, which have developed from differing scales of interest and focus processes. Land-model development in some of these other applications has informed advances in land models for climate simulation, as in representation of vegetation and hydrologic processes. Because land models do not

include all climate system processes, they can be expected in the future to engage other disciplines and encompass a wider range of processes, especially as resolution increases.

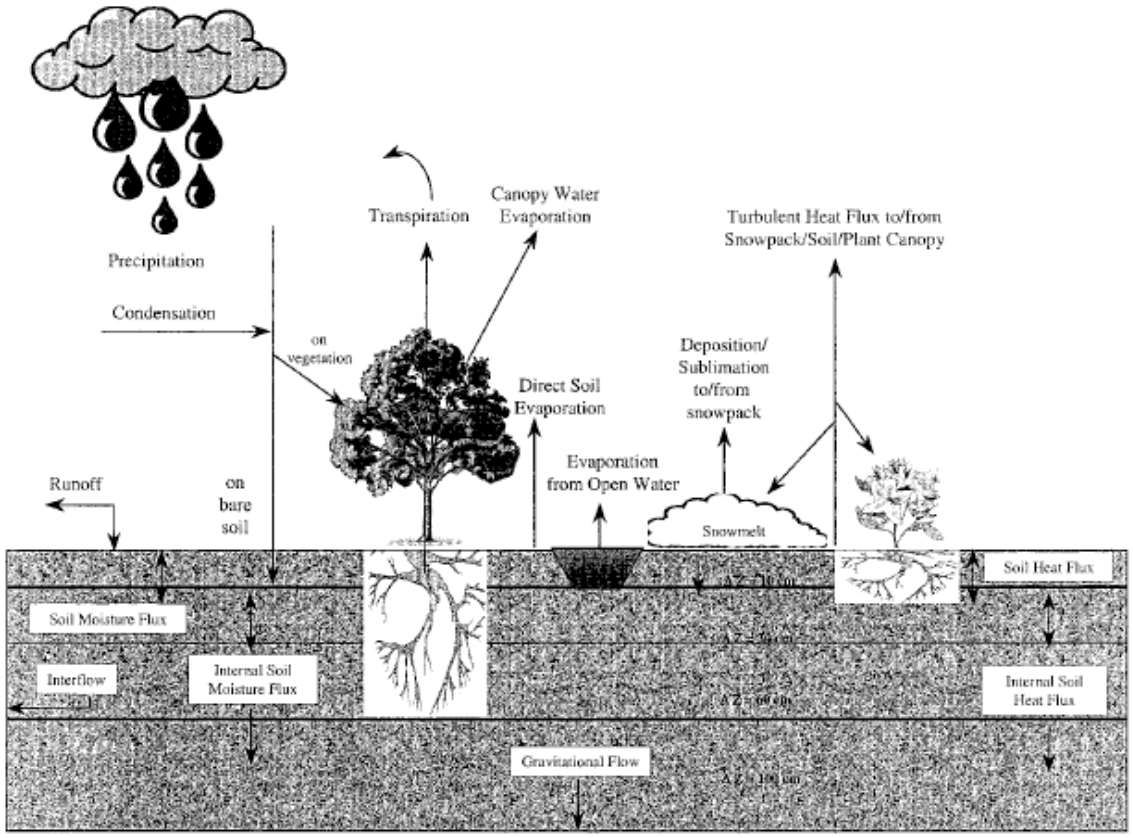

Figure LS-1. Schematic of physical processes in a contemporary land model (from Chen and Dudhia, 2001).

Sea Ice Models, including parameterizations and evaluation

General overview: All the considered climate models have sea ice components that are both dynamic and thermodynamic. That is, the models include the physics for ice movement as well as the physics that is related to energy and heat within the ice. The differences in the various models relate primarily to how complex the code for the dynamics is in determining the representation of ice rheology and their use of parameters.

There are two dynamical codes that are in common use in ice models, the standard Hibler viscous-plastic (VP) rheology (Hibler, 1979; Zhang and Rothrock, 2000) and the more complex elastic-viscous-plastic (EVP) rheology of Hunke and Dukowicz (1997). The EVP method explicitly solves for the ice stress tensor, while the VP solution uses an implicit iterative approach. The solutions are similar (Hunke and Zhang, 1997). The NOAA-GFDL models [Delworth et al., 2005] and the NCAR-CCSM3 (Collins et al., 2005) use the EVP rheology, while the NASA-GISS models use the VP implementation. The EVP is more efficient, especially when using multiple processors.

The thermodynamics portions of the codes also vary in their implementation. Previous climate models generally used the thermodynamics code of Semtner (1976). This classic sea ice model includes one snow layer and two ice layers with constant heat conductivities and a simple parameterization of the brine (salt) content. The NOAA-GFDL models continue to use the Semtner structure with three layers but extend the code relating to brine content in the upper ice layer to be represented by variable heat capacity (Winton, 2000). The NCAR-CCSM3 and NASA-GISS models use variations of the Bitz and Lipscomb (1999])thermodynamics (Briegleb et al., 2002). The code accounts for more of the physical processes within the ice, including the melting of internal brine regions and conserves energy.

The prognostic variables of the sea ice components of the separate climate models are similar to their ocean counterpart, that is the NOAA-GFDL and NCAR-CCSM use velocity, temperature and volume while the NASA-GISS models use velocity, enthalpy, and mass. The amounts of snow and ice for the layers are also computed with each model defining the number of ice layers and ice categories differently. The NOAA-GFDL models use a snow layer, two ice layers and five ice-thickness categories. The NCAR-CCSM3 model has a snow layer, four ice layers, and six ice categories. The NASA-GISS model includes one snow layer, three ice layers, and two ice categories. There is variation among the models on how ice categories are defined, but all include a "no ice" category. The resolution of the sea-ice component is the same as the ocean components of a

specific climate model: NASA-GISS is at a relatively low resolution of 4°x5°, while the NOAA-GFDL and NCAR-CCSM models are on the order of 1°.

Parameterizations:

Albedo: As an important feedback to the atmosphere, the albedo (the proportion of incident radiation reflected off a surface) of the snow and ice plays a significant role in the climate system. All the sea ice component models parameterize the albedo to some extent. Figure XXX from Curry et al. (1995) illustrates the interrelations of the sea-ice system and how the albedo is a function of the snow or ice thickness, ice extent, open water, and the surface temperature, along with other factors, including the spectral band of the radiance. The various models treat the different contributions to the total albedo in similar ways, but vary on the details. For example, the NCAR-CCSM3 sea-ice component does not include dependence on the solar elevation angle (Briegleb et al., 2002), while the NASA-GISS model does (Schmidt et al., 2006). Both of these models include the contribution of melt ponds (Ebert and Curry, 1993; Schramm et al., 1997) The NOAA-GFDL model follows Briegleb et al. (2002), but accounts for the differences in spectral contributions using fixed ratios (Delworth et al. 2006).

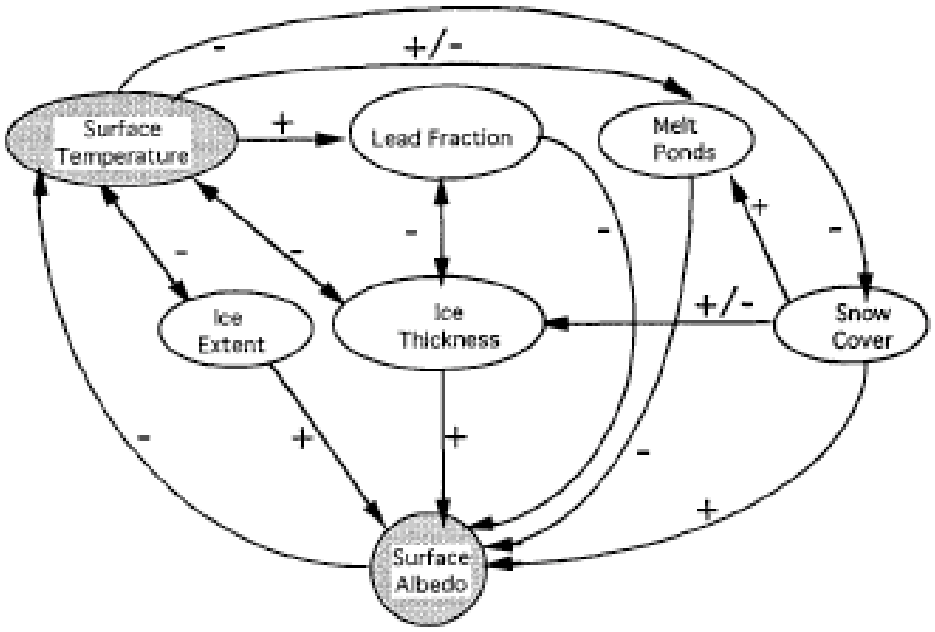

FIG. 6. Schematic diagram of the sea ice–albedo feedback mechanism. The direction of the arrow indicates the direction of the interaction. A "+" indicates a positive interaction (an increase in the first quantity leads to an increase in the second quantity) and a "−" indicates a negative interaction (an increase in the first quantity leads to a decrease in the second quantity). A "±" indicates either that the sign of the interaction is uncertain or that the sign changes over the annual cycle.

From Curry et al. (1995)

Other parameterizations: Additional parameters include reference values for defining ice salinities, strengths, roughness, and drag coefficients. Details of these parameters can be found in the references listed above which describe the basic sea-ice models of the various groups.

Component coupling and coupled model evaluation

We describe in the following some of the key aspects of the model development process at the three U.S. groups that contributed models to the Fourth Assessment of the IPCC, with particular focus on those aspects most relevant for simulation of the 20th century global mean temperature record on the one hand, and the model's climate sensitivity on the other hand. We begin with some general comments on the model development process. (The next few paragraphs could be deleted or moved somewhere else)

The complexity of the climate system, and our inability to resolve all relevant processes in our models, result in a host of choices for development teams to make. Differing expertise, experience, and interests result in distinct development pathways for each climate model. While we eventually expect to see model convergence, forced by increasing insights into the working of the climate system, we are still far from that limit today in several important aspects of the models. Given this level of uncertainty, multiple modeling approaches are clearly needed.

Models differ in their details primarily because development teams have differing ideas concerning the underlying physical mechanisms relevant for the less well-understood aspects of the system. Secondarily, the models may also be adjusted in different ways, consistent with the team's views as to the plausible ranges of parameters in the model, so as to optimize the fit to observations deemed to be of particular importance. How does one come to an agreement on how much a realistic ENSO period is worth as compared with the simulation of the precipitation over the Amazon or the diurnal cycle of convection over the US, if a change in the treatment of subgrid scale moist convection alters all of these simultaneously? Decisions are typically make through qualitative evaluations and compromise amongst competing individual preferences within the team, rather than through a predetermined metric that weights all conceivable climate statistics emerging from the model. The basis for these decisions is difficult to document. Through interviews with those involved, it is, however, possible to describe those factors that were given the most weight in each case.

Members of the three U.S teams described here hold various views on the most likely value of climate sensitivity, but rarely with much conviction, and there is agreement that it is best to avoid engineering the models to posses a particular value of sensitivity, at least at the stage in the development efforts in which one is looking for optimal model configurations. Especially if one is willing to compromise on some measures of fitness, one can control the models' sensitivity to some extent. There may be value, for example, in engineering models with exceptionally high and low sensitivities in different ways, to see if confrontation with different sets of observations can rule them out. But this

approach towards systematic generation of a spectrum of sensitivities was not followed by any of these three teams.

The Geophysical Fluid Dynamics Laboratory of NOAA conducted a thorough restructuring of their atmospheric and climate models over more than five years prior to its delivery of a model to the CMIP-3/IPCC database in 2004, partly in response to need for modernizing the software engineering and partly in response to new ideas in modeling the atmosphere, ocean, and sea ice. The differences between the resulting models and the previous generation of climate models at GFDL are sufficiently varied and substantial, that mapping out exactly why climate sensitivity and other aspects of the climate simulations differ between these two generations of models would be very difficult and has not been attempted. Unlike the earlier generation, the new models do not use flux adjustments.

The new atmospheric models developed at GFDL for global warming studies are referred to as AM2.0 and AM2.1 (GFDL Atmospheric Model Development Team, 2006). A key point of departure from previous models at GFDL was the adoption of a new "grid-point" numerical core for solving the fluid dynamical equations for the atmosphere. Much of the atmospheric development was based on running the model over observed seas surface temperature and sea ice boundary conditions over the period 1980-2000, with a focus on both the mean climate and the response of the atmosphere to ENSO variability in the tropical Pacific. Given the basic model configuration, several subgrid closures were varied to optimize aspects of the climate. Modest improvements in the midlatitude wind field were obtained by adjusting a part of the model referred to as “orographic gravity wave drag” which accounts for the effects of the force exerted on the atmosphere by unresolved topographic features ("hills"). Substantial improvements in tropical rainfall and its response to ENSO resulted from an optimization of parameters as well, especially the treatment of vertical transport of horizontal momentum by moist convection.

The ocean model chosen for this development was the latest version of the Modular Ocean Model developed over several decades at GFDL, notable new features in this

version being a grid structure better suited to simulating the Arctic ocean and a framework, that has been nearly universally accepted by ocean modelers in recent years, for sub-gridscale mixing that avoids unphysical mixing between oceanic layers of differing densities (Gent and McWilliams, 1990). A new sea ice model with the structure that has proven itself in the past decade in several models, with a "viscous-plastic" rheology and multiple ice thickness/lead classes in each grid box. The land model chosen was relatively simple, with vertically resolved soil temperature but retaining the “bucket hydrology” from the earlier generation of models.

The resulting climate model was studied, restructured, and tuned for an extended period , with particular interest in optimizing the structure and frequency of the models spontaneously generated EL Nino events, minizing surface temperature biases, and moiantaining an Atlantic overturning circulation of sufficient strength. During this development phase climate sensitivity was monitored by integrating the model to equilibrium with doubled CO2 when coupled to a "flux-adjusted slab" ocean model A single model modification reduced the model’s sensitivity from a value of 4.0-4.5 K to values between 2.5 and 3.0 K. The change responsible for this reduction was the inclusion of a new model of mixing in the planetary boundary near the Earth’s surface. It was selected for inclusion in the model because it generated more realistic boundary layer depths and near surface relative humidities. The reduction in sensitivity resulted from modifications to the low level cloud field; the size of this reduction was not anticipated.

Aerosol distributions used by the model were computed off-line from the MOZART-II model as described in Horowitz, et al. (2003). No attempt was made to simulate the indirect aerosol effects (interactions between clouds and aerosols) as the confidence in the schemes tested was deemed insufficient for inclusion in the model. In the 20th century simulations, solar variations followed the prescription of Lean, et al. (1995), while volcanic forcing was estimated from obervations.
Well-mixed greenhouse gas concentrations used standard sources, while tropospheric ozone etc. Stratospheric ozone was prescribed, with the Southern Hemisphere ozone hole

prescribed, in particular, in the 20th century simulations. A new detailed land-use history provided a time-history of vegetation-types.

Final tuning of the global energy balance of the model, using two parameters in the cloud prediction scheme, was conducted by examining control simulations of the fully coupled model using fixed 1860 and 1990 forcings. The IPCC-relevant runs of the resulting model (CM2.0) were provided to the CMIP-3/IPCC database under considerable time pressure.

The simulations of the 20th century with time-varying forcings provided to the database were the first simulations of this kind generated with this model. There was no retuning of the model, and no iteration of the aerosol or any other time-varying forcings, at this point.

Model development efforts proceeded in the interim, and a new version of the model emerged rather quickly in which the numerical core of the atmospheric model was replaced by a "finite-volume" code (Lin and Rood, 1996)), substantially improving the wind fields near the surface. These improved winds in turn resulted in improved extratropical ocean circulation and temperatures. ENSO variability increased in this model, to unrealistically large values. But the efficiency of the ocean code was also improved substantially, and with a retuning of the clouds for global energy balance, the new model, CM2.1, was deemed to be a substantial enough improvement to warrant generating a new set of runs for the database. CM2.1 when run with a slab ocean model was found to have a somewhat increased sensitivity, (3.3K). However, the transient climate sensitivity, the global mean warming at the time of CO2 doubling in a fully-coupled model with 1%/yr increasing CO2, is actually slightly smaller than in CM2.0 . The solar, aerosol, volcanic, and greenhouse gas forcings are identical in the two models. The global mean temperature simulations included in Fig. xx are those generated by CM2.1

The CCSM Development Path

Note: The following is the abstract from the Collins, et al (2006) Journal of Climate paper describing CCSM3. It will be replaced with a development description after consulation with the CCSM developers.

A new version of the Community Climate System Model (CCSM) has been developed and released to the climate community. CCSM3 is a coupled climate model with components representing the atmosphere, ocean, sea ice, and land surface connected by a flux coupler. CCSM3 is designed to produce realistic simulations over a wide range of spatial resolutions, enabling inexpensive simulations lasting several millennia or detailed studies of continentalscale dynamics, variability, and climate change. This paper will show results from the configuration used for climate-change simulations with a T85 grid for the atmosphere and land and a grid with approximately 1-degree resolution for the ocean and sea-ice. The new system incorporates several significant improvements in the physical parameterizations. The enhancements in the model physics are designed to reduce or eliminate several systematic biases in the mean climate produced by previous editions of CCSM. These include new treatments of cloud processes, aerosol radiative forcing, land-atmosphere fluxes, ocean mixed-layer processes, and sea-ice dynamics. There are significant improvements in the sea-ice thickness, polar radiation budgets, tropical sea-surface temperatures, and cloud radiative effects. CCSM3 can produce stable climate simulations of millennial duration without ad hoc adjustments to the fluxes exchanged among the component models. Nonetheless, there are still systematic biases in the ocean-atmosphere fluxes in coastal regions west of continents, the spectrum of ENSO variability, the spatial distribution of precipitation in the tropical oceans, and continental precipitation and surface air temperatures. Work is underway to extend CCSM to a more accurate and comprehensive model of the Earth's climate system.

The GISS Development Path

Recent development of the climate model at GISS mirrors work at GFDL. The most recent version of the atmospheric GCM, modelE, resulted from a substantial reworking of the previous version, model II'. While the model physics has become more sophisticated, execution by the user is simplified as a result of modern software, including fortran-90, version control, make files for compilation, and most of all, improved model documentation embedded within the code and accompanying web pages. The model can be downloaded from the GISS website by outside users, and is designed to run on myriad platforms ranging from laptops to a variety of multi-processor computers, partly as the result of the rapidly shifting computing environment at NASA. The most recent (post-AR4) version can be run on an arbitrarily large number of processors.

Historically, GISS has eschewed flux adjustment. Nonetheless, the net energy flux at the top of atmosphere and surface have been reduced to near zero, by adjusting the threshold relative humidity for water and ice cloud formation, two parameters that are otherwise weakly constrained by observations. Near-zero fluxes at these levels are necessary to minimize drift of either the ocean or the coupled climate.

To assess the sensitivity of the climate response to the treatment of the ocean, modelE has been coupled to a slab-ocean model with prescribed horizontal heat transport, along with two ocean GCMs. One GCM, the Russell ocean (Russell et al 1995), has 13 vertical layers and horizontal resolution of 4 degrees latitude by 5 degrees longitude, and is mass conserving (rather than volume conserving like the GFDL MOM). Alternatively, modelE is coupled to the Hybrid Coordinate Ocean Model (HYCOM), an isopycnal model developed originally at the University of Miami (Sun and Bleck 2006). HYCOM has 2 degree latitude by 2 degrees longitude resolution at the equator, with the latitudinal spacing decreasing poleward with the cosine of latitude. A separate rectilinear grid is used in the Arctic to avoid the polar singularity, and joins the spherical grid around 60 N.

Climate sensitivity to doubling of CO2 depends upon the ocean model due to differences in sea-ice. For the slab-ocean model, the climate sensitivity is 2.7 C, and 2.9 C for the Russell ocean (Hansen et al 2005). As at GFDL, no effort is made to match a particular

sensitivity, nor is the sensitivity or forcing adjusted to match twentieth century climate trends (Hansen et al 2007). Aerosol forcing is calculated from prescribed concentration, computed offline by a physical model of the aerosol life cycle. In contrast to the GFDL and NCAR models, modelE includes a representation of the aerosol indirect effect. Cloud droplet formation is related empirically to the availability of cloud condensation nuclei, which depends upon the prescribed aerosol concentration (Menon and Del Genio 2005).

Flexability is emphasized in model development (Schmidt et al 2006). ModelE is designed for a variety of applications, ranging from simulation of stratospheric dynamics and the middle atmosphere response to solar forcing, to projection of twenty-first century trends in surface climate. Horizontal resolution is typically 4 degrees latitude by 5 degrees longitude, although twice the resolution is typically used for studies of cloud processes. The model top has been raised from 10 mb (as in the previous model II') to 0.1 mb, so that the top has less influence upon the stratospheric circulation. Coding emphasizes `plug-and-play' structure, so that the model can be easily adapted for future needs, such as fully interactive carbon and nitrogen cycles.

Model development is devoted to improving the realism of individual model parameterizations, such as the planetary boundary layer, or sea-ice dynamics. Because of the variety of applications, relatively little emphasis is placed upon optimizing the simulation of specific phenomena such as El Nino or the Atlantic thermohaline circulation; as noted above, successful reproduction of one phenomena usually results in a sub-optimal simulation of another. Nonetheless, some effort was made to reduce biases in previous versions of the model that emerged from the interaction of various features of the model, such as subtropical low clouds, tropical rainfall, and variability of the stratospheric winds. Some of the model adjustments were structural, as opposed to the adjustment of a particular parameter: for example, the introduction of a new planetary boundary layer parameterization that reduced the unrealistic formation of clouds in the lowest model level (Schmidt et al 2006).

Because of their uniform horizontal coverage, satellite retrievals are emphasized for model evaluation, like Earth Radiation Budget Experiment fluxes at TOA, Microwave Sounding Unit channels 2 (troposphere) and 4 (stratosphere) temperatures, and International Satellite Cloud Climatology Project (ISCCP) diagnostics. Comparison to ISCCP is through a special algorithm that samples the GCM output to mimic data collection by an orbiting satellite. For example, high clouds may include contributions from lower levels in both the model and the downward looking satellite instrument. This satellite perspective within the model allows a rigorous comparison to observations. In addition to satellite retrievals, some GCM fields like zonal wind are compared to in situ observations adjusted by the ERA-40 reanalyses. Surface air temperature is taken from the Climate Research Unit (Jones et al 1999).

Common problems The CCSM and GFDL Development Teams met at several times during this period to compare experiences and discuss common biases in the two models. A topic of considerable discussion and concern, for example, was the tendency for too strong an equatorial cold tongue in the Eastern Equatorial Pacific and associated problems with the pattern of precipitation (often referred to as the "double ITCZ problem"). It was noted in these meetings that the climate sensitivities of the two models had converged to some extent from an earlier generation in which the NCAR model was on the low end of the canonical sensitivity range of 1.5–4.5K, while the GFDL model had been near the high end. This convergence in the global mean was considered by the teams to be coincidental; it was not a consequence of any specific actions taken so as to engineer convergence, and did not reflect convergence either in the specifics of the cloud feedback processes that resulted in these sensitivity changes, nor in the regional temperature changes than make up these global mean values.

A procedure common to each of these three models, and to all other comprehensive climate models, is a tuning of the global mean energy balance. A climate model must be in balance at the top of the atmosphere and globally averaged, to within a few tenths of a

W/m2 in its control (pre-1860) climate if it is to avoid temperature drifts in 20th and 21st century simulations that would obscure the response to the imposed changes in greenhouse, aerosol, volcanic, and solar forcings. Especially because of the difficulty in modeling clouds, but even in the clear sky, untuned models do not currently possess this level of accuracy in their radiative fluxes. The imbalances are more typically range up to 10 W/m2. Parameters in the cloud scheme are then altered to create a balanced state, often taking care that the individual components of this balance, the absorbed solar flux and emitted infrared flux, are individually in agreement with observations, since these help insure the correct distribution of the heating between atmosphere and ocean. This is occasionally referred to as the "final tuning" of the model, to distinguish it from the various choices made with other motivations while one is configuring the model.

The need for this final tuning does not preclude the use of these models for global warming simulations, in which the radiative forcing is itself of the order of several W/m2. Consider for example, the study of Ramaswamy et al. (2001) of the effects of modifying the treatment of the "water vapor continuum" in a climate model. This is an aspect of the radiative transfer algorithm in clear sky in which there is significant uncertainty. While modifying the treatment of the continuum can change the top-of-atmosphere balance by more than 1 W/m2, the effect on climate sensitivity is found to be insignificant. The change in radiative transfer in this instance alters the outgoing infrared flux by roughly 1% , and it affects the sensitivity (by altering the derivative of the flux with respect to temperature) by roughly the same percentage. But a change in sensitivity of this magnitude, say from 3K to 3.03K, is of little consequence given uncertainties in the cloud feedbacks. It is some aspects of the models that affect the strengths of temperature-dependent feedbacks that are of particular concern, not errors in mean fluxes per se.

Reductive vs. holistic evaluation of models: In order to evaluate models, appreciation is needed of their structure: which variables are prescribed, which are predicted. Most importantly, one needs to appreciate the extent to which the physical basis of the model is empirical or based on physical principles in which we have high confidence? We can place different kinds of models used in climate science on a spectrum ranging from more

reductive, physically based to more empirical and holistic. This distinction between reductive and holistic modeling is most easily understood by considering an example.

Figure xx shows the time evolution over the 20th century of the rainfall over the Sahel region of Africa. As is not uncommon in climate science, the accuracy of this data has been questioned; a discussion of precipitation data quality in this region can be found in Dai et al. (2004). Also not uncommon in climate science, hidden behind the surface of this seemingly unremarkable time series is the profound imprint of these variations on economies and societies, in this case especially the stark human suffering associated with the drought period in the 1970's and 80's.

It has been argued that these variations in Sahel rainfall were primarily forced by variations in sea surface temperature. In addressing this hypothesis, one temporarily puts aside the question of why these ocean temperatures varied. Using standard statistical techniques one can search for a functional relationship between the rainfall time series and the observed ocean temperature variations in this period and find those that fit these variations most accurately and parsimoniously. One such function is obtained by computing anomalies of surface temperature over the North Atlantic and the Indian Ocean from the century long averages, multiplying the North Atlantic anomaly (in degrees Celsius) by +0.4 and the Indian anomaly by -0.5, and then interpreting the result as the percent change in precipitation over the Sahel It is clearly a special purpose model; it can do nothing else other than predict Sahel rainfall as a function of Atlantic and Indian Ocean SSTs. It does not address the underlying mechanisms by which the temperature changes in these ocean basins affect African rainfall.

Alternatively, the observed sea surface temperatures were input into t the atmosphere/land component of the GFDL climate model used in the IPCC assessments, In this case the entire global field of ocean surface temperature plays the role of a boundary condition, or constraint, on the model.

This class of model evolves the state of the atmosphere/land system forward in time, starting from some initial condition. It consists of rules that generate this state (temperature, winds, water vapor, clouds, rainfall rate, water storage in the land, land surface temperature) from the preceding state, in this case one half hour earlier. By this process it evolves the "weather" over Africa and the rest of the Earth. To change the result , one would need to modify these rules. Besides Sahel rainfall, , this model generates a host of other results that can be compared to observations. Changing the rules of time evolution defining the model would change all of these other aspects of the model, including the weather and climate in other regions of the world besides Africa.

We refer to this model as being "reductive" in that it does not deal directly, or "holistically", with a high level climate output such as Sahel rainfall averaged over some period, but rather attempts to simulate the inner workings, or dynamics, of the climate system at a much finer level of granularity. To the extent that the simulation is successful and convincing, with analysis and manipulation of the model one can hope to uncover the detailed physical mechanisms underlying this causal connection. The resulting fit may or may not be as good as the fit obtained with the explicitly tuned statistical model, but a reductive model ideally provides a different level of confidence in its explanatory and predictive power, deriving, if successful, from the fact that one is simulating many aspects of the climate system simultaneously with the same set of physically-based rules of atmospheric dynamics.

It is still important to ask the question of whether a result such as this one for Sahel rainfall is itself the result of "tuning." Were certain choices made in the model development process so as to optimize this fit to Sahel rainfall, possibly sacrificing the quality of other aspects of the model output? (In this case, the answer from those familiar the process, is no, African rainfall variations over time were not examined by the development team.) Given uncertainties in some of the dynamical rules on which the model is based, there is clear value in comparing this result with that obtained with other attempts at modeling the atmospheric/land climate. In this case, several other models (Hoerling et al. 2006do produce qualitatively similar results.

Most of our interest in this report centers on the coupled atmosphere/ocean/land/cryosphere models used to simulate the changes in climate expected in the coming centuries. Suppose one examines Sahel rainfall in a coupled-atmosphere ocean model of this sort, in which the SSTs are predicted rather than prescribed, with the model only forced by estimated historical variations in well-mixed greenhouse gases, ozone, volcanic and anthropogenic aerosols, solar forcing, and changes in land use. The SSTs are now part of the solution and one's approach to validation needs to be adjusted accordingly; the SST variations of interest are themselves partly forced and partly due to internal variability of the coupled system. The result in Fig, xx is produced with the GFDL CM2.1 model. One solves this system multiple times, with different initial conditions, and focuses on both the ensemble mean evolution and the spread and characteristics of variability of the individual realizations. The ensemble mean evolution isolates the response to the changing model forcings – in this case, the ensemble mean shows a gradual drying trend which, with additional calculations and analysis one could hope to partition into the contributions from the individual forcing agents, natural and anthropogenic. Some of the individual realizations should resemble the observations, to illustrate that the observed evolution is a possible solution of the model system. Fig. xx shows, as an example, one realization from CM2 that agrees best with the observed Sahel time series.

Now consider another aspect of climate variations in the latter part of the 20th century. The latitude of the maximum in the surface westerlies in the Southern Hemisphere (the "Roaring 40's") has moved poleward over the past few decades, as illustrated in Fig yy for the summer season. This shift is estimated in the figure using the ERA40 reanalysis . This data set has also been critically examined: a recent paper comparing a closely related time series to individual radiosonde stations can be found in Marshall et al.(??, ref missing) . This poleward displacement of the circulation is often referred to as the excitation of the positive phase of the Southern Annular Mode, and is thought to have influenced the warming of the Antarctic peninsula as well as the drought in Southwest

Australia. It has been suggested that this shift is in large part caused by the development the ozone hole in the Antarctic stratosphere, and that warming of the troposphere has contributed as well .Also shown in this figure is the result from five integrations of GFDL's CM2.1 climate model. With considerable variability between realizations, the model simulates a trend of about the observed size. Just as in the case of Sahel rain, the trend in Southern Hemisphere winds was not studied during this model's development process

In the absence of these and other comparable model solutions, it would be easy to be skeptical about the ability of ozone depletion in the stratosphere to move the Roaring 40's polewards. Limited data in this region makes it difficult to construct useful statistical models that illuminate the underlying dynamics. But climate models such as this one provide hope for disentangling the importance of tropospheric warming, ozone depletion, and natural variability for this shift.

Finally, we show in Fig zz the globally averaged change in lower stratospheric temperature, as measured by the T4 channel of the Microwave Sounding Unit, and compare these temperatures to those simulated by exactly the same simulations of CM2.1 that produced the the Sahel rainfall and Southern Hemispheric winds trends already described

Our confidence in its explanatory and predictive power of climate models grows based on their ability to simulate many aspects of the climate system *simultaneously* with the same set of physically based rules. Results from other models besides GFDL's CM2.1 could be used to make this same point. Strengths and weaknesses vary from model to model, a subject of intensive analysis within the climate modeling community. For example, the trends in Northern Hemisphere circulation over the past few decades are more poorly simulated by CM2.1 than are the trends in the Southern Hemisphere. Other models share this deficiency – what is the distinction between the two hemispheres that makes the Northern Hemisphere trends more difficult to capture – more complex interactions with the land surface? more delicate interactions between troposphere and stratosphere? subtle controls on the strength of the meridional overturning circulation in the Atlantic Ocean?

The simulation of the mean climate is itself a non-trivial metric in these models, since they produce this climate by generating weather and then averaging this weather over time. But how does one translate the qualities of a climate simulation into a level of confidence in the model's ability to predict climate change? The time-averaged Sahel rainfall in CM2.1, for example, is roughly 15% larger than in the observations. Is it important that the model has a wet bias in this region of a magnitude comparable to the variations under discussion? Is the size of the mean bias a useful measure of the quality of a model, or should one focus primarily, on the simulations of climate change? This class of question is a difficult one, and remains a research issue in many cases. It reappears explicitly or implicitly in much of the discussion to follow.

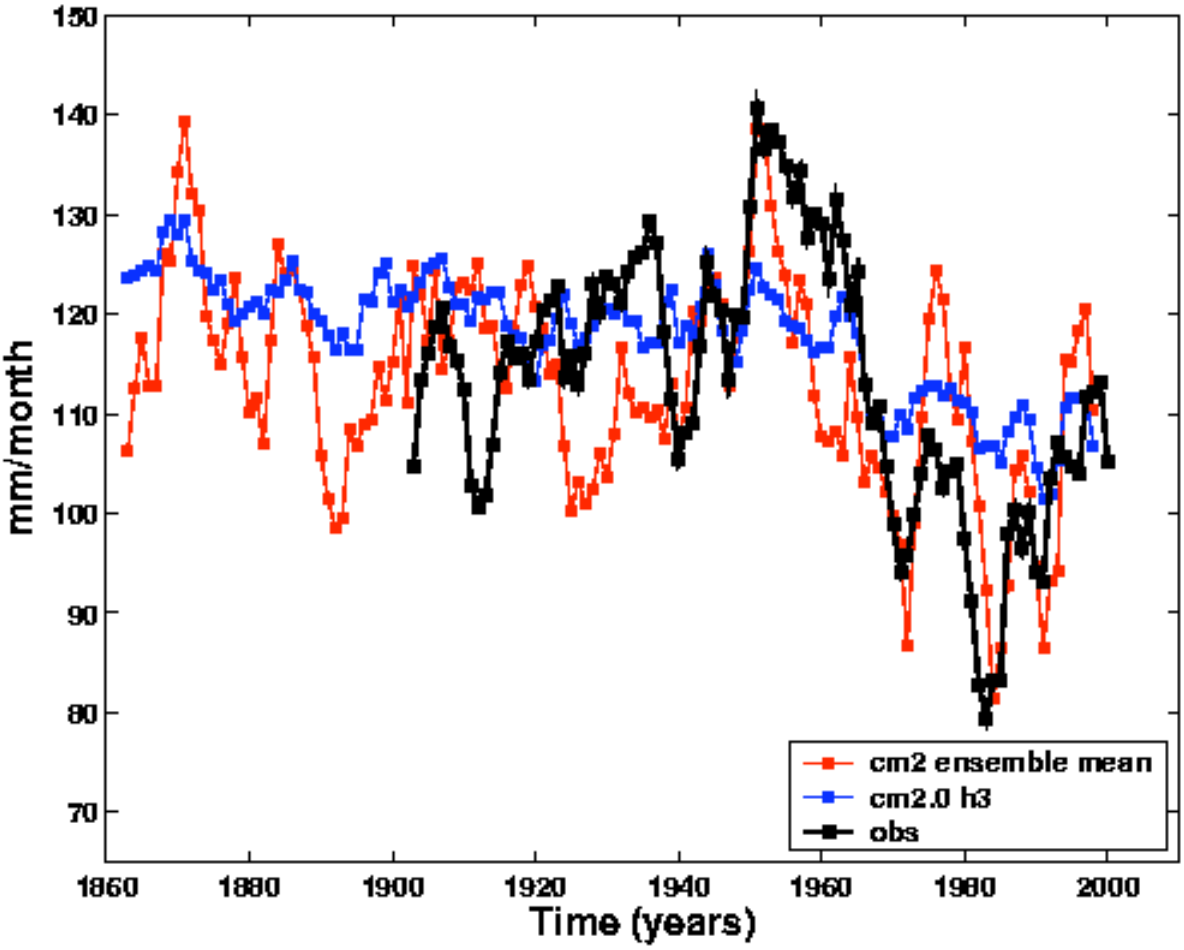

Fig xx from above discussion

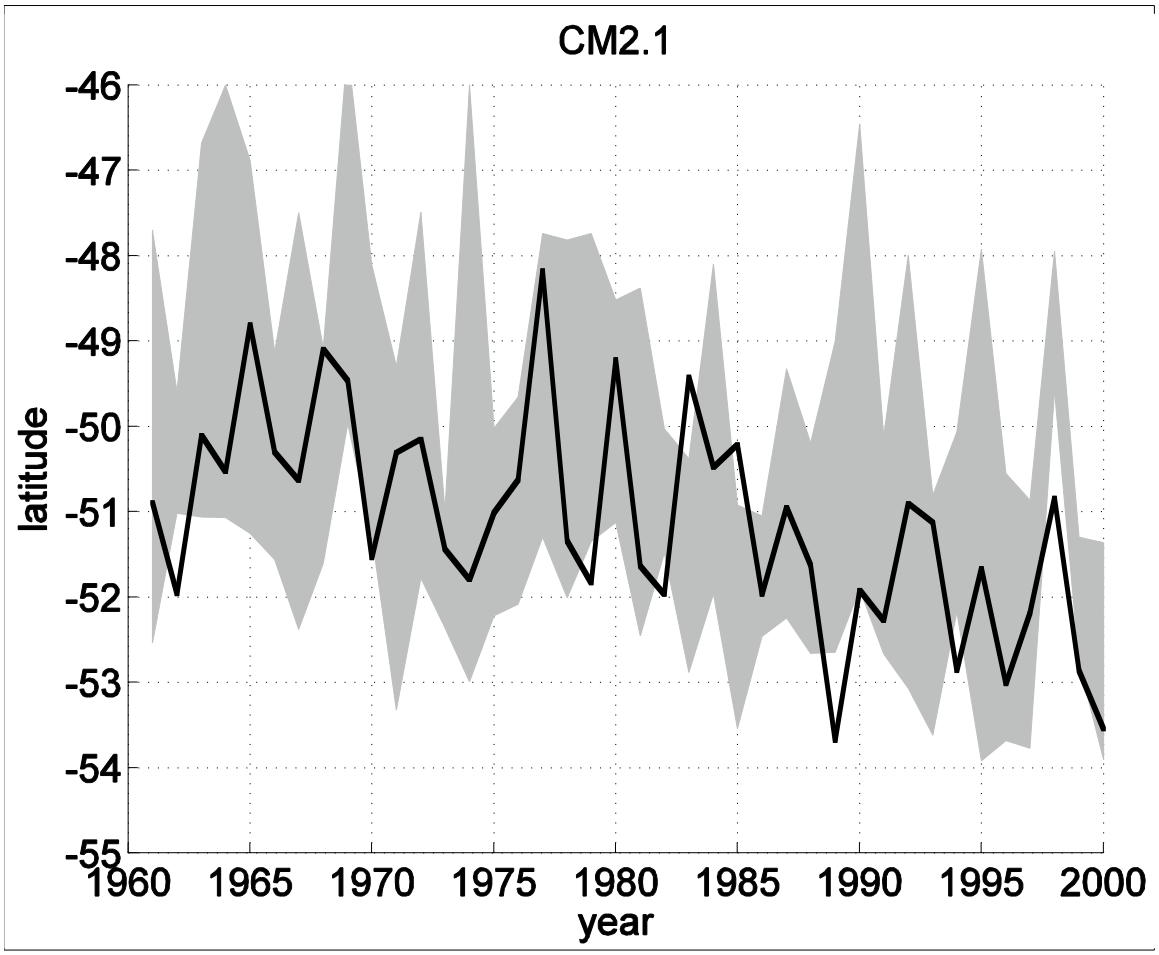

Fig yy in above discussion

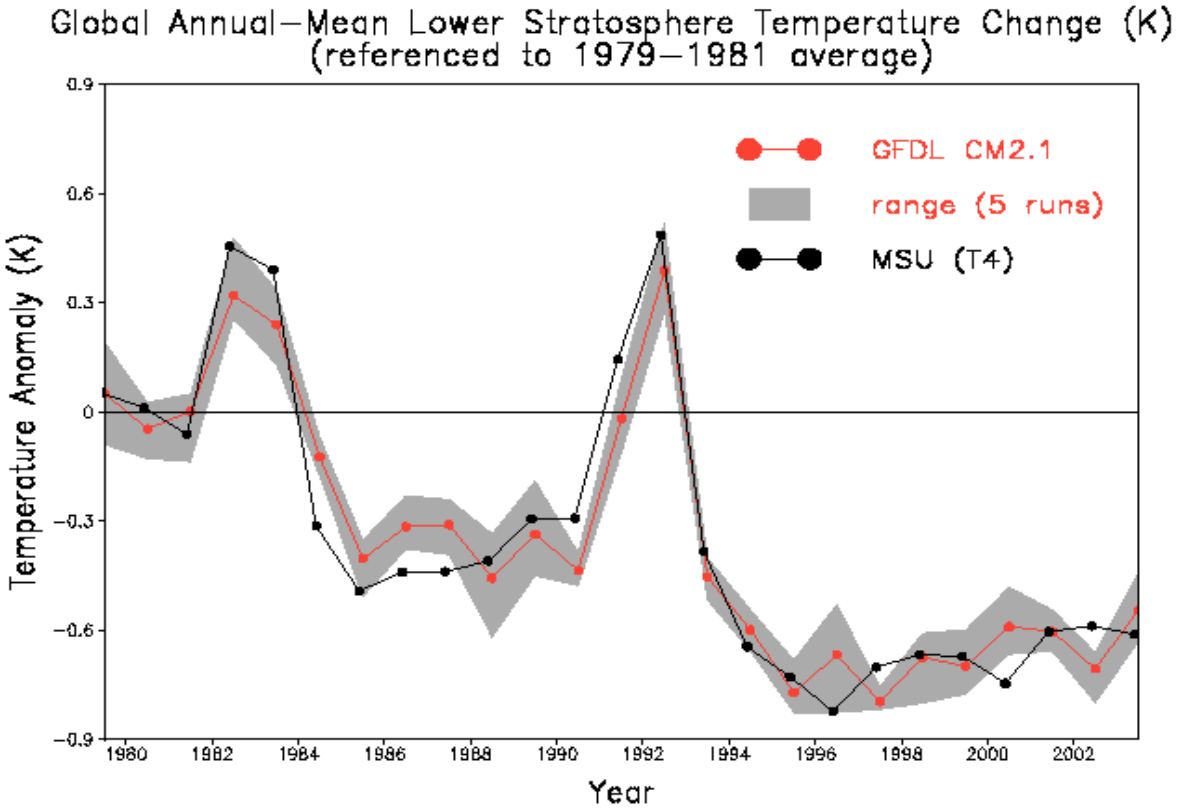

1
2

3

4 Fig zz in above discussion

5

6

Climate simulations discussed in this report

Three types of climate simulation are discussed in this report. They differ according to the climate forcing factors used as input to the models:

Control runs use constant forcing. (The name "control runs" originated in comparing them with the other simulation types discussed below.) The Sun's energy output and the atmospheric concentrations of carbon dioxide and other gases and aerosols do not change in control runs. As with the other types of climate simulation, day-night and seasonal variations occur, as well as internal "oscillations" like ENSO (see below). Other than these variations, the control run of a well-behaved climate model is expected to reach a steady state eventually.

Values of control-run forcing factors are typically set to match present-day conditions, and model output is then compared with present-day observations. Actually, the present climate is affected not only by current forcing but also by the history of forcing over time—in particular past emissions of greenhouse gases—but present-day control run output and observations are expected to agree fairly closely if models are reasonably accurate. We compare model control runs with observations in Chapter V below.

Idealized climate simulations are aimed at understanding important processes in models and in the real world. They include experiments in which the amount of atmospheric carbon dioxide increases at precisely 1% per year (about twice the present rate of increase) or doubles instantaneously. The carbon dioxide doubling experiments are typically run until the simulated climate reaches a steady state in equilibrium with the enhanced greenhouse effect. Until the mid-1990s, idealized simulations were often employed to assess possible future climate changes including human-induced global warming. Recently, however, the more realistic time-evolving simulations defined immediately below have been used for making climate predictions. We discuss idealized simulations and their implications for climate sensitivity in Chapter IV below.

Time-dependent climate forcing simulations are the most realistic, especially for eras in which climate forcing is changing rapidly such as the 20th and 21st centuries. Input for the 20th century simulations includes observed time-varying values of solar energy output, atmospheric carbon dioxide, and other climate-relevant gases and aerosols including those produced in volcanic eruptions. Each modeling group uses its own best estimate of these factors. There are significant uncertainties in many of them, especially atmospheric aerosols, so that different models use somewhat different input for their 20th century simulations. We discuss these simulations in Chapter V after comparing control runs with observations.

Time-evolving climate forcing is also used as input for modeling future climate change. This subject is discussed in CCSP Synthesis and Assessment Product 3.2. Finally, we mention for the record simulations of the distant past (various time periods ranging from the early Earth up to the 19th century). These simulations are not discussed in this report, but some of them have been used to loosely "paleocalibrate" simulations of the more recent past and the future (Hoffert and Covey, 1992; Hansen et al., 2006; Hegerl et al., 2006).

Chapter III – The Added Value of Regional Climate Model Simulations

Types of downscaling simulations

This section focuses on downscaling using three-dimensional models based on fundamental conservation laws, i.e., numerical models with a similar basis as GCMs. There are three primary approaches to numerical downscaling: limited-area models (Giorgi and Mearns, 1991; McGregor, 1997; Giorgi and Mearns, 1999; Wang et al., 2004), stretched grid models (e.g., Deque et al., 1995; Fox-Rabinovitz et al., 2001, 2006) and uniformly high-resolution atmospheric GCMs (AGCMs) (e.g., Brankovic and Gregory, 2001; May and Roeckner, 2001; Duffy et al., 2003; Coppola and Giorgi, 2005). The last approach is sometimes called "time-slice" climate simulation because the AGCM simulates a portion of the period simulated by the parent, coarser resolution GCM that supplies boundary conditions to it. The limited-area models, also known as regional climate models (RCMs), have the most widespread use. All three approaches use interactive land models, but sea-surface temperatures and sea ice are generally specified from observations or an atmosphere-ocean GCM.

RCMs, as limited-area models, cover only a portion of the planet, typical a continental domain or smaller. They require lateral boundary conditions from observations, such as atmospheric analyses (e.g., Kanamitsu et al. 2002, Uppala et al. 2005), or a global simulation. They may also use grids nested inside a coarser RCM simulation to achieve higher resolution in subregions (e.g. Liang et al., 2001; Hay et al., 2006). Stretched-grid models, like the high-resolution AGCMs, simulate the globe, but with spatial resolution varying horizontally. Highest resolution may focus on one (e.g. Deque and Piedelievre, 1995; Hope et al., 2004) or a few regions (e.g., Fox-Rabinovitz et al., 2002). In some sense, high-resolution AGCMs are a limiting case of stretched-grid simulations where the grid is uniformly high everywhere.

Highest spatial resolutions are most often several tens of kilometers, though some (e.g., Grell et al., 2000a,b; Hay et al., 2006) have simulated climate with resolutions as

small as a few kilometers using multiply nested grids. Duffy et al., (2003) have performed multiple AGCM time-slice computations using the same model to simulate resolutions from 310 km down to 55 km. Such approaches expose changes in climate with resolution. Higher resolution generally yields improved climate, especially for fields with high spatial variability, such as precipitation. For example, some studies show that higher resolution does not have a statistically significant advantage in simulating large-scale circulation patterns but it does yield better monsoon precipitation forecasts and interannual variability (Mo et al., 2005) and precipitation intensity (Roads et al., 2003). However, improvement is not guaranteed: Hay et al. (2006) find deteriorating timing and intensity of simulated precipitation versus observations in their inner, high-resolution nests, even though the inner nest improves resolution of topography. Extratropical storm tracks in a time-slice AGCM may shift poleward relative to the parent, coarser GCM (Stratton, 1999; Roeckner et al., 2006) or lower resolution versions of the same AGCM (Brankovic and Gregory, 2001), thus yielding an altered climate with the same sea-surface temperature distribution as the parent model.

Spatial resolution affects the length of simulation periods because higher resolution requires shorter time steps for numerical stability and accuracy. Required time steps scale with the inverse of resolution and can be one or two orders of magnitude smaller than AOGCM time steps. Since increases in resolution are most often applied to both horizontal directions, this means that computation demand varies inversely with the cube of resolution. Although several RCM simulations have lasted 20 to 30 years (Christensen et al., 2002; Leung et al., 2004; Plummer et al., 2006) and even as long as 140 years (McGregor, 1999) with no serious drift away from reality, stretched-grid, time-slice AGCM and RCM simulations typically last from months to a few years. Vertical resolution usually does not change with horizontal resolution, though Lindzen and Fox-Rabinovitz (1989) and Fox-Rabinovitz and Lindzen (1993) have expressed concerns about the adequacy of vertical resolution relative to horizontal resolution in climate models.

Higher resolution in RCMs and stretched-grid models must also satisfy numerical constraints. Stretched-grid models whose ratio of coarsest to finest resolution exceeds a factor of roughly three are likely to produce inaccurate simulation due to truncation error

(Qian et al., 1999). Similarly, RCMs will suffer from incompletely simulated energy spectra and thus loss of accuracy if their resolution is roughly 12 times or more finer than the resolution of the source of lateral boundary conditions, which may be a coarser RCM grids (Denis et al., 2002, 2003; Laprise, 2003; Antic et al., 2004, 2006; Dimitrijevic and Laprise 2005). In addition, these same studies indicate that lateral boundary conditions should be updated more frequently than twice per day.

Additional factors also govern ingestion of lateral boundary conditions (LBCs) by RCMs. LBCs are most often ingested in RCMs by damping of the model's state toward the LBC fields in a buffer zone surrounding the domain of interest (Davies, 1976; Davies and Turner, 1977). If the buffer zone is only a few grid points wide, the interior region may suffer phase errors in simulating synoptic-scale waves (storm systems), with resulting error in the overall regional simulation (Giorgi et al., 1993). Spurious reflections may also occur in at boundary regions (e.g., Miquez-Macho et al., 2005). RCM boundaries should be where the driving data are of optimum accuracy (Liang et al., 2001), but placing the buffer zone in a region of rapidly varying topography can induce surface pressure errors due to mismatch between the smooth topography implicit in the coarse resolution driving data and the varying topography resolved by the model (Hong and Juang 1998). Domain size may also influence RCM results. If a domain is too large, the model's interior flow may drift from the large-scale flow of the driving data set (Jones et al., 1995). However, too small a domain overly constrains interior dynamics, preventing the model from generating appropriate response to interior mesoscale-circulation and surface conditions (Seth and Giorgi, 1998). RCMs appear to perform well for domains roughly the size of the contiguous United States. Fig. RM-1 shows that the daily, root-mean-square difference (RMSD) between simulated and observed (reanalysis) 500 hPa heights is generally within observational noise levels (roughly 20 m).

Because simulations from the downscaling models may be analyzed for periods as short as a month, model spin-up is important (e.g., Giorgi and Bi, 2000). During spin-up the model evolves to conditions representative of its own climatology, which may differ from the sources of initial conditions. The atmosphere spins up in a matter of days, so the key factor is spin-up of soil moisture and temperature, which evolve more slowly. Equally important, data for initial conditions is often lacking or has low spatial

resolution, so that initial conditions may be only a poor approximation to the model's climatology. Spin-up is especially relevant for downscaling because these models are presumably resolving finer surface features than coarser models, with the expectation that the downscaling models are providing added value through proper representation of these surface features. Deep soil temperature and moisture, at depths of 1–2 meters, may require several years of spin up. However, these deep layers generally interact weakly with the rest of the model, so shorter spin-up times are used. For multi-year simulations, 3-4 years appears to be a minimal requirement (Christensen, 1999; Roads et al., 1999). This ensures that the upper meter of soil has a climatology in further simulation that is consistent with the evolving atmosphere.

Many downscaling simulations, especially with RCMs, are for periods much shorter than two years. Such simulations likely will not use multi-year spin up. Rather, these studies may focus on more rapidly evolving atmospheric behavior that is governed by lateral boundary conditions, including extreme periods like drought (Takle et al., 1999) or flood (Giorgi et al., 1996; Liang et al., 2001; Anderson et al., 2003). Thus, they assume that the interaction with the surface, while not negligible, is not strong enough to skew the atmospheric behavior studied. Alternatively, relatively short regional simulations may specify, for sensitivity study, substantial changes in surface evaporation (e.g., Paegle et al., 1996), soil moisture (e.g., Xue et al., 2001) or horizontal moisture flux at lateral boundaries (e.g., Qian et al., 2004).

Even with higher resolution than standard GCMs, models simulating regional climate still need parameterizations for subgrid-scale processes, most notably atmospheric convection, boundary-layer dynamics, surface-atmosphere coupling, radiative transfer and cloud microphysics. Often, these parameterizations are the same or nearly the same as used in GCMs. However, all parameterizations make assumptions that they are representing the statistics of subgrid processes, and so implicitly or explicitly they require that the grid box's area in the real world would have sufficient samples to justify the stochastic modeling. For some parameterizations, such as convection, this assumption becomes doubtful when grid boxes become only a few kilometers in size (Emanuel 1994). In addition, models simulating regional climate may include circulation characteristics, such as rapid mesoscale circulations (jets) whose interaction with subgrid

processes like convection and cloud cover differs from the larger scale circulations resolved by typical GCMs. This factor is part of a larger issue, that parameterizations may have regime dependence, performing better for some conditions than others. For example, the Grell (1993) convection scheme is responsive to large-scale tropospheric forcing, whereas the Kain and Fritsch (1993) scheme is heavily influenced by boundary-layer forcing. As a result, the Grell scheme simulates better the propagation of precipitation over the U.S. Great Plains that is controlled by the large-scale tropospheric forcing, while the Kain–Fritsch scheme simulates better late afternoon convection peaks in the southeastern U.S. that are governed by boundary-layer processes (Liang et al., 2004). As a consequence, parameterizations for regional simulation may differ from their GCM counterparts, especially for convection and cloud microphysics. In some instances, the regional simulation may have resolution of only a few kilometers and the convection parameterization may be discarded (Grell et al., 2000). A variety of parameterizations exist for each of these phenomena, with multiple choices often available in a single model (e.g., Grell et al., 1994; Skamarock et al., 2005).

The chief reason for performing regional simulation, whether by an RCM, a stretched-grid model or a time-slice AGCM, is to resolve behavior considered important for a region's climate that a global model does not resolve. Thus, regional simulation should have clearly defined regional-scale (mesoscale) phenomena targeted for simulation. These include, for example, effects of mountains (e.g., Leung and Wigmosta, 1999; Grell et al., 2000; Zhu and Liang, 2007), jet circulations (e.g., Takle et al., 1999; Anderson et al., 2001; Anderson et al., 2003; Byerle and Paegle, 2003) and regional ocean-land interaction (e.g., Kim et al., 2005; Diffenbaugh et al. 2004). The most immediate value, then, of regional simulation is to explore how such phenomena operate in the climate system, which becomes a justification for the expense of performing regional simulation. Phenomena and computational costs together influence the design of regional simulations. Simulation periods and resolution are balances between sufficient length and number of simulations for climate statistics versus computational cost. For RCMs and stretched-grid models, the sizes of regions targeted for high resolution simulation are determined in part by where the phenomenon occurs.

In the context of downscaling, regional simulation offers the potential to include phenomena affecting regional climate change that are not explicitly resolved in the global simulation. When given boundary conditions corresponding to future climate, regional simulation can then indicate how these phenomena contribute to climate change. Results, of course, are dependent on the quality of the source of the boundary conditions (Pan et al., 2001; de Elía et al., 2002), though use of multiple sources of future climate may lessen this vulnerability and offer opportunity for probabilistic estimates of regional climate change (Raisanen and Palmer, 2001; Giorgi and Mearns, 2003; Tebaldi et al., 2005). Results also depend on the physical parameterizations used in the simulation (Yang and Arritt, 200; Vidale et al., 2003; Déqué et al., 2005; Liang et al., 2006). Advances in computing power suggest that typical GCMs will eventually operate at resolutions of most current regional simulations (a few tens of kilometers), so that understanding and modeling improvements gained for regional simulation can promote appropriate adaptation of GCMs to higher resolution. For example, interaction between mesoscale jets and convection appears to require parameterized representation of convective downdrafts and their influence on the jets (Anderson et al., 2007), behavior not required for resolutions that do not resolve mesoscale circulations.

Because of the variety of numerical techniques and parameterizations employed in regional simulation, many models and versions of models exist. Side-by-side comparison (e.g., Takle et al., 1999; Anderson et al., 2003; Fu et al., 2005; Frei et al., 2006; Rinke et al., 2006) generally shows no single model appearing as best versus observations, with different models showing superior performance depending on the field examined. Indeed, the best results for downscaling climate simulations and estimating climate-change uncertainty may come from assessing an ensemble of simulations (Giorgi and Bi, 2000; Yang and Arritt, 2002; Vidale et al., 2003; Déqué et al., 2005). Such an ensemble may capture much of the uncertainty in climate simulation, offering an opportunity for physically based analysis of the climate changes and also the uncertainty of the changes. Several regional models have performed simulations of climate change for parts of North America, but at present, there have been no regional projections using an ensemble of regional models simulating the same time periods with the same boundary conditions. Such systematic evaluation has occurred in Europe [PRUDENCE

(Christensen et al. 2002) and ENSEMBLES (Hewitt and Griggs 2007) projects] and is starting in North America with the North American Regional Climate Change Assessment Program (NARCCAP 2007).

Empirical downscaling

Empirical, or statistical, downscaling is an alternative approach to obtaining regional-scale climate information (Kettenberg et al., 1996; Hewitson and Crane, 1996; Giorgi et al., 2001; Wilby et al., 2004, and references therein). It uses statistical relationships to link resolved behavior in GCMs with climate in a targeted area. The size of the targeted area can be as small as a single point. So long as significant statistical relationships occur, empirical downscaling can yield regional information for any desired variable, such as precipitation and temperature, as well as variables not typically simulated in climate models, such as zooplankton populations (Heyen et al. 1998) and initiation of flowering (Maak and von Storch, 1997). The approach encompasses a range of statistical techniques from simple linear regression (e.g., Wilby et al., 2000) to more complex applications, such as those based on weather generators (Wilks and Wilby, 1999), canonical correlation analysis (e.g., von Storch et al,. 1993) or artificial neural networks (e.g., Crane and Hewitson, 1998). Empirical downscaling can be very inexpensive compared to numerical simulation when applied to just a few locations or using simple techniques. This together with the flexibility in targeted variables has led to a wide variety of applications for assessing impacts of climate change.

There has been some side-by-side comparison of methods (Wilby and Wigley, 1997; Wilby et al., 1998; Zorita and von Storch 1999; Widman et al., 2003). These studies have tended to show fairly good performance of relatively simple versus more complex techniques and to highlight the importance of including moisture as well as circulation variables when assessing climate change. There also has been comparison of statistical downscaling and regional climate simulation (Kidson and Thompson, 1998; Mearns et al., 1999; Wilby et al., 2000; Hellstrom et al., 2001; Wood et al., 2004; Haylock et al., 2006), with neither approach distinctly better or worse than the other.

Strengths and limitations of regional models

We focus here on numerical models simulating regional climate without discussing empirical downscaling because the wide range of applications using the latter undermines making a general assessment of strengths and limitations.

The higher resolution in regional-scale simulations provides quantitative value to climate simulation. With finer resolution, one can resolve mesoscale phenomena contributing to intense precipitation, such as stronger upward motions (Jones et al., 1995) and coupling between regional circulations and convection (e.g., Anderson et al., 2007). Time-slice AGCMs show intensified storm-tracks relative to their parent model (Solman et al. 2003, Roeckner et al., 2006). Thus, although regional models may still miss the most extreme precipitation (Gutowski et al., 2003, 2007), they can give more intense events that will be smoothed in coarser resolution GCMs. The higher resolution also includes other types of scale-dependent variability, especially short-term variability such as extreme winds and locally extreme temperature that coarser resolution models will smooth and thus inhibit.

Mean fields also appear to be simulated somewhat better on average versus coarser GCMs because spatial variations are potentially better resolved. Thus, Giorgi et al. (2001) report typical errors in RCMs of less than 2˚C temperature and 50% for precipitation for regions $10^5 - 10^6$ km^2. Large-scale circulation fields tend to be well simulated, at least in the extratropics (Fig. RM-1).

As alluded to above, regional-scale simulations also have phenomenological value, simulating processes that GCMs either cannot resolve or can resolve only poorly. These include internal circulation features such as the nocturnal jet that imports substantial moisture to the center of the United States and couples with convection (e.g., Byerle and Paegle, 2003; Anderson et al., 2007). These processes often have substantial diurnal variation and are thus important to proper simulation of regional diurnal cycles of energy fluxes and precipitation. Some processes require resolving surface features too coarse for typical GCM resolution, such as rapid topographic variation and its influence on precipitation (e.g., Leung and Wigmosta, 1999; Hay et al., 2006) and climatic influences of bodies of water like the Gulf of California (e.g., Anderson et al., 2001) and the North American Great Lakes (Lofgren, 2004) and their downstream influences. In addition, regional simulations resolve land-surface features that may be important for

climate-change impacts assessment, such as distributions of crops and other vegetation (Mearns, 2003; Mearns et al., 2003), though care is needed to obtain useful information at higher resolution (Adams et al., 2003).

An important limitation for regional simulations is that they are dependent on boundary conditions supplied from some other source. This applies to all three forms of numerical simulation (RCMs, stretched-grid models, time-slice AGCMs), since they all typically require input sea-surface temperature and ocean ice. Some RCM simulations have been coupled to a regional ocean-ice model, with mixed-layer ocean (Lynch et al., 1995, 2001) and a regional ocean-circulation model (Rummukainen et al., 2004) but this is not common. In addition, of course, RCMs require lateral boundary conditions. Thus, regional simulations by these models are dependent on the quality of the model or observations supplying the boundary conditions. This is especially true for projections of future climate.

Careful evaluation is also necessary to show differences, if any, between the large-scale circulation of the regional simulation and its driving data set. Generally, any tendency for the regional simulation to correct biases in the parent GCM's large-scale circulation should be viewed with caution (Jones et al., 1995). RCM should not normally be expected to correct large-scale circulation problems of parent model, unless there is a clearly understood physical basis for the improvement. Clear physical reasons for the correction due to higher resolution, such as better rendition of physical processes like topographic circulation (e.g., Leung and Qian, 2003), surface-atmosphere interaction (Han and Roads, 2004) and convection (Liang et al., 2006), must be established. Otherwise, the regional simulation may simply have errors that counteract the parent GCM's errors, which undermines confidence of projected future climate.

RCMs may also exhibit difficulty in outflow regions of the domain, especially for domains with relatively strong cross-boundary flow, such as extratropical domains covering a single continent or less. The difficulty appears to arise because storm systems may track across the RCM's domain at a different speed that in the driving-data source, resulting in a mismatch of circulations at boundaries where storms would be moving out of the domain. Also, there are always unresolved scales of behavior, so the regional simulations are still dependent on the quality of their parameterizations for the scales

explicitly resolved. Finally, the higher computational demand due to shorter time steps limits the length of typical simulations to two to three decades or less (e.g., Christensen et al., 2002; NARCCAP, 2007), with few ensemble simulations.

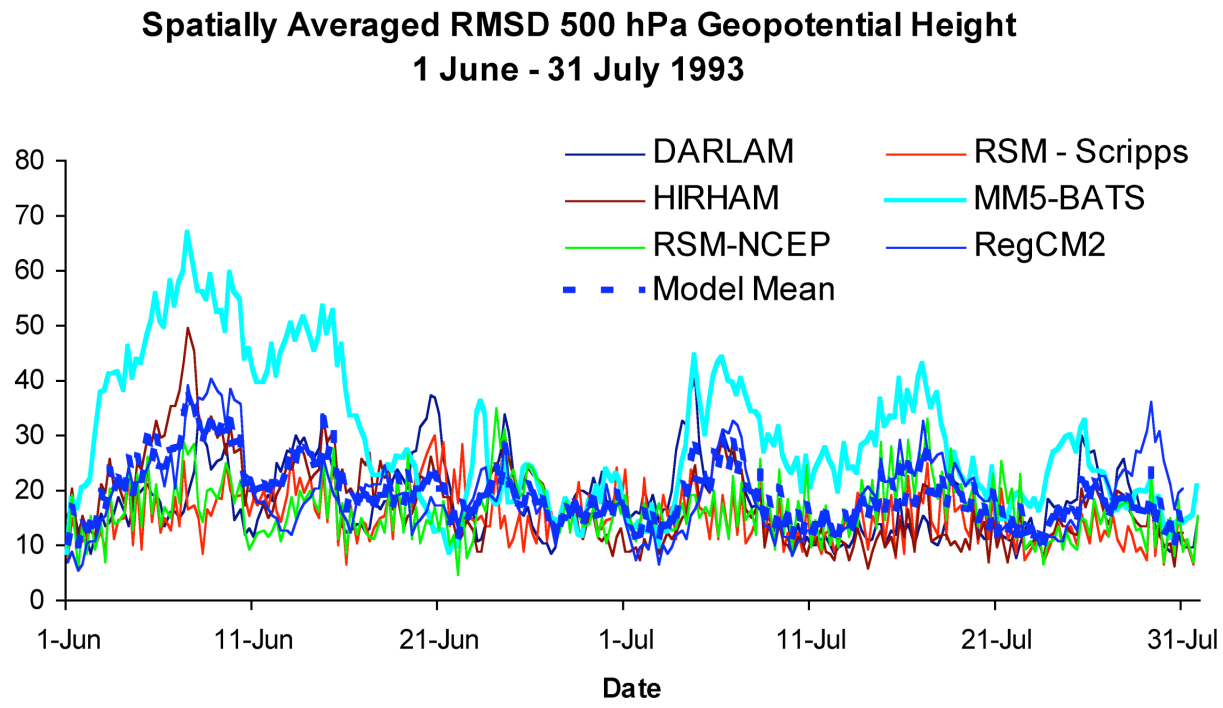

Fig. RM-1. Daily root-mean-square differences (RMSD) in 500 hPa height between observations (reanalysis) and 6 models participating in the PIRCS 1b experiment (Anderson et al., 2003). RMSD values averaged over the simulation domain inside the boundary-forcing zone. Also shown is the mean curve for the 6 models. (y-axis scale: meters).

Chapter IV – Model Climate Sensitivity

"Climate sensitivity" is a quantitative measure of how much Earth's climate responds to a given amount of forcing. The forcing is external to the climate system and may arise from changing the energy output of the Sun, the properties of the planetary surface, or the atmospheric amounts of heat-trapping gases (greenhouse gases) or small particles (aerosols). Climate sensitivity provides a simple indication of how Earth would actually respond to the totality of real-world climate forcing factors.

The climate system's response to any forcing is determined by a number of internal feedback processes that can amplify or dampen the initial effect of the forcing. The most important feedback processes, involving ocean circulation and atmospheric humidity and clouds, have proved difficult to assess. In this report we summarize estimates of climate sensitivity without explicit discussion of feedback processes.

The net trapping of heat that would occur if changes in atmospheric concentrations occurred very quickly is often used to quantify climate forcing. A nearly instantaneous change in one or more of the atmosphere's constituents is an idealized, unrealistic scenario, but it serves a useful purpose. Direct heat-trapping and heat-rejecting (albedo) properties are fairly well characterized for the most significant greenhouse gases and aerosols. As a result, the climate forcing that would occur if specified atmospheric changes took place may be calculated with moderate uncertainty (Ramaswamy et al., 2001). For example, suddenly doubling the atmospheric amount of carbon dioxide would add energy to the lower atmosphere at the rate of about 4 Watts per square meter for the first few months after the doubling took place (Hansen et al., 1981). Eventually temperatures would increase (and climate would change in other ways such as changing precipitation) in response to this forcing, Earth would radiate more heat to space, and the 4 W m^{-2} imbalance would be redressed.

The concept of encapsulating global climate sensitivity in a single number appeared early in the development of climate models (Schneider and Mass, 1975). Today, three different

numbers are in common use. All three involve changes in global and annual mean surface or near-surface temperature. The global and annual mean is obtained by averaging over both Earth's total area and the cycle of the seasons (e.g. Earth's present-day global and annual mean surface temperature is about 15°C). *Transient climate response* or TCR is defined as warming due to 1% per year increasing atmospheric carbon dioxide, taken at the moment that carbon dioxide doubles (about 70 years after the increase begins). *Equilibrium warming* is defined as the analogous long-term surface warming after atmospheric carbon dioxide has been doubled but thereafter held constant, and the climate is allowed to reach a new steady state, as described in the example above. *Effective climate sensitivity* is defined as the equilibrium warming that would be expected—based on model behavior at the time of atmospheric carbon dioxide doubling—if feedback processes in the climate system remained fixed thereafter.

Historically, equilibrium warming due to doubled atmospheric carbon dioxide has been the most common measure of climate sensitivity. Dividing it by the associated climate forcing (4 W m^{-2}) gives a climate sensitivity ratio in units of °C / (W m^{-2}). This ratio can be used as a scale to predict the global and annual mean temperature change due to other kinds of forcing, provided that one assumes mean surface warming varies linearly with forcing. The assumption of linearity is a reasonable first approximation for solar and greenhouse-gas forcing but not for all types of forcing (Ramaswamy et al., 2001). Even in cases for which the assumption is reasonable, it must be remembered that it leads to an estimate of equilibrium warming. The actual time-evolving or transient response of the climate will differ from the equilibrium response in magnitude and also, to some extent, in geographical pattern (Schneider and Thompson, 1981; Manabe et al., 1991).

Equilibrium warming is difficult to obtain from AOGCMs because the deep ocean takes a great deal to time to fully respond to changes in climate forcing. To avoid unacceptably lengthy computer simulations, equilibrium warming is usually estimated from a modified climate model in which the ocean component is replaced by a simplified, fast-responding "slab ocean model." The modified model, however, can give a different result from the original and presumably more accurate AOGCM. To address this problem, effective

climate sensitivity ΔT_e may be defined in terms of TCR, climate forcing ΔF and the flux of energy into the ocean surface ΔF_o (Cubasch et al. 2001):

$$\Delta T_e = \Delta F_{2x} / (\Delta F - \Delta F_o) \times TCR$$

where $\Delta F_{2x} \approx 4$ W m^{-2} is climate forcing due to doubled atmospheric carbon dioxide. For an AOGCM experiment in which atmospheric carbon dioxide is doubled, $\Delta F_{2x} = \Delta F$ and the ratio above ≥ 1, so that $\Delta T_e \geq$ TCR. If the experiment were continued until the climate system is allowed to reach a new steady state, $\Delta F_o = 0$ and ΔT_e = TCR = equilibrium warming. In short, effective climate sensitivity is defined to be (a) identical to the equilibrium warming due to doubled atmospheric carbon dioxide in simulations that obtain this quantity directly, and (b) the best estimate of equilibrium warming from simulations that have not yet reached equilibrium.

The three leading families of US models exemplify the climate sensitivity of modern AOGCMs. Kiehl et al. (2006) examined the sensitivity of three successive versions of the Community Climate System Model developed over a period of a decade: CSM1.4, CCSM2 and CCSM3. Stouffer et al. (2006) and Hansen et al. (2006) similarly studied the most recent GFDL and GISS models, respectively. These (and other) models differ in their details because development teams have differing ideas concerning the underlying physical mechanisms relevant for the less well-understood aspects of the system. The complexity of the climate system, together with our inability to explicitly represent all relevant processes in models, result in a host of choices to be made by development teams. Differing expertise, experience, and interests result in distinct development pathways for each climate model. While we eventually expect to see model convergence forced by increasing knowledge of the real climate system, we are still far from that limit today. The models are also adjusted in different ways, consistent with plausible ranges of model parameters, so as to optimize the fit to observations deemed to be of particular importance.

Resulting sensitivity values for the three families of US models are shown in Table IV(1) below (including a slight correction of effective sensitivity values by personal communication from J. T. Kiehl). Members of model development teams held various views on the most likely value of climate sensitivity, but rarely with much conviction, and there was agreement that it is best to avoid engineering the models to posses a particular value of sensitivity. Hence, deliberate generation of particular sensitivity values was not followed by any of these three teams.

Table IV(1)

Model	**TCR**	**Effective sensitivity**	**Equilib. warming***
CSM1.4	1.4°C	2.1°C	2.0°C
CCSM2	1.1°C	1.6°C	2.3°C
CCSM3	1.5°C	2.6°C	2.5°C
GFDL CM2.0	1.6°C		2.9°C
GFDL CM2.1	1.5°C		3.4°C
GISS Model E			2.7-2.9°C

In the last column, only the higher GISS Model E value is obtained with a full AOGCM. All other values of equilibrium warming in the table are obtained with the ocean component replaced by a slab ocean model. For the full-AOGCM version of CCSM3, equilibrium warming due to doubled atmospheric carbon dioxide may be inferred from Meehl et al. (2006). Their Figure 3a-b shows the mean warming that results from imposing two IPCC SRES emissions scenarios (A1B and B1) for the years 2000-2100 and then holding atmospheric concentrations of gases and aerosols constant from 2100 to 2300, by which time the mean temperatures are approximately constant. The SRES emissions scenarios imply a more complex and uncertain radiative forcing than increasing atmospheric carbon dioxide, but scaling the Meehl et al. results, one obtains ~2°C equilbrium warming due to doubled atmospheric carbon dioxide, consistent with the CCSM3 slab ocean model version.

Comparing different columns within a single row of the table shows that both the effective climate sensitivity and the equilibrium warming are greater than TCR for any given model. This is because TCR is measured before the deep ocean, with its large thermal inertia, has had time to warm fully in response to doubled atmospheric carbon dioxide. It also appears that the effective climate sensitivity is usually close to the equilibrium warming. This result suggests that in typical models, the most important feedback processes have come into play by the time of atmospheric carbon dioxide doubling.

Comparing different rows within any single column, it is apparent that a wide range of sensitivity values are obtained by different models even if the definition of sensitivity is the same. The range for equilibrium warming is particularly striking and persistent. Nearly three decades ago, Charney (1979) judged the model-implied range of equilibrium warming due to doubled atmospheric carbon dioxide to be 1.5-4.5°C, a three-fold span of possibilities. As indicated in the table, this range has narrowed for recently developed models, but a systematic exploration of plausible input parameters for one AOGCM gives a 5-95 percentile range of ~2-6°C, again a three-fold span (Piani et al. 2005, Knutti et al. 2006). The low end of the range is more certain than the high end (Bierbaum et al. 2003, Soden and Held 2006).

The variation among models is less for TCR than for equilibrium warming because enhanced equilibrium sensitivity correlates with enhanced heat transport to the deep ocean, and these two effects cancel to some extent in transient simulations (Covey et al. 2003). Apart from the anomalous CCSM2, model TCR varies by less than 15% in the table above. Systematic exploration of model input parameters gives a wider range, 1.5-2.6°C, similar to that found in extensive multi-model studies (M. Collins et al. 2006).

It has proved difficult to identify the reasons behind the variation of climate sensitivity among models. As a result, we cannot completely understand why different models give different answers to the same fundamental question about climate change, let alone determine which answer is “right.” Studies of the CCSM family of models provide an

example of the problem. Kiehl et al. (2006) found that a variety of factors are responsible for differences in climate sensitivity among the models of this family. Most notably, the generally lower sensitivity of CCSM2 that is evident in the table is mainly due to a single change (relative to CSM1.4 and CCSM3) in the model's algorithm for simulating convective clouds. CCSM3's formulation reflects intensive efforts to represent climate processes more accurately than its predecessors CSM1.4 and CCSM2, but it cannot be proven that the resulting global climate sensitivity is closer to real-world truth.

The CCSM and GFDL development teams met at several times during the development of CCSM3 and CM2 (see table entries above) to compare experiences and discuss common systematic errors in the two models. It was noted in these meetings that CCSM and GFDL climate sensitivities had converged to some extent from an earlier generation in which CCSM2 was on the low end of the "canonical" sensitivity range of 1.5-4.5°C, while the corresponding GFDL model was near the high end. This convergence in sensitivity was considered by the teams to be coincidental; it was not a consequence of any specific actions taken so as to engineer convergence.

These results illustrate the principle that climate sensitivity is itself highly sensitive to model input assumptions (Mitchell et al. 1989). As an example, figure IV(1) below shows how equilibrium warming due to doubled atmospheric carbon dioxide varied during the development of the most recent GFDL models. The dramatic drop in sensitivity between model versions p10 and p12.5.1 was unexpected. It followed a reformulation of the model's treatment of processes in the lower atmospheric boundary layer.

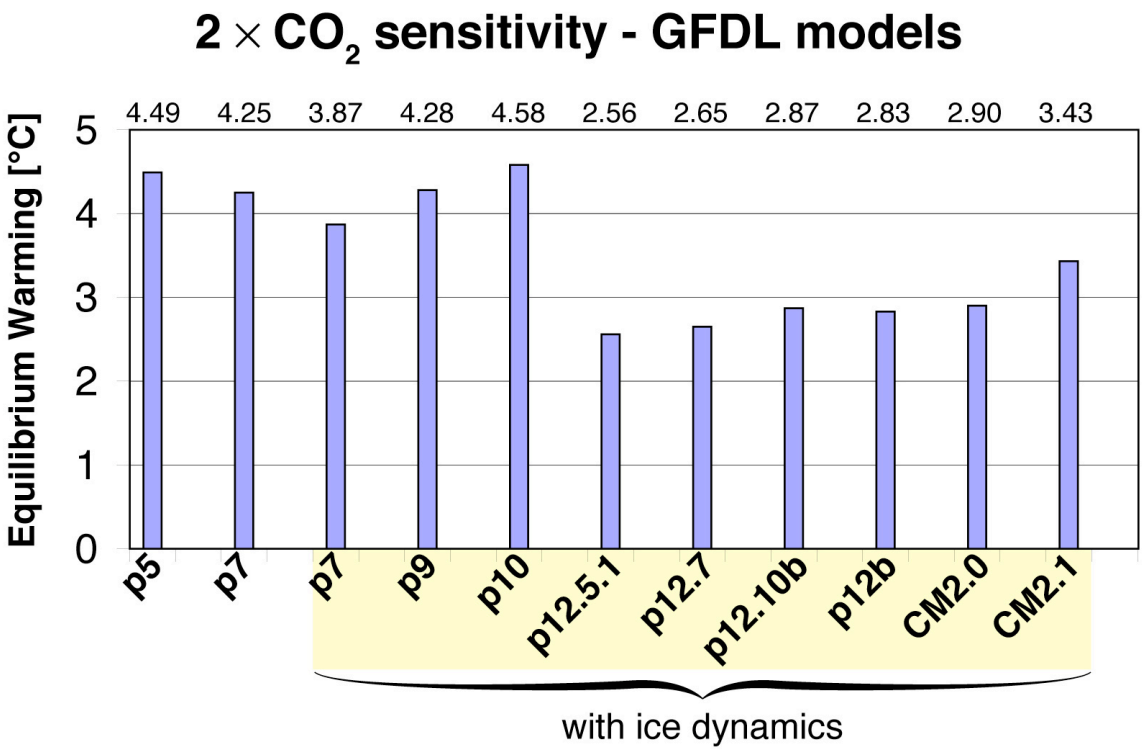

Figure IV(1): Equilibrium global mean near-surface warming due to doubled atmospheric carbon dioxide from intermediate ("p") model versions leading to GFDL's CM2.0 and CM2.1. Equilibrium warming was assessed by joining a simplified slab ocean model to the atmosphere, land and sea ice AOGCM components. The later versions include sea ice motion (dynamics) as well as sea ice thermodynamics.

[Possible Contribution from GISS models goes here]

Despite all this "bouncing around" of model-simulated equilibrium warming due to doubled atmospheric carbon dioxide, no credibly formulated AOGCM seems to have gone far outside the range 1.5–4.5°C (Cubash et al. 2001), at least on the low end (Piani et al., 2005; Knutti et al., 2006). A newly developed model that obtained a much different value than the norm would of course be subject to close scrutiny, but if its input

assumptions were plausible, it's hard to imagine such a model not being published or at least informally discussed among climate modelers.

The possibility remains that a strong negative feedback is missing in all current models, including the parameter-variation studies discussed above, due to generic flaws such as a tendency to overly "diffuse" water vapor (a strong greenhouse gas) and oversimplifications of other aspects of the hydrologic cycle. Discrepancies between observations and model simulations of humidity, clouds and related quantities (e.g. Clement and Soden 2005) have been used to infer such missing feedbacks. It would be difficult, however, to reconcile a very low real-world sensitivity value with the climate changes observed during recent decades (Andronova and Schlesinger, 2001; Forest et al.,, 2001) and inferred for the more distant past (Hansen et al. 1993; Covey et al., 1996).

Better understanding of Earth's climate sensitivity, with potential reduction in its uncertainty, will require better understanding of the multitude of climate feedback processes that operate in the real world. Humidity and clouds and their effects on energy flows are particularly important but difficult to observe (e.g. Lindzen et al., 2001 vs. Hartmann and Michelsen, 2002—this complicates using observations to test models). Hope nevertheless remains that new observations and theoretical models will narrow the uncertainty in climate sensitivity (Bony et al., 2006).

Cloud Feedbacks

Clouds reflect solar radiation to space, cooling the Earth-atmosphere system. Clouds also trap infrared radiation, keeping the Earth warm. The net effect depends on the height, location, microphysical and radiative properties of clouds, and their appearance of time with respect to the seasonal and diurnal cycles of the incoming solar radiation. Cloud feedback refers to the variations of these effects that can either amplify or moderate a climate change. Uncertainties of cloud feedbacks in climate models have been identified as the leading contributor of model sensitivity to climate forcing (e.g., Cess et al, 1990; Randall et al., 2000; Zhang, 2004; Stephens, 2005; Bony et al., 2006; Soden and Held 2006). The fidelity of cloud feedbacks in climate models is therefore important to the reliability of their prediction of future climate change.

Several diagnostic methods have been used to evaluate and understand cloud feedbacks in AGCMs. One is to calculate the partial radiative perturbation (PRP) due to variation of clouds in a climate change (e.g., Hansen et al., 1984; Wetherald and Manabe, 1988; Zhang et al., 1994; Soden et al., 2004; Soden and Held 2006). A second method is to use the variation of cloud radiative forcing (CRF) in a climate change simulation (Cess and Potter, 1988). CRF describes the difference of radiative transfer due to the presence of clouds. The CRF approach is more commonly used because of its convenience of calculation and the availability of satellite data for this diagnostics. While there are differences between the diagnostic feedbacks from the two approaches (Zhang et al. 1994; Coleman 2003; Soden et al., 2004), they tend to capture similar inter-model differences and physical processes. Both diagnostics also correlate well with the magnitude of simulated climate warming from models. Cloud feedback can also be more accurately calculated from climate change simulations with and without interactive clouds (Wetherald and Manabe, 1988). This approach however requires multiple climate change integrations of the model.

Early GCM cloud feedback studies include Hansen et al. (1984) with the GISS GCM and Wetherald and Manabe (1988) with the GFDL GCM by using the PRP approach. Positive

cloud feedbacks were diagnosed. Cess et al. (1990) used the surrogate climate change of plus and minus 2^{o}K over the oceans and diagnosed the cloud feedback in 19 GCMs. They showed a wide range of values from negative to strongly positive. The sensitivity of cloud feedback to model representation of clouds was more directly demonstrated in Senior and Mitchell (1993, 1996), who used the same unified GCM at the UK Met Office (UKMO) with only small modifications to the cloud scheme. In one modified version, cloud particle size is calculated based on the cloud liquid amount through an empirically observed relationship. In the standard version, particle size is fixed. In another version, sub-grid scale distribution of total water within a GCM grid is changed from a triangle distribution to a top-hat distribution. These modifications were all within uncertainties of model physical parameterizations. The three versions however exhibited large differences in cloud feedbacks from negative to positive values, leading to different equilibrium global warming from 1.9^{o}C to 5.5^{o}C in response to doubling CO_2 in the atmosphere. Many subsequent studies with other GCMs also showed large sensitivity of cloud feedbacks to the formulation of model physics (e.g., Le Treut et al., 1994; Yao and Del Genio, 2002; Soden et al., 2004; Yokohata et al., 2005).

To improve the understanding of cloud feedback processes in models, recent studies have also focused on the response of clouds to dynamical circulation conditions. Williams et al. (2003), Bony et al. (2004), and Wyant et al. (2006) showed that in the tropical region, the CRF response differs most between models in subsidence regimes, which also suggests a dominant role for low-level clouds in the diversity of tropical cloud feedbacks. Others also diagnosed errors in the simulation of particular cloud regimes or in specific dynamical conditions (Klein and Jakob, 1999; Tselioudis et al., 2000;; Webb et al., 2001, Norris and Weaver, 2001; Jakob and Tselioudis, 2003; Williams et al., 2003; Bony et al., 2004; Lin and Zhang, 2004; Ringer and Allan, 2004; Bony and Dufresne, 2005; Del Genio et al., 2005; Williams et al., 2006; Wyant et al., 2006). Zhang et al. (2005) evaluated clouds in ten AGCMs and showed that even though they simulate reasonable radiation balance at the top of the atmosphere, models have systematic compensatory cloud biases. Common among them are overestimation of optical thick clouds and

underestimation of middle and low clouds. Such biases may affect the ability to simulate cloud feedback in a climate change.

Soden and Held (2006) evaluated cloud feedbacks in 12 AR4 coupled models using PRP calculations. They showed positive cloud feedback in all models, ranging from the smallest magnitude of 0.14 W/m2/K in the CCSM to the largest value of 1.18 $W/m^2/K$ in the MPI ECHAM5. These values translate to a range of global warming of 2.2^oK to 4.9^oK assuming a forcing of 4 W/m2 and a feedback parameter of 2 $W/m^2/K$ without clouds (-3.2 $W/m^2/K$ from Planck's law,1.0 $W/m^2/K$ from water vapor and temperature lapse rate, 0.2 $W/m^2/K$ from surface albedo). Bony et al. (2005) analyzed the sensitivity of CRF in 15 AR4 coupled models in the tropics from 30^oS to 30^oN. They reported a CRF sensitivity range of -2.0 $W/m^2/K$ to 1.6 $W/m^2/K$ in the models. These ranges can be compared with results from earlier PRP results of -0.10 $W/m^2/K$ to 1.40 $W/m^2/K$ in Coleman (2003) and the early CRF range of -1.10 $W/m^2/K$ to 3.00 $W/m^2/K$ in Cess et al. (1990). The range of difference among GCMs has become smaller over the years, pointing to a slight negative feedback to positive feedback that is weaker than water vapor feedback. The range however is still substantial.

A recent study with super-parameterization (Wyant et al. 2006), in which CRMs were used to replace traditional parameterization in a GCM, showed negative cloud feedback parameter of -0.9 $W/m^2/K$ in the surrogate climate change of Cess et al. (1990) with the CRF approach. It was shown that the negative cloud feedback is primarily due to an increase in low cloud fraction and liquid water in tropical regions of moderate subsidence as well as substantial increases in high-latitude cloud fraction. Using the same experimental framework, Miura et al. (2005) carried out experiments of a global CRM with 7 km resolutions; they showed that climate sensitivity in the model is significantly reduced relative to a conventional GCM because of increased amount of extratropical clouds in warmer climate.

Several questions remain to be answered about cloud feedbacks in GCMs. First, the physical mechanisms of cloud feedbacks are still not clear. Some of the proposed possibilities include feedbacks from changes of cloud amount, cloud liquid water content, and cloud height, but they are model specific (Somerville and Remer 1984). Second, it is not clear how accurate a model should simulate observed clouds for it to reliably simulate cloud feedback processes. Another question is whether cloud feedbacks can be diagnosed from using different observed modes of climate variability (Tsushima et al. 2005; Williams et al. 2006). Answers to these questions will be important to understand the robustness of cloud feedbacks in climate models.

Disparities In Imposed Radiative Forcing

While increases in the concentration of greenhouse gases provide the largest change in radiative forcing during the twentieth century (IPCC AR4), other forcings must be considered to account for the observed change in surface air temperature. The burning of fossil fuels that releases greenhouse gases into the atmosphere can also create aerosols (small liquid droplets or solid particles that are temporarily suspended in the atmosphere) that cool the planet by reflecting sunlight back to space. In addition, there are changes in land use that change the reflectivity of the Earth's surface, as well as variations in sunlight impinging on the Earth, among other forcings. In this section, we discuss the extent to which twentieth century radiative forcing is known. In practice, this forcing varies among the models. Compared to the pre-industrial, present-day forcing in GISS modelE is 1.77 W/m2 (Hansen et al. 2007), but 2.8 W/m2 in the GFDL CM2.1 model (Knutson et al 2006). Variations in radiative forcing among models introduce uncertainty in the simulation of twentieth century climate change along with its attribution.

Greenhouse gases like carbon dioxide and methane have long atmospheric lifetimes on the order of decades, which allows them to be thoroughly mixed throughout the atmosphere. Trends in concentration are consistent throughout the world, and have been measured routinely since the International Geophysical

Year in 1958. Measurements of the gas bubbles trapped in ice cores give the concentration prior to that date. While changes in greenhouse gas concentration are accurately known, the associated radiative forcing varies among climate models. This is because GCM radiative calculations need to be computationally efficient, necessitating various approximations to the exact calculation based upon first principles. Using changes in well-mixed greenhouse gases, including carbon dioxide, methane, nitrous oxide and chlorofluorocarbons, measured between 1860 and 2000, Collins et al (2006) compared the radiative forcing computed by climate models (including NCAR, GFDL, and GISS). The GCM values were further compared to line-by-line (LBL) calculations, where fewer approximations are made, and differences result mainly from the omission of particular absorption bands (Collins et al 2006). The median LBL forcing at the top of the model by greenhouse gases is 2.1 W/m2, and the corresponding median among the climate models is higher by only 0.1 W/m2. However, the standard deviation among model estimates is 0.30 W/m2 (compared to 0.13 for the LBL models), which corresponds to a large fractional variation in greenhouse forcing among the models. In general, forcing calculated by the NCAR and GISS models are on the high side of estimates, while the GFDL model is low. For a doubling of greenhouse gas concentration, NCAR and GISS calculate forcing at the top of the atmosphere of 3.95 and 4.06 W/m2, respectively, while the GFDL model calculates 3.50 W/m2 compared to the all-model average of 3.67 +/- 0.28 W/m2 (W. Collins, personal communication). These calculations assume temperature and moisture profiles typical of the summer mid-latitudes, and exclude the effect of clouds, which introduce additional uncertainty into the computed forcing. Even though changes in greenhouse gas concentration are precisely measured over the last century, the associated radiative forcing among the American models over this period varies by at least 10 percent or a few tenths of a W/m2.

Aerosols have short lifetimes, on the order of a week or so, that prevents them from dispersing uniformly throughout the atmosphere, in contrast to well-mixed greenhouse gases. Consequently, aerosol concentrations have large spatial

variations, which are currently not measured with sufficient detail. Global radiative forcing by aerosols has historically been estimated using physical models of aerosol creation and dispersal constrained by the available observations. Recent estimates center around -1.5 W/m2 (Anderson et al., 2003). Satellite retrievals are increasingly used to provide estimates based upon actual measurements. Estimates range from 0.35 0.25 W/m2 (Chung et al 2005) to -0.5 0.33 W/m2 (Yu et al 2006) to -0.8 0.1 W/m2 (Bellouin et al 2005). That these estimates do not overlap suggests that there are assumptions that are not represented in the formal uncertainty analysis of each study. In particular, each calculation must decide how to extract the anthropogenic fraction of aerosol within each column. Because aerosol species are not retrieved directly, and the instruments cannot identify the original source region, this extraction is uncertain. In the absence of species identification, the optical properties used in the calculation of radiative forcing are also imprecisely known. Future satellite instruments will identify aerosol type with greater accuracy, improving the forcing estimates.

For now, global forcing by aerosols is estimated by the IPCC AR4 as -0.2 +/- 0.2 W/m2, according to models, and -0.5 +/- 0.4 W/m2, based upon satellite estimates. This represents increased certainty compared to the 2001 IPCC estimate of -0.9 +/- 0.5 W/m2. However, this represents only the direct radiative forcing by aerosols: that is, the change in the radiative fluxes through scattering and absorption of photons by aerosol droplets or particles. Aerosols also act as cloud condensation nuclei, and alter radiative forcing by clouds. For example, an increase in aerosol number increases the condensation nuclei available for cloud droplet formation, which has the potential to increase cloud droplet number. If the total cloud water is unchanged by the aerosols, the cloud will nonetheless be brighter because a larger number of smaller cloud droplets provides a larger cross-sectional area for reflection of sunlight. This is the first aerosol indirect effect (Twomey 1977). Smaller cloud droplets slow the coalescence and growth of rain droplets, reducing precipitation efficiency and extending the cloud lifetime: the

second aerosol indirect effect (Albrecht 1989). Aerosol changes to cloud droplet density can also alter dynamical mixing within the cloud, affecting cloud cover and lifetime (Ackerman et al, 2004). Because of the complex interactions between aerosols and dynamics along with cloud microphysics, the aerosol indirect effect is very difficult to measure directly, and model estimates vary widely. This effect was generally omitted from the IPCC AR4 models, although it was included in GISS modelE where it increased cloud cover corresponding to twentieth century forcing of -0.87 W/m2 (Hansen et al 2007). This negative forcing is the most obvious reason that the total twentieth-century forcing in the GISS model is smaller compared to GFDL despite the larger greenhouse gas forcing in the former (Table 1).

Other model forcings include variability of solar irradiance and volcanic aerosols. Satellites provide the only measurements of these quantities at the top of the atmosphere. Prior to the satellite era in the 1970's, solar variations are inferred using records of sunspot area and number (Foukal et al 2006), which are converted into irradiance variations using an empirical relation. The American models all use the solar reconstruction by Lean et al (1995) with subsequent updates. Prior to the satellite era, volcanic aerosols are inferred from measurements of aerosol optical depth. The radiative calculation requires aerosol amount and particle size, which is inferred using empirical relations with optical depth derived from recent eruptions. The GFDL and GISS models use updated versions of the Sato et al (1993) eruption history, while NCAR uses Ammann et al (2003).

Satellite measurements indicate increasing absorption of longwave radiation at the top of the atmosphere by greenhouse gases during recent decades (Harries et al 2001). Nonetheless, the total radiative imbalance at the top of the atmosphere, summed over all wavelengths, which is related to the global net forcing and global surface temperature response, is currently too small to be measured directly, necessitating the use of first principle calculations (in the case of

greenhouse gases) or models with a larger empirical component (as for aerosols).

In general, we note that comparison of radiative forcing during the twentieth century IPCC AR4 runs is difficult because of incomplete documentation currently provided by the modeling groups. Moreover, there are different definitions of forcing, depending upon whether the stratosphere or troposphere is allowed to adjust (Hansen et al 2005), although differences in the resulting estimates are usually slight. Nonetheless, an important step toward understanding differing estimates of twentieth century temperature change would be to document more completely the various contributions to the total radiative forcing.

Table 1: Contributions to radiative forcing (W/m2) in the twentieth century in GISS modelE (1880-2003), GFDL CM2.1 (1861-2000), and NCAR.

	GISS	GFDL	NCAR
GHG	2.50		
Ozone	0.28		
Tropos Aerosols (direct)	-0.38		
Tropos Aerosols (indirect)	-0.87	-	-
Strat Aerosols	0.00		
Solar	0.24		
Snow Albedo	0.05		
Land Use	-0.09		
All together	1.77	2.8	

Water Vapor Feedback

The simulation of the water vapor distribution in the atmosphere is central to many aspects of climate modeling, including climate sensitivity. Analysis of the radiative feedbacks in the PCMDI/AR4 database (Soden and Held, 2006). reaffirms that water

vapor feedback, the increase in infrared opacity due to the increase in water vapor as the climate warms, is fundamental to the responses in those models to increases in carbon dioxide. The strength of the water vapor feedback in these models is typically close in magnitude but slightly weaker than that obtained by assuming that relative humidity, H, remains unchanged as the climate warms. When the interaction with other temperature-dependent feedbacks are considered, water vapor feedback of this strength increases the climatic sensitivity of a typical model by at least a factor of two (Held and Soden, 2000).

A trend towards increasing column water vapor in the atmosphere consistent with model predictions has been documented from microwave satellite measurements (Trenberth, et al, 2005). These studies increase confidence in the model's vapor distributions more generally, but they do not directly address the water vapor feedback issue. Due to the particular radiative characteristics of water vapor, this feedback is primarily a consequence of increases in water vapor in the tropical upper troposphere. Studies of vapor trends in this region are therefore of central importance. Soden (2006) presents analysis of radiance measurements (from the infrared sounder on the NOAA xx satellites) that relative humidity H has remained unchanged in the upper tropical troposphere over the past xx yrs, which combined with MSU temperature measurements, provides our best evidence that water vapor in this region is increasing.

One can use observations of interannual variability in water vapor to help judge the value of model simulations. Recently, Minchswaner, Dessler, and Sawaengphokhai (2006) have compared the interannual variability in humidities in the highest latitudes of the tropical troposphere, as measured by infrared limb sounding satellites, with PCMDI/AR4 20^{th} century simulations. Both models and observations show some negative correlation between H and tropical temperatures, due to in large part to a tendency for H in the relatively warm El-Nino years and higher values in cold La Nina years. However, there is a suggestion that the magnitude of this co-variation is underestimated in most of the models. Looking across the models, there is also a tendency for models with larger interannual variations in H to also produce larger reductions in H in this region in response to global warming, suggesting that this deficiency in interannual variability

might be relevant for climate sensitivity. This study provides indirect evidence that the strength of water vapor feedback might be overestimated t in models, but the part of the atmosphere sampled directly by this technique produces only a small fraction of the global feedback.

The potential for the uncertainties in cloud feedbacks to impact water vapor feedbacks in the tropics, through evaporation of condensate, remains under discussion (Lindzen-IRIS). But analyses examining the extent to which tropical humidities can be understood without considering sources from condensate (Sherwood, Dessler) continue to suggest that effect of this kind are small.

The CMIP-3/IPCC simulations of the water vapor climatology have also been critically analyzed (Pierce et al, 2006 (GRL), others). Despite uncertainties in the observations, some systematic deficiencies are clear, especially a tendency towards too much humidity in middle latitudes in the midtroposphere. This is a plausible consequence of the too low resolution in climate models, but the relevance of this deficiency for climate sensitivity remains unclear.

Chapter V: Model simulation of major climate features

A. Mean climate

Monthly mean near-surface temperature is well simulated by modern OGCMs. This success occurs despite the freedom of models to "choose" their surface temperatures. Most of these models now allow the ocean and atmosphere the to exchange heat and water without explicitly forcing agreement with observation by artificial adjustment to air-sea fluxes (i.e. without "flux adjustment"). The following figure quantifies the extent of agreement between simulations by several models and observations for both temperature and precipitation (the triangular points will be discussed in Chapter VI below). Each model's temperature or precipitation simulation produces a single point on the diagram, but in the figure, the range of results from all the models are shown as shaded areas:

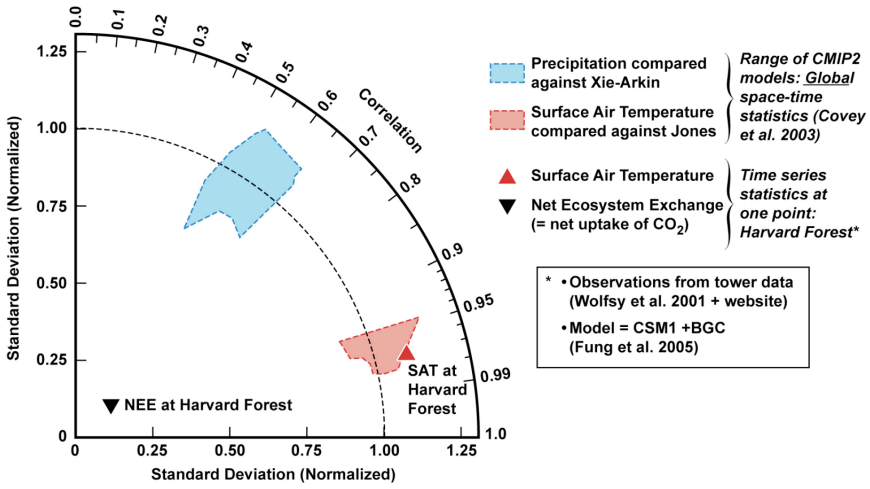

Note: This figure shows results from the CMIP2 database (Covey et al. 2003). Though it won't make much difference, we should update it using the CMIP3 database.

This type of diagram (Taylor 2001) displays the overall space-time correlation between simulated and observed variables as an angular coordinate. 100% perfect correlation would place a point along the horizontal direction to the right, while zero correlation would place a point along the upward vertical direction. Looking at the red-shaded area that depicts the range of near-surface temperature simulations, one sees a remarkable 95-98% correlation with observations. The second independent (radial) coordinate in the diagram gives the ratio of simulated to observed amplitude for the variations that are being correlated. A value of 1.0 indicates perfect agreement of the amplitudes. In this coordinate system, complete agreement between simulation and observation in both dimensions would place a point where the dashed semicircle and the horizontal line intersect. The distance from this point to the actual point for any given model is proportional to the combined root-mean-square model error in both space and time dimensions. Temperature points for all of the models lie very close to complete agreement with observation—indeed nearly within the uncertainty range of the observations themselves (Covey et al. 2003).

For monthly mean precipitation, AOGCM simulations are considerably less precise than for temperature. The figure shows that overall space-time correlation between models and observations is ~50-60%. Qualitative examination of latitude-longitude maps shows that AOGCMs generally reproduce the observed broad patterns of precipitation amount and year-to-year variability (A. Dai, 2006: Precipitation characteristics in eighteen coupled climate models, J. Climate, in press). The most prominent error is that models lacking flux adjustment fail to simulate the observed northwest-to-southeast orientation of a large region of particularly heavy cloudiness and precipitation in the Southwest Pacific Ocean (the Southwest Pacific Convergence Zone or SPCZ). Instead, these models produce an unrealistic set of Inter-Tropical Convergence Zones in two parallel lines straddling the Equator: a "double ITCZ" pattern. The double-ITCZ error has been frustratingly persistent in climate models despite much effort to correct it, including intensive

discussion between the CCSM and GFDL climate modeling groups in the The average day-night cycle of temperature and precipitation in AOGCMs exhibits general agreement with observations, although simulated cloud formation tends to start too early in the day. Another discrepancy between models and observations appears upon sorting precipitation into light, moderate and heavy categories. Models reproduce the observed extent of moderate precipitation (10-20 mm / day) but underestimate the extent of heavy precipitation and overestimate the extent of light precipitation (Dai 2006). Additional model errors appear when precipitation is studied in detail for particular regions, e.g. within the US (Ruiz-Barradas, A., and S. Nigam, 2006: IPCC's 20th Century Climate Simulations: Varied Representations of North American Hydroclimate Variability, Journal of Climate, in press).

Taking examples from two of the US model families discussed in Chapter 4, one finds that AOGCM-simulated and observed maps of surface temperature and even precipitation appear rather similar at first sight. Constructing simulated-minus-observed "difference maps," however, reveals monthly and seasonal mean temperature and precipitation errors up to ~10°C and 7 mm / day respectively at some points (W. Collins et al. 2006 Figs. 14 and 5 [bottom] , Dellworth et al. 2006 Fig. 17):

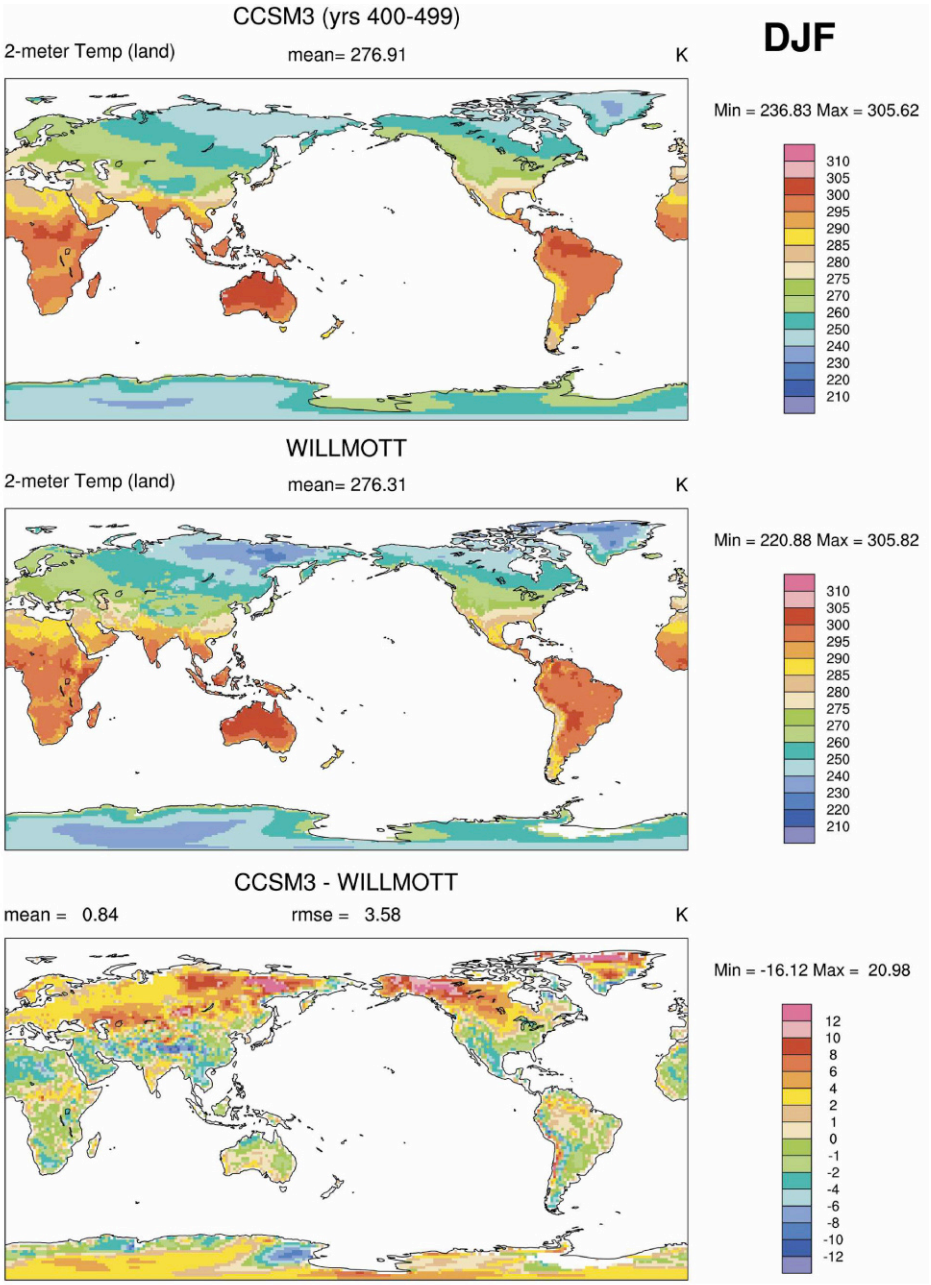

CCSM3 annual mean simulated-minus-observed sea surface temperature [°C]

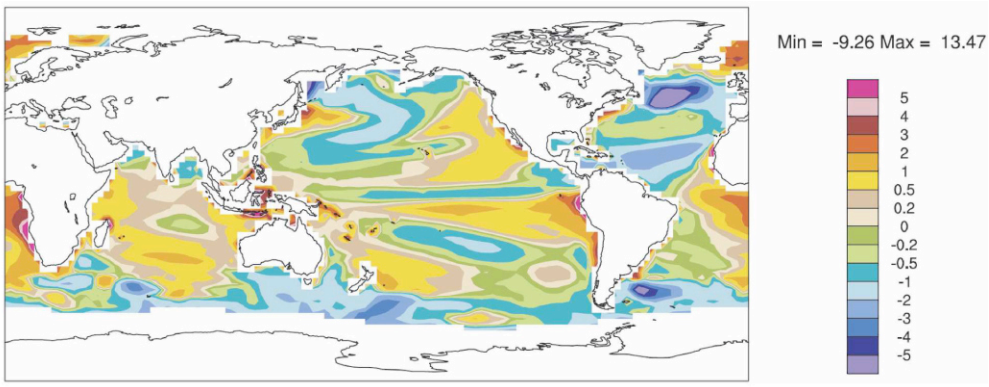

The CCSM3 temperature difference maps exhibit the largest errors in the Arctic (note scale change in last frame), where continental wintertime near-surface temperature is overestimated. AOGCMs find this quantity particularly difficult to simulate because, for land areas near the poles in winter, models must resolve a strong temperature inversion (warm air overlying cold air).

Observed and model-simulated precipitation [mm / day]

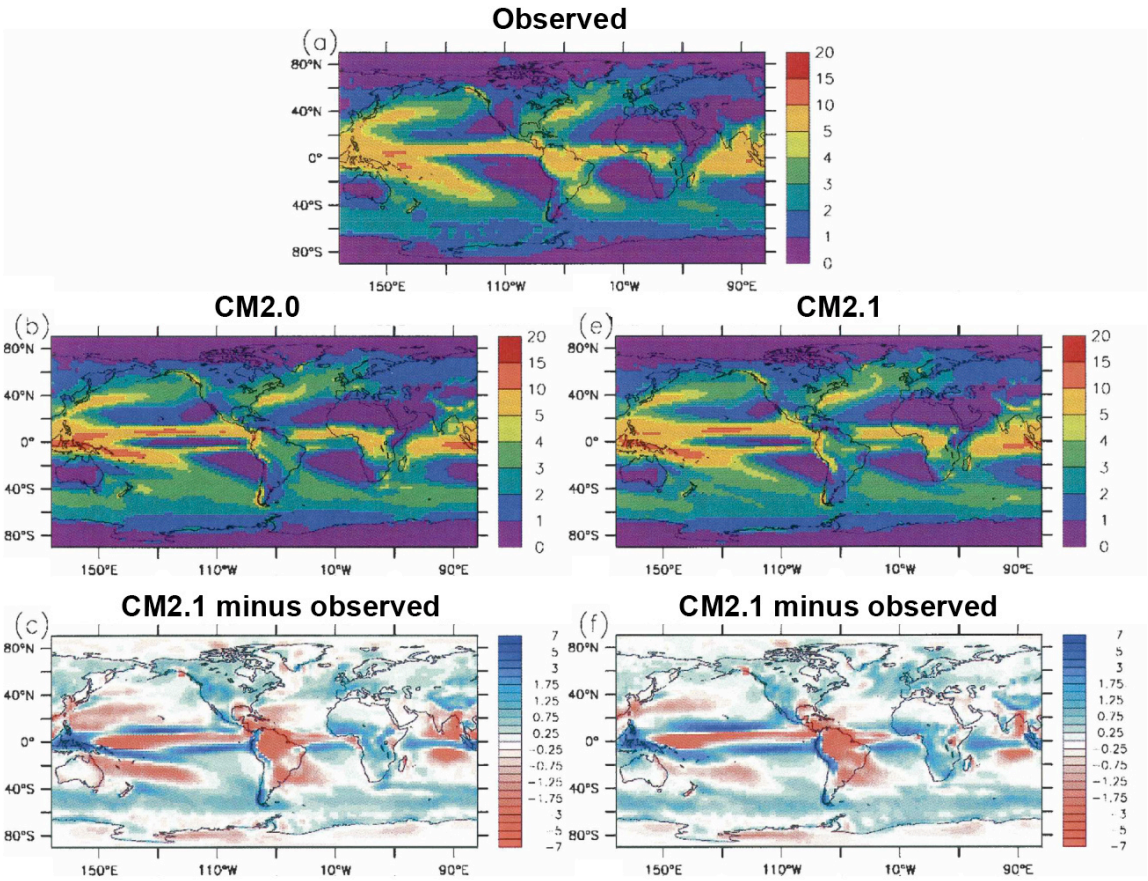

The GFDL precipitation difference maps reveal significant widespread errors in the tropics, most notably in the ITCZ region discussed above and in the Amazon River basin, where precipitation is underestimated by several millimeters per day. Similar precipitation errors appear in the following table of CCSM3 results (Collins et al. 2006 Table 2):

Region	CCSM3-simulated precip	Error
Southeast USA (30-40°N, 80-100°W)	2.4 mm / day	−24%
Amazon basin (10°S-10°N, 60-80°W)	4.5 mm / day	−28%
Southeast Asia (10-30°N, 80-110°E)	3.1 mm / day	−24%

AOGCM precipitation errors have serious implications for "Earth system" models with interactive vegetation, because such models use the simulated precipitation to calculate plant growth (see Chapter VI below). Errors of the magnitude shown above would

produce an unrealistic distribution of vegetation in an Earth system model, e.g. by spuriously deforesting the Amazon basin.

To sum up: modern AOGCMs generally simulate large-scale mean climate with considerable accuracy, but the models are not reliable for aspects of mean climate in some regions, especially precipitation.

B. 20th century trends

Modern AOGCMs are able to simulate not only the time-average climate but also changes (trends) of climate during over the past century or more. For example, the following figure shows results from one model featured in the IPCC Third Assessment Report (Summary for Policymakers, Houghton et al. 2001):

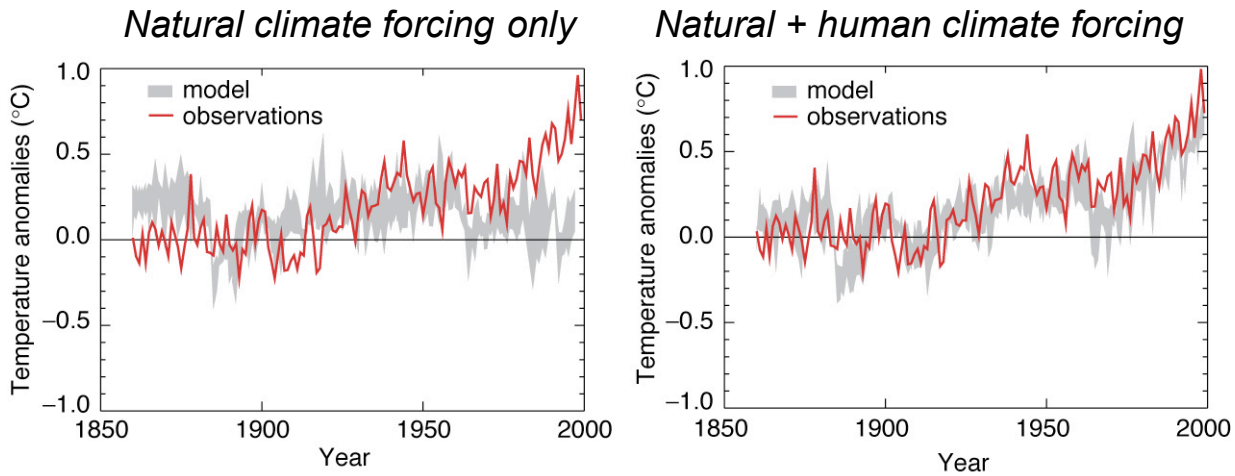

The figure shows globally averaged near-surface temperature over the period 1850-2000 as observed (red line) and as modeled under a variety of initial conditions (gray shading). The precise initial conditions, especially deep ocean temperature and salinity, are not known for 1850. The width of the gray band thus indicates uncertainty in model-simulated temperature arising from our lack of knowledge of initial conditions. Both left- and right-hand sides of the figure show the same observations. The model simulations on the left include natural climate forcing from solar energy output variations and volcanic eruptions. Those on the right also include human-caused (anthropogenic) changes in atmospheric greenhouse gases—mainly carbon dioxide and methane—and pollutants like sulfate aerosols. Comparison of the two sides of the figure makes it obvious that including anthropogenic effects in the model leads to much better agreement with observation. In particular, global warming during the past few decades is successfully simulated by the model, but only if it takes anthropogenic emissions of greenhouse gases and aerosols into account.

The results shown above for one model generalize to the entire set of AOGCMs used in the most recent IPCC assessment. Models typically exhibit good agreement with observed near-surface temperature trends not only for the global mean (Min, S.-K., and A. Hense, 2006: A Bayesian assessment of climate change using multi-model ensembles.

Part I: Global mean surface temperature, Journal of Climate 19: 3237-3256) but also for most individual continents (Min, S.-K., and A. Hense, 2006: A Bayesian assessment of climate change using multi-model ensembles. Part II: Regional and seasonal mean surface temperature, J. Climate, in press). At smaller scales the model simulation of trends is less accurate. For example, model-simulated trends do not consistently match the observed lack of 20th century warming in the central US (Kunkel, K.E., X.-Z. Liang, J. Zhu, and Y. Lin, Can CGCMs simulate the Twentieth Century "warming hole" in the central United States, Journal of Climate, in press). Observed trends in climate extremes such as heat-wave frequency and frost-day occurrence are also simulated with basic reliability by the latest generation of AOGCMs (Tebaldi, C., K. Hayhoe, J.M. Arblaster, G.A. Meehl, 2006: Going to the extremes: An intercomparison of model-simulated historical and future changes in extreme events, Climatic Change, in press).

The US AOGCMs again provide examples of the general model behavior discussed above. All three produce time series of 20th century global mean near-surface temperature very similar to the figure above. Furthermore, the longitude-latitude map of trends from GISS Model E agrees reasonably well with the observed spatial distribution (Hansen et al. 2006 Fig. 11):

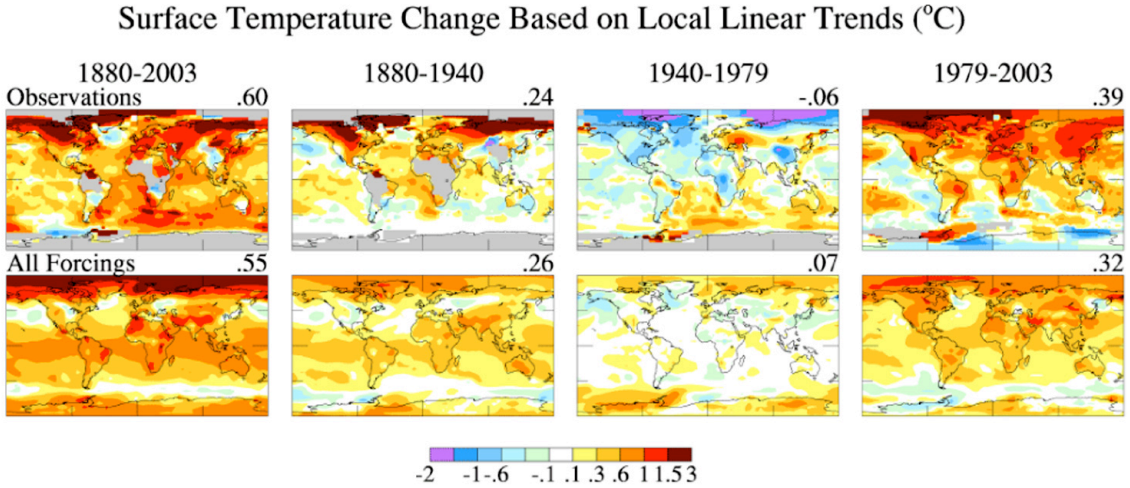

The figure shows general agreement between the model and observations not only for the overall period 1880-2003, but also for the segments 1880-1940 and 1979-2003, which encompass periods of early and late 20th century warming. Amplification of warming and cooling at high northern latitudes is the most obvious feature in the observations. For the period 1940-1979, the model simulates only a small change in global mean temperature in agreement with observations, but it fails to simulate the strong north polar cooling observed for this period. As a result, the model-simulated global mean temperature change (upper right corner of each frame) for 1940-1979 is slightly positive rather than slightly negative as observed. For both 20th century warming periods, the model simulates but underestimates the high-latitude amplification of global warming.

Finally, the CCSM3 simulates 4.7 cm of global mean sea level rise during the 20th century (Meehl et al. 2006). The actual value of sea level rise is 3-5 times as large, but the model does not include melting glaciers and ice sheets, and therefore it simulates only the part of sea level rise due to expansion of ocean water from heating.

Annular Modes

The simulated annular patterns during the late twentieth-century are highly correlated with the observed spatial pattern of sea-level pressure, though the modes represent too large a percentage of total temporal variability within each hemisphere (Miller, et al 2006). In response to increasing concentrations of greenhouse gases and tropospheric sulfate aerosols in the 20th century, the multi-model average exhibits a positive annular trend in both hemispheres, with decreasing sea-level pressure (SLP) over the pole and a compensating increase in mid-latitudes. However, the models underestimate the coupling of stratospheric changes (from volcanic aerosols) to annular variations at the surface, and may not simulate the full response to increasing GHGs)

Ocean structure and circulation

A set of ocean characteristics or metrics (sea surface temperature, ocean heat uptake, meridional overturning and ventilation, sea level variability and global sea level rise) is used to describe the realism of the ocean in the climate models.

Sea surface temperature: The sea surface temperature (SST) plays a critical role in the determination of the climate and the predictability of the changes. In general, when the simulated fields of SST are compared to observational fields there is improvement in the models' representation of the mean SST. *Delworth et al*. [2006] (**see their Figure 2**) compares the CM2.0 and CM2.1 mean SST field averaged over a period of 100 years to the Reynolds SST observational climatology. With an improved atmospheric core and a different viscosity parameter value, the later version (CM2.1) of the GFDL climate model produces a reduced cold bias in the northern hemisphere. The CCSM3.0 model also has improved its simulation of SST primarily in the handling of the processes associated with the mixed layer of the upper ocean waters [*Danabasoglu et al*. 2005]. The improvement in the representation of the SST is apparent especially in the eastern tropical Pacific [**see Figure 5 in *Collins et al.* 2006**]. An inter-model comparison of the 50 year global SST trend for each model is shown in *Zhang and McPhaden* [2006] [**Their Figure 15**]. The SST trends range from a low of 0.1°C/50yrs to a high of about 0.6°C/50yrs, with the observational trend estimate given as about 0.43°C/50yrs. The figure also shows that within a group, the estimates significantly vary. This distribution of values in SST trends shows that improvements in any model's representation of SST are dependent on both advances in the ocean and atmospheric components.

Meridional overturning circulation and ventilation: The circulation process related to the transportation heat and freshwater throughout the global oceans is referred to as thermohaline circulation. The Atlantic portion of this process is called the Atlantic meridional overturning circulation (AMOC). Tropical and warm waters flow northward via the Gulf Stream and North Atlantic Current and these waters are important for keeping Europe relatively warm. The southward flow occurs when water is sub-ducted in the regions of the Labrador Sea and Greenland Seas and occurs when the freshening of the surface waters become denser and flow down the slope to deeper depths. Similar processes occur at locations in the Southern Ocean. Ventilation is the process by which

these dense surface waters are carried into the interior of the ocean. The important climate parameter is the rate at which this process occurs, the so-called "ventilation rate". It has been suggested that this pattern of circulation if it becomes weaker (i.e. less warmer water flowing towards Europe) will impact the climate. It is thus important to understand how well the ocean component simulates the observed estimates of these overturning processes.

Schmittner et al. [2005] examined the performance of the models in reproducing the observed meridional overturning in 4 of the 5 US models. The authors examined a small ensemble set of simulations to quantify the uncertainty in the models' representation of 20th century AMOC transports. To make their estimate, they evaluated the global temperature (T), the global salinity (S), the pycnocline depth (D), the surface temperature and surface salinity in the Atlantic (SST, SSS), and calculations of the overturning at 3 locations ~in the Atlantic. Their results suggest that temperature is simulated the most successfully on the large scale and that the overturning transports at 24°N are close (~18Sv) to the observed measurements (~15.8Sv). However, the maximum mean overturning transports in these models are too high (23.2, 31.7, 27.7, and 30.9 Sv: *Schmittner et al*. [2005] and 21.2 Sv from *Bryan et al.* [2006]) than the observed value (17.7 Sv). Table 1 shows a reduced version of Table 1 from *Schmittner et al*. [2005] that shows the root mean errors (RMS) for the various quantities as compared to observations. The authors do not attempt to explain why the models are different from each other and from observations, rather, that there is a broad range in the value of these metrics for a set of climate models.

Table 1

Model	T_{global}	S_{global}	D_{global}	SST_{NAtl}	SSS_{NAtl}	D_{NAtl}	$AMOC_{24N}$ (15.8) (SV)
GFDL-2.0	0.20	0.43	0.57	0.34	0.53	0.75	0.16 (18.3)
GISS-AOM	0.66	0.75	2.29	0.43	0.79	3.48	0.22 (19.2)

GISS-EH	0.31	0.76	1.57	0.61	1.12	1.85	0.34 (21.1)
GISS-ER	0.69	0.82	2.06	0.65	1.11	2.40	0.13 (17.9)

From Schmittner et al. [2005] Table 1. RMS Errors for the Individual Models; RMS errors are normalized by the standard deviation of the observations unless otherwise stated. *Schmittner et al*. 2005; "Observation-based estimates of the AMOC at 24 N from *Ganachaud and Wunsch* [2000] *and Lumpkin and Speer* [2003], at 48 N from *Ganachaud* [2003], and its maximum value in the North Atlantic from *Smethie and Fine* [2001] *and Talley et al.* [2003], as well as temperature, salinity, and pycnocline depth observations from the World Ocean Atlas 2001 [*Conkright et al*., 2002] are used to evaluate the climate models."

The global overturning circulation can also be quantified by also examining the realism of the transports through the Drake Passage. The passage, between the tip of South America and the Antarctic Peninsula provides a constrained passage to measure the flow between two large ocean basins. The observed mean transport is around 135 Sv. *Russell et al.* [2006] estimate the flow in the passage for a subset of the climate models (Table 2). There is a wide range in the simulated mean values. The interaction between the atmospheric and ocean component models appears to be important in reproducing the observed transport. The strength and location of the zonal wind stress correlates with how well the transport reflects observed values.

TABLE 2

Model	ACC (Sv)	$d\rho/dy$ (kg m^{-3})	Total τ_x 10^{12} N	Max τ_x (N m^{-2})	Lat of max τ_x
Observational estimate	135	0.58	6.5	0.161	52.4
GISS-ER	266	0.62	4.3	0.107	46.0
GISS-AOM	202	0.38	2.9	0.166	43.5
GFDL-CM2.1	135	0.58	6.1	0.162	51.0

GFDL-CM2.0	113	0.56	4.5	0.149	46.0
GISS-EH	-6	0.43	3.6	0.096	46.0

Reduced From Table 1 *Russell et al.* [2006] Various parameters related to the strength of the ACC. The ACC transport is the integral of the zonal velocity across the Drake Passage at 69°W. The density gradient (d/dy) is the zonally averaged density difference between 65° and 45°S. The total ACC-related wind stress (total) is the integral of the zonal wind stress over the Drake Passage channel (54°–64°S). The maximum westerly wind stress (max) is the maximum of the zonally averaged wind stress that is located at the latitude given by Lat max. The observed ACC strength is from *Cunningham et al.* (2003). The observed density gradient is calculated from the World Ocean Atlas 2001 (*Conkright et al.* 2002). The observed wind data are from the NCEP long-term mean *(Kistler et al.* 2001). NA indicates data not archived at PCMDI

Tropical Pacific Ocean: On scales of years to decades, the tropical ocean varies significantly. The climate changes related to the El Nino – Southern Oscillation events (ENSO) are well-known to effect local weather, ecosystems, and parts of our socio-economic life [e.g. *McPhaden et al.* 1998]. It is necessary to understand how the climate models perform in reproducing the observed variability of the tropical ocean to understand the uncertainty in future estimates of these phenomena. Several recent papers have analyzed the performance of the current generation of climate simulations with a focus on the tropical ocean. *van Oldenborgh, et al.* [2005] show that the periodicities of the ENSO events are reasonable (but trend to being too short), while the amplitude and skewness of the events vary widely. From their analyses, the simulations at resolutions smaller than 3° are able to better represent the ENSO pattern than those at the lowest resolutions (Table 3). Similarly, *Capotondi et al.* [2006] found the average dominant interannual timescale to be somewhat shorter than observed. In addition, it was found that the location where the variability is the maximum and meridional extent of it is significantly correlated with a particular model's zonal wind stress pattern. This relationship is consistent with observations. *Zhang and McPhaden* [2006] examined the interaction between the tropical and subtropical Pacific within the present climate models. Observations have shown that measurements of transports in the central and eastern Pacific are inversely correlated with SST implying a link between the shallow meridional

overturning component of the subtropical cell and tropical SST. [*McCreary and Lu*, 1994]. While the models show a significant correlation of the two quantities, the variability is underestimated. While there are still discrepancies between these climate models and observations, significant improvement has been made in the models' representation of the tropical ocean and ENSO variability. It is important to note that the non-physical corrections to the surface fluxes made in previous generations of climate models are no longer required with the improvements that have been incorporated within this generation of models.

Table 3

Analysis/model	Pattern	Period (yr)	Amplitude	Skewness
SSTOIv2/Kaplan	**160 W–<90 W**	**2.5–6**	**0.25**	**0.54**
CCSM3	160 W–100 W	2–2.5	0.22	–0.06
GFDL-CM2.0	175 E–115 W	1.5–3.5	0.32	0.14
GFDL-CM2.1	180 –105 W	2–6	0.39	0.31
GISS-AOM	140 E–<90 W	1–10	0.09	–0.01
GISS-EH	150 W–100 W	1.5–4	0.16	–0.20
GISS-ER	170 W–<90 W	2.5–8	0.07	–0.18

From: von Oldenborgh et al. 2006 Table 2. Only US models listed "Properties of the first EOF and associated time series (PC) of detrended monthly SST in the region 10°S–10°N, 120°E–90°W. The pattern denotes the longitudes of the contour of 80% of the peak value, the period denotes the height of the power spectrum at 50% of the peak value." Bold line is the observational data. Skewness is defined as quantity to determine whether SST are larger during an El Nino than during the La Nina phase. "

Northward Heat Transport: A common metric used to quantify the realism in ocean models is the northward transport of heat. This integrated quantity (from top to bottom and across latitude bands) gives an estimate of how heat moves within the ocean and is important in balancing the overall heat budget of the Earth. The calculations for the ocean's northward heat transport in the current generation of climate models show that

the models reasonably represent the observations [*Delworth et al*. 2006, *Collins et al*. 2006, and *Schmidt et al*. 2006 **- It would be nice to see these figures --- see figures at end -- combined, if possible**]. The current models have significantly improved over the last generation (IPCC TAR) in the Northern Hemisphere. Comparisons of the simulated values to the observed values for the North Atlantic are within the uncertainty of the observations. In the Southern Hemisphere, the comparisons in all the models are not as good, with the Indian Ocean transport estimates contributing to a significant part of the mismatch.

Heat Content: Related to the heat transport is the ocean's heat content itself. This can be thought of how realistically the models reproduce the uptake of heat. An evaluation of the temporally evolving ocean heat content in the suite of climate models for the AR4 shows the models abilities to simulate the zonally integrated annual and semi-annual cycle in heat content. In the middle latitudes [*Gleckler et al.* 2006], the models do a reasonable job while there is a broad spread of values for the tropical and polar regions. This analysis showed that the models replicate the dominant amplitude of the annual cycle along with its phasing in the mid-latitudes **[figures 1 & 3 From Gleckler**]. At high latitudes, the comparisons with observations are not as consistent. While the annual cycle and global trend are reproduced, analyses of the models [e.g. *Hansen et al.* 2005] show that they do not simulate the decadal changes in estimates made from observations [*Levitus et al.* 2001]. Part of the difficulty of comparisons at high latitudes and at long periods is the paucity of observational data [*Gregory et al.* 2004].

Global mean sea level rise: Two separate physical processes contribute to the sea level rising: 1) the thermal expansion of the ocean from an increase in the heat uptake by the ocean (steric component) and 2) the addition of freshwater from precipitation, continental ice melt, and/or river runoff (the eustatic component). The current ocean component of all the models except the NASA GISS models, conserve volume. In practice, the first component can be easily computed from a model's primary variables. The second contribution maybe considered as a freshwater flux into the ocean. The various ocean models handle the process in different ways. With the addition of a free surface in the

current generation of ocean models, the freshwater flux into the oceans can be included directly [*Griffies et al*. 2001]. In other cases, the mass or freshwater contribution is computed by quantities estimated by land/ice sheet components of the climate model [e.g. *Church et al.,* 2005, *Gregory et al.*, 2006]. In general, the state-of-the-art climate models underestimate the combined global mean sea level rise as compared to tide gauge and satellite altimeter estimates while the rise for each of the separate components is within the uncertainty of the observed values. The reason for this is an open research question and may relate to either observational sampling or not correctly accounting for the all the eustatic contributions. The steric component to the global mean sea level rise is estimated to be 0.40+/-0.05mm/yr from observations [*Antonov et al.* 2005]. The models simulate a similar, but somewhat smaller rise [*Gregory et al.*, 2006, *Meehl et al.* 2005]. There are also significant differences in the magnitudes of the decadal variability between the observed and the simulated sea level or SSH. It most be noted, however, that progress is been made over the previous generation of climate models. When atmospheric volcanic contributions are included, for example, ocean models of the current generation capture the observed impact on the ocean (a decrease in the global mean sea level). **Figure xx from *Church et al*. 2006** gives an example of a few models and their de-trended estimate of the historic global mean sea level that shows the influence of including the additional atmospheric constituents in changing the steric height of the ocean.

Delworth et al. 2006 Figure 2

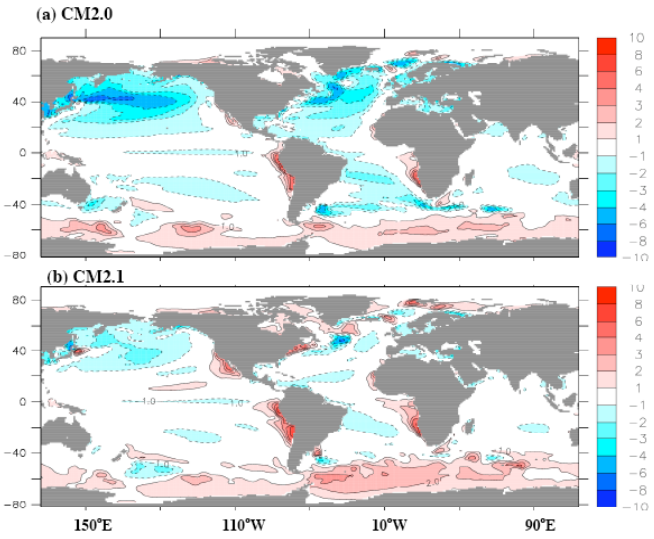

Fig. 2 Maps of errors in simulation of annual mean sea-surface temperature (SST). Units are K. The errors are computed as model minus observations, where the observations are from the ReynoldsSST data (provided by the NOAA-CIRES Climate Diagnostics Center, Boulder, Colorado, USA, from their Web site at http://www.cdc.noaa.gov/). (a) CM2.0 (using model years 101-200). (b) CM2.1 (using model years 101-200). Contour interval is 1K, except that there is no shading for values between 1 K and +1 K.

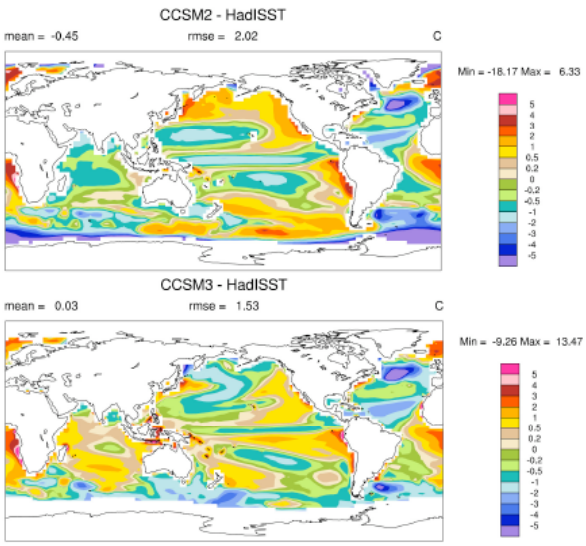

From Collins, et al 2006 Figure 5

Differences in annual-mean surface temperature between CCSM2 and the HadISST data set

(Rayner et al. 2003) (top); corresponding differences for CCSM3 (bottom).

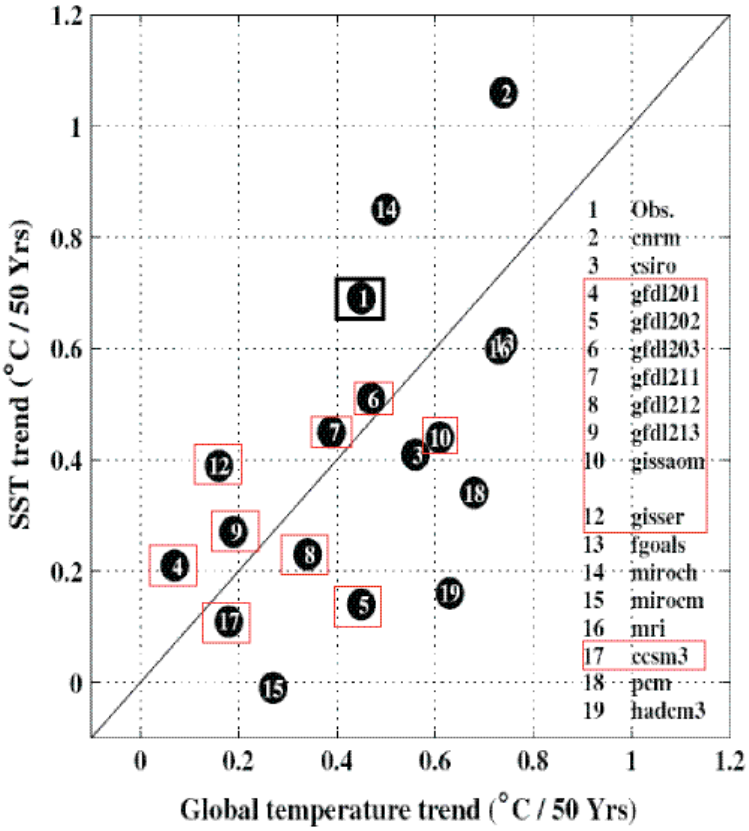

From Fig. 15. Zhang & McPhaden, 2006)

Scatter plot of the SST trends averaged in the central and eastern tropical Pacific (9 S–9 N and 90–180 W), and global mean surface temperature trends. Correlation of the model results is 0.58, of higher magnitude than the 95% significance level of 0.46. The 1:1 line is drawn for clarity.

[RTT] The red boxes denote US Climate models and the black box is the relationship computed from observations.

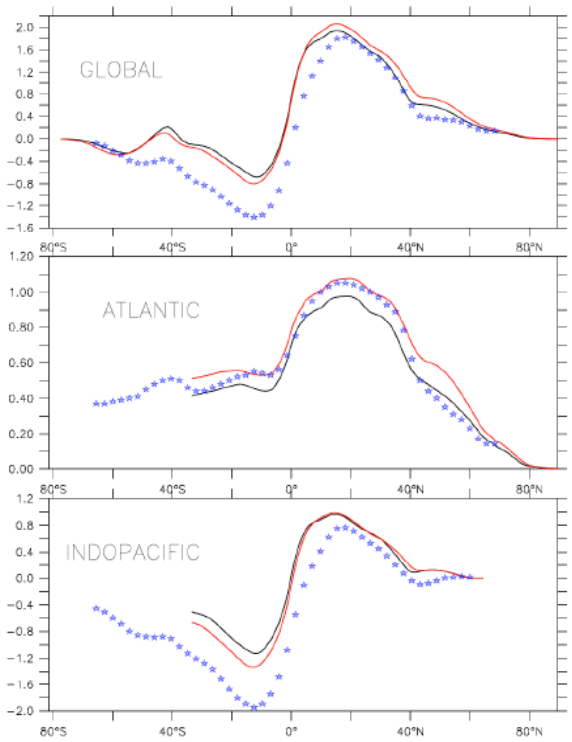

Fig. 11 Simulated northward oceanic heat transport. Units are Petawatts (10^{15} W). Black line is for CM2.0 1990 control integration, and red line is for CM2.1 1990 control integration. Asterisk symbols denote observational estimates based on Trenberth and Caron (2001).

1

2 **Above from *Delworth et al. 2006***

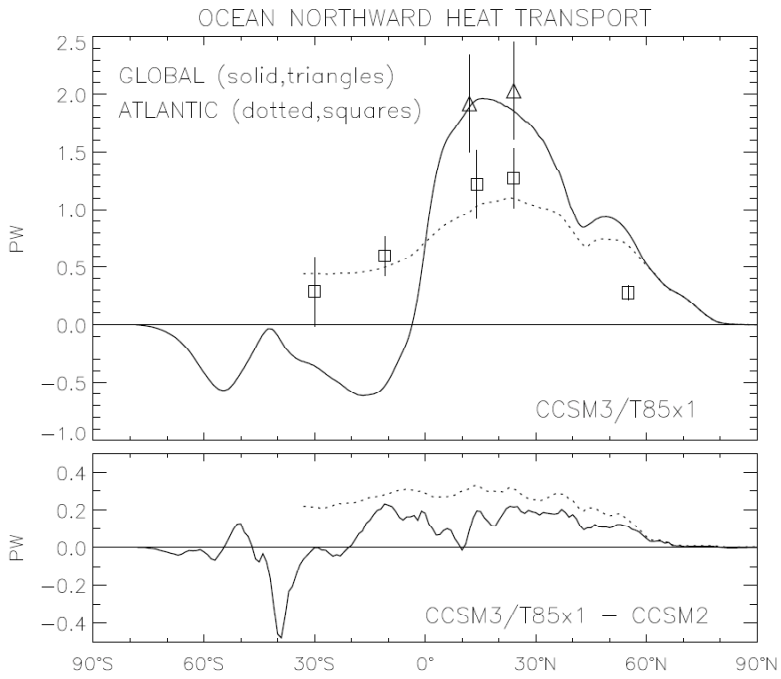

From Collins et al 2006. Figure 7: Northward total transport of heat in the ocean model from integrals across the Atlantic (dotted) and around the globe (solid). The model values include the resolved and parameterized eddy components and the isopycnal diffusion. The squares and pluses are, respectively, the Atlantic and global results of individual section analyses compiled by Bryden and Imawaki (2001). Uncertainties in the observational estimates are typically +/-3 PW.

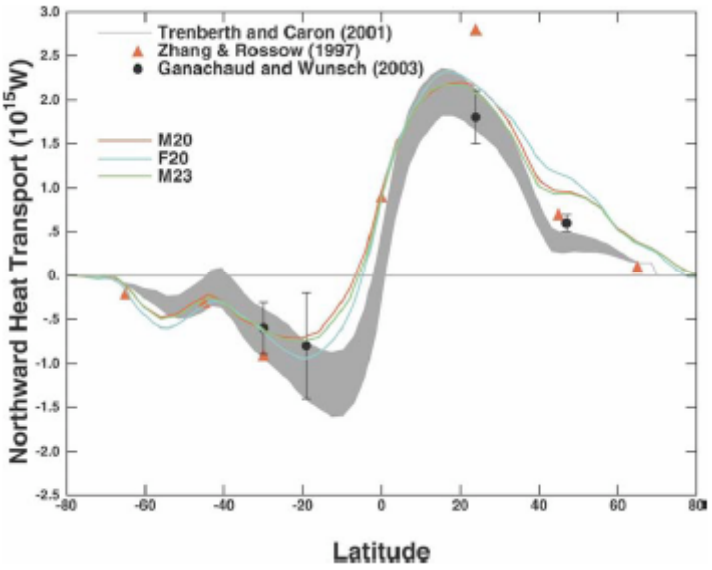

FROM Schmidt et al. 2006. FIG. 11. Implied annual mean poleward ocean heat

transports from the integrated *q* fluxes calculated from the climatological model runs and comparison with residual calculations (with error bars) from the NCEP reanalysis (Trenberth and Caron 2001), from the ISCCP remotely sensed fluxes (Zhang and Rossow 1997), and from ocean inverse calculations (Ganachaud and Wunsch 2003).

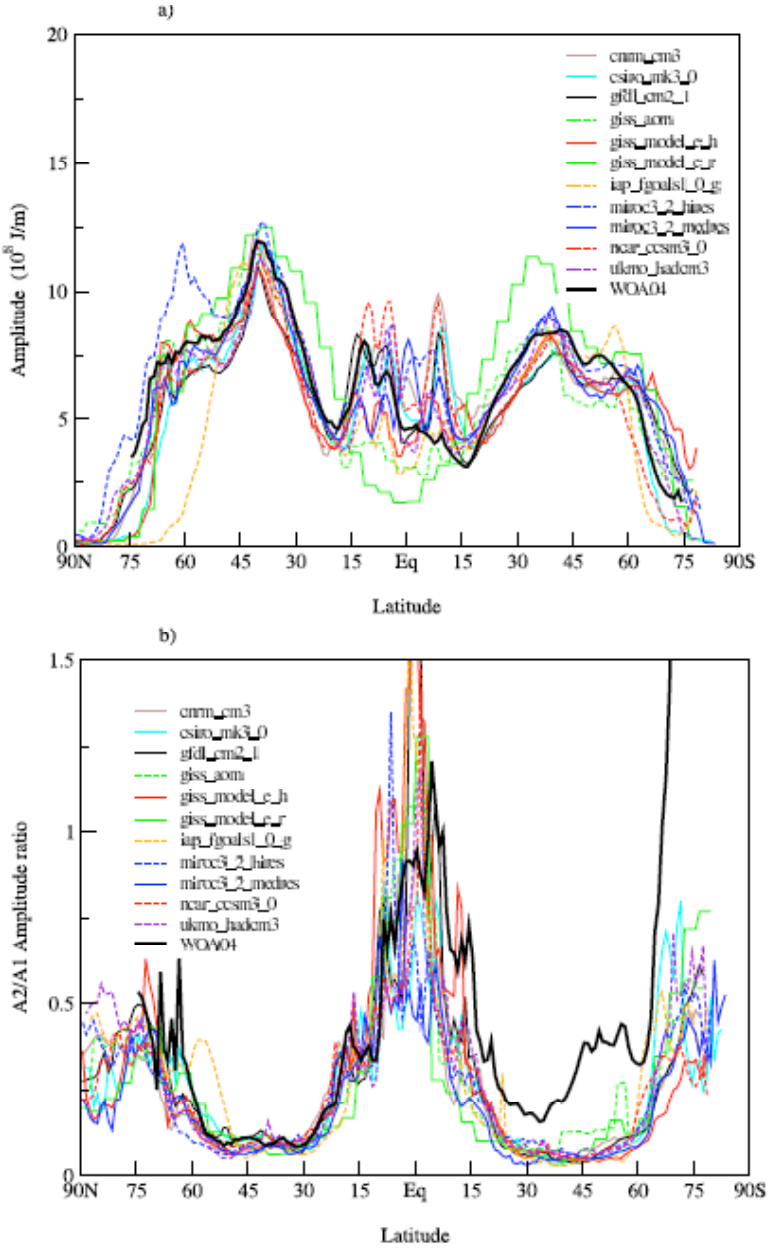

From Glecker et al. 2006 .Figure 1. Observed (WOA04) and simulated zonally integrated ocean heat content (0–250 m): (a) annual cycle amplitude (10^8J/m^2) and (b) semiannual/annual (A2/A1).

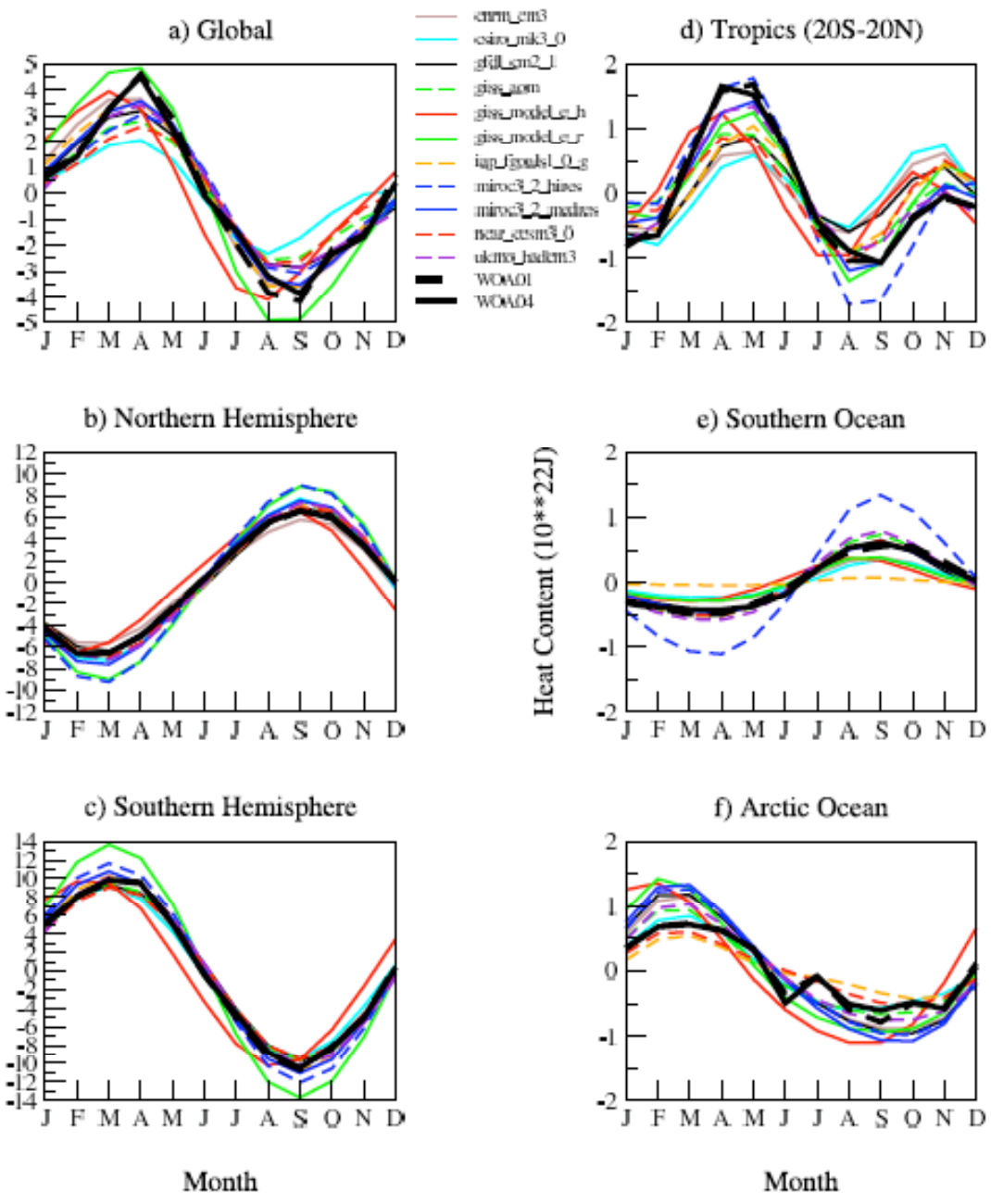

From Glecker et al., 2006, Figure 3. Annual cycle of observed (WOA04) and simulated basin average global ocean heat content (0–250 m). Units are 10^{22}J. Arctic Ocean is defined as north of 60 N, and Southern Ocean is south of 60 S.

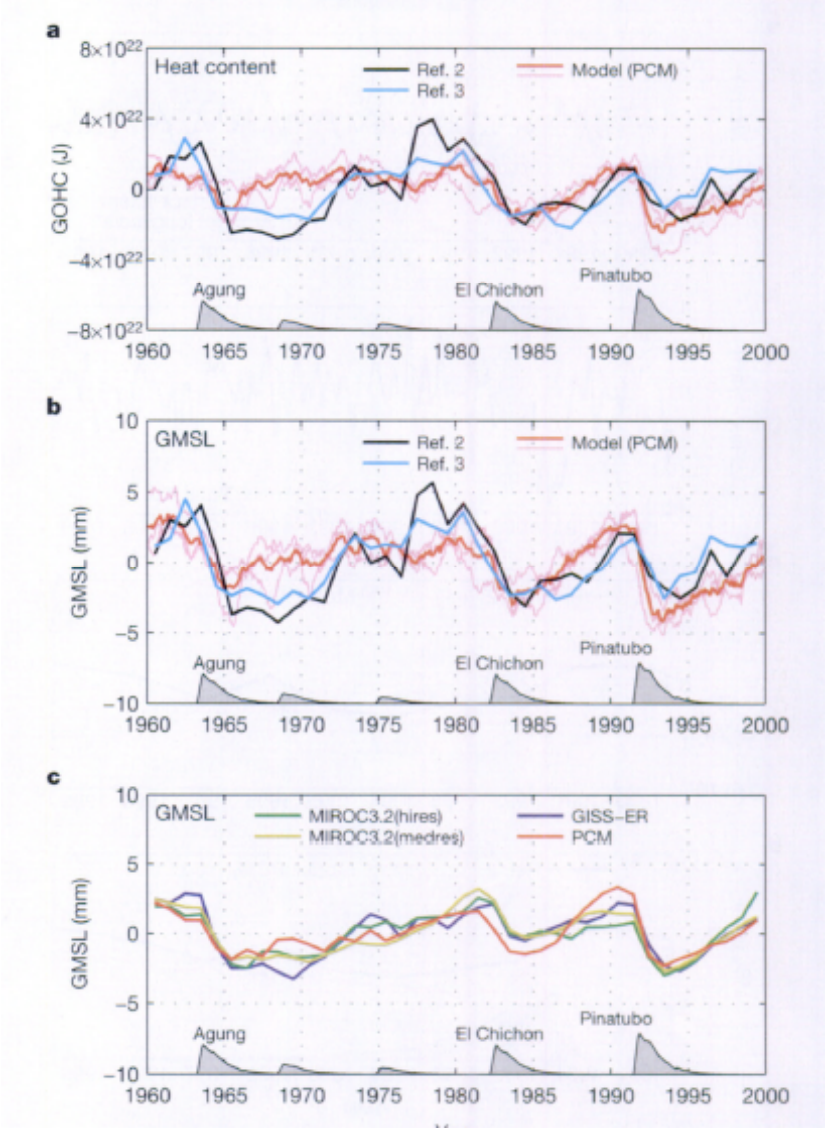

Figure 2 | Observed and modelled GOHC and GMSL for the period 1960–2000. The response to volcanic forcing, as indicated by the differences between the pairs of PCM simulations for GOHC (**a**) and the GMSL (**b**) is shown for the ensemble mean (bold line) and the three ensemble members (light lines). The observational estimates[2,3] of GOHC and GMSL are shown by the black and blue bold lines. For **a** and **b**, all results are for the upper 300 m only and have been detrended over the period 1960–2000. **c**, The ensemble mean (full depth) GMSL for the GISS-ER, MIROC3.2(hires), MIROC3.2(medres) and the PCM models (after subtracting a quadratic) are shown.

[From *Church, et al*, 2005]

C. Simulation of specific climate dynamical features

Monsoons

Meteorologists define the monsoon as a seasonal circulation driven by a temperature contrast between land and an adjacent ocean. While the land is heated intensely during the summer, sending buoyant air aloft to condense and precipitate, the ocean is heated over a deeper layer, moderating the warming. Air is driven by this regional temperature contrast toward the warm land, where it ascends before returning offshore. Conversely, the monsoon circulation reverses during winter when the land cools more rapidly, and the temperature difference drives air out toward the warmer ocean where it rises. While a coastal sea breeze is also driven by the temperature contrast between land and ocean, the monsoon is distinguished by its continental scale. The onshore flow is so extensive that it is deflected by the Earth's rotation. Over the Arabian Sea, for example, surface air flows toward the east and northeast during the Northern Hemisphere summer, rather than traveling directly north toward the Asian continent.

The word `monsoon' derives from the Arabic word for season, and over land rain is often restricted to summer within a monsoon climate, when the circulation wrings rainfall from the moist air. While the monsoon takes its name from a language spoken by traders around the Arabian Sea, this circulation reaches far beyond the periphery of the Indian Ocean, and local cultures have their own words for the monsoon: for example, Mei-yu in China, Chang-ma in Korea, and Bai-yu in Japan. Over a billion people are dependent upon the arrival of the monsoon rains for water and irrigation for agriculture. Continental rainfall is supplied mainly by evaporation from the nearby ocean. This limits the reach of monsoon rains to the distance over which moisture can be transported onshore. Variations in the spatial extent of the monsoon from year to year determine which inland regions experience a drought.

The Asian monsoon during NH summer is the most prominent example of the monsoon circulation, dominating global rainfall during this season. However, the seasonal reversal of winds and distinct rainy season also indicate monsoon circulations in West Africa and the Amazon basin. In addition, during NH summer, air flows off the eastern Pacific Ocean toward Mexico and the American southwest, while over the Great Plains of the United States, moisture from the Gulf of Mexico brings an annual peak in rainfall. Thus, the climate in these regions is also described as monsoonal.

Because of the geographic extent of the Asian monsoon, the fidelity of climate model simulations is weighed according to metrics from a variety of regions. Kripalani et al. (2007) judged that three-quarters of the eighteen analyzed coupled models (including the GFDL CM2.0 and 2.1 models, along with the NCAR PCM and GISS modelE-R) match the timing and magnitude of the summertime peak in precipitation over East Asia between 100 and 145E and 20 to 40N that is evident in the NOAA NCEP Climate Prediction Center Merged Analysis of Precipitation (CMAP, Xie and Arkin 1997). However, only half of these models (including both GFDL CGCMs) were able to reproduce the observed spatial distribution of monsoon rainfall, and its extension along the coast of China toward the Korean peninsula and Japan. Considering a broader range of longitude (40-180E) that includes the Indian subcontinent, Annamalai et al (2007) found that only six of eighteen CGCMs (including both GFDL models) were significantly correlated with the observed spatial pattern of CMAP precipitation during June through September. These six models also included a realistic simulation of ENSO variability, which is known to influence interannual variations in the Asian summer monsoon. Kitoh and Uchiyama (2007) computed the spatial correlation and root-mean-square

error of simulated precipitation over a similar region and found the GFDL models in the top tercile, with the GISS modelE-R in the bottom.

During NH winter, the Asian surface winds are directed offshore: from the northeast over India, and the northwest over East Asia. The two American models included in the comparison of the simulated East Asian winter monsoon by Hori and Ueda (2006), GFDL CM2.0 and GISS modelE-R, generally reproduce the observed spatial distribution of sea level pressure and 850mb zonal wind.

In response to increasing greenhouse gases, summer precipitation is expected to increase in the twenty-first century (Kripalani et al 2007 Kimoto 2005). However, the circulation strength in both winter and summer is expected to weaken (Kimoto 2005, Ueda et al 2006), consistent with simple physical arguments by Held and Soden (2006).

Observed variability of the West African monsoon is related to variations of ocean temperature in the Gulf of Guinea. The drying of the Sahel during the late twentieth century, and the attendant societal impacts, is related to the inland extent of the monsoonal circulation. Cook and Vizy (2006) found that slightly over half of the 18 analyzed coupled models reproduced the observed maximum in precipitation over land during June through August. Of these models, only six reproduced the anti-correlation between Gulf of Guinea ocean temperature and Sahel rainfall. The GISS modelE-H and both GFDL models were among the most realistic.

It is unresolved whether the late-twentieth century Sahel drought is due to natural or human influences. Hoerling et al (2006) argue that anthropogenic forcings during this period have little effect upon the Sahel, based upon the average response of eighteen coupled models. In

contrast, Biasutti and Giannini (2006), compare Sahel rainfall between simulations with observed twentieth century forcings (such as greenhouse gas and aerosol concentrations), constant (climatological) forcing, and increasing greenhouse gases. They suggest that the observed late-twentieth century trend was externally forced, predominately by anthropogenic aerosols. This conclusion is based upon the average behavior of the models considered. It is supported in particular by the GFDL and GISS models. It is currently unclear how to resolve these contrasting conclusions, because they are based upon different methods and comparisons of models. Both studies agree that the Sahel drought is the result of ocean warming in the Gulf of Guinea, compared to the NH subtropical Atlantic. The disagreement is how forcing by greenhouse gases and aerosols have changed the contrast in ocean temperature between these two regions.

Rainfall over the Sahel and Amazon are anti-correlated: when the Gulf of Guinea warms, rainfall is generally reduced over the Sahel but increases over South America. Amazon rainfall also depends upon the eastern equatorial Pacific, and during an El Nino, rainfall is reduced in the Nordeste region of the Amazon. Li et al (2006) compare the hydrological cycle of eleven CGCMs over the Amazon during the late-twentieth and twenty-first centuries. Based upon a comparison to CMAP rainfall, the GISS modelE-R is among the best, with the GFDL CM2.1 and NCAR CCSM3 models similarly ranked. Despite this fidelity, the models make disparate predictions for the twenty-first century. In the GISS modelE-R, the equatorial Pacific warms more in the west, resembling a La Nina event. This, together with warming in the Gulf of Guinea, is associated with an increase in Amazon rainfall. While the NCAR CCSM3 predicts a comparable increase, the GFDL CM2.1 exhibits a decrease and lengthening of the Amazon dry season.

The studies of Li et al (2006) along with Ammamalai et al (2007) note that future changes in the South American and Asian monsoons are intimately tied to the response of El Nino in the twenty-first century. Expected temperature changes in the eastern equatorial Pacific are discussed in section V.F. Here, we note that a consensus is yet to emerge adding to uncertainty in monsoonal changes.

The ability of climate models to simulate NH summer rainfall over the US Great Plains and Mexico was summarized by Ruiz-Barradas and Nigam (2006). Among the American models, the GISS modelE-H matches the annual cycle of precipitation over the Great Plains and Mexico most closely. It is also one of two models to simulate interannual variations in precipitation that are significantly correlated with observed variability during the second half of the twentieth century. The observed predominance of moisture import from the Gulf of Mexico compared to local evaporation is most closely reproduced by the NCAR PCM. Moisture import is excessive in the GISS modelE-H, whereas as evaporation contributes too large a fraction in the GFDL CM2.1.

Polar climates

Polar simulation is important not only for polar regions themselves, but also because changes in polar climate can have global impact. Changes in polar snow and ice cover affect the Earth's albedo and thus the amount of insolation heating the planet (e.g., Holland and Bitz 2003, Hall 2004, Dethloff et al. 2006). Concern has also emerged about potential melting of glaciers and ice sheets in Greenland and Antarctica that could produce substantial sea-level rise (Arendt et al. 2002, Braithwaite and Raper 2002, Alley et al. 2005). Polar regions thus require accurate simulation for projecting future climate change and its impacts.

Polar regions present unique environments and, consequently, challenges for climate modeling. The obvious are processes involving frozen water. While not unique to

polar regions, they are more pervasive there. These processes include seasonally frozen ground and permafrost (Lawrence and Slater 2005, Yamaguchi et al. 2005) and seasonal snow cover (Slater et al. 2001), which can have significant sub-grid heterogeneity (Liston 2004), and clear-sky precipitation, especially in the Antarctic (King and Turner 1997, Guo et al. 2003). Polar radiation also has important characteristics that test the ability of models to handle extreme geophysical behavior, such as longwave radiation in clear, cold environments (Hines et al. 1999, Chiacchio et al. 2002, Pavolonis et al. 2004) and cloud microphysics in the relatively clean polar atmosphere (Curry et al. 1996, Pinto et al. 2001, Morrison and Pinto 2005). In addition, polar atmospheric boundary layers can be very stable (Duynkerke and de Roode 2001, Tjernström et al. 2004, Mirocha et al. 2005), and stable boundary layers remain an important area for model improvement.

Confidence in climate model projections of future climate is greatly increased if it can be shown that climate models can accurately simulate the current climate state, and much effort has gone into this type of analysis (e.g. Collins et al. 2006, Delworth et al. 2006). In particular climate models should be able to reproduce both long-term and short-term variations in climate including daily, seasonal, interannual, and decadal variability. The primary mode of Arctic interannual variability is the Arctic Oscillation (Thompson and Wallace 1998), also referred to as the Northern Annual Mode (NAM), which is related to the North Atlantic Oscillation (Hurrell 1995). The primary mode of Antarctic interannual variability is the Southern Annular mode (SAM) (Thompson and Wallace 2000), also known as Antarctic Oscillation. Coupled global climate models have shown skill in simulating the NAM (Fyfe et al. 1999, Shindell et al. 1999, Miller et al. 2006), although in some cases too much of the variability in sea level pressure is associated with the NAM in these models (Miller et al. 2006). Global climate models also realistically simulate the SAM (Fyfe et al. 1999, Cai et al. 2003, Miller et al. 2006), although some details of the SAM (e.g. amplitude and zonal structure) show disagreement between global climate model simulations and reanalysis data (Raphael and Holland 2006; Miller et al. 2006).

Less attention has been given to the ability of global climate system models to simulate shorter-duration climate and weather variability. Uotila et al. (2007) and Cassano et al. (2007) evaluated the ability of an ensemble of 15 global climate-system

models to simulate the daily variability in sea level pressure in the Antarctic and Arctic. In both polar regions, it was found that the 15-model ensemble was not able to reproduce the daily synoptic climatology, with only a small subset of the models accurately simulating the frequency of the primary synoptic weather patterns identified in global reanalysis data sets. Vavrus et al. (2006) assessed the ability of seven global climate models to simulate extreme cold-air outbreaks in the Northern Hemisphere, and found that the spatial pattern of the outbreaks was accurately reproduced in the models, although some details differed.

Attention has also been given to the ability of regional climate models to simulate polar climate. In particular, the Arctic Regional Climate Model Intercomparison Project (ARCMIP) (Curry and Lynch 2002) engaged a suite of Arctic regional atmospheric models to simulate a common domain and period over the western Arctic. Rinke et al. (2006) evaluated the spatial and temporal patterns simulated by 8 ARCMIP models, and found that the model ensemble agreed well with global reanalyses, despite some large errors for individual models. Tjernstrom et al. (2005) evaluated near-surface properties simulated by 6 ARCMP models. In general surface pressure, air temperature, humidity, and wind speed were all well simulated, as were radiative fluxes and turbulent momentum flux. Tjernstrom et al. (2005) found that turbulent heat flux was poorly simulated, and that over an entire annual cycle the accumulated turbulent heat flux simulated by the models was an order of magnitude larger than the observed turbulent heat flux (Fig. PA-1).

Although simulations of polar climate display agreement with observed behavior, as indicated above, there remains room for improvement. In global models, polar simulation may be affected by errors in simulating other regions of the planet, but much of the difference from observations and uncertainty about projected climate change stems from current limitations in polar simulation. These limitations include missing or incompletely represented processes and poor resolution of spatial distributions.

As with other regions, model resolution affects simulation of important processes. In the polar regions, surface distributions of snow depth vary markedly, especially when snow drifting occurs. Improved snow models are needed to represent such spatial heterogeneity (e.g., Liston 2004), which will continue to involve scales smaller than

resolved for the foreseeable future. Frozen ground, whether seasonally frozen or occurring as permafrost, presents additional challenges. Modeling soil freeze and thaw continues to be a challenging problem as characteristics of energy and water flow through the soil affect temperature changes, and such fluxes are poorly understood (Yamaguchi et al. 2005).

Frozen soil affects surface and subsurface hydrology, which influences the spatial distribution of surface water with attendant effects on other parts of the polar climate system such as carbon cycling (e.g., Gorham 1991, Aurela et al. 2004), surface temperature (Krinner 2003), and atmospheric circulation (Gutowski et al. 2007). The flow of fresh water into polar oceans potentially alters their circulation, too. Surface hydrology modeling typically includes limited, at best, representation of subsurface water reservoirs (aquifers) and horizontal flow of water at both the surface and below surface. These features limit the ability of climate models to represent changes in polar hydrology, especially in the Arctic.

Vegetation has been changing in the Arctic (Callaghan et al. 2004) and projected warming, which may be largest in regions where snow and ice cover retreat, may produce further changes in vegetation (e.g., Lawrence and Slater 2005). Current models use static distributions of vegetation, but dynamic vegetation models will be needed to account for changes in land-atmosphere interactions influenced by vegetation.

A key concern in climate simulations is how projected anthropogenic warming may alter ice sheets on land, whose melting could raise sea levels substantially. At present, climate models do not include ice-sheet dynamics and thus cannot account directly for how ice sheets might change, possibly changing heat absorption from the sun and atmospheric circulation in the vicinity of the ice sheets.

How well each of the processes above is represented in climate simulation depends in part on model resolution. Distributions of snow, ice sheets, surface water, frozen ground and vegetation have important spatial variation on scales smaller than the resolutions of typical contemporary climate models. Finer resolution is thus needed. Part of this need may be satisfied by regional models simulating just a polar region. Because both the northern and southern polar regions are within circumpolar atmospheric circulations, their synoptic coupling with other regions is more limited than is the case

with midlatitude regions embedded in the westerlies (e.g., Wei et al. 2002), which could allow polar-specific models that focus on ant/arctic processes, in part to improve modeling of surface-atmosphere exchange processes (Fig. PA-1). While each of the above processes have been simulated in finer scale, stand-alone models, their interactions as part of a climate system also need to be simulated and understood.

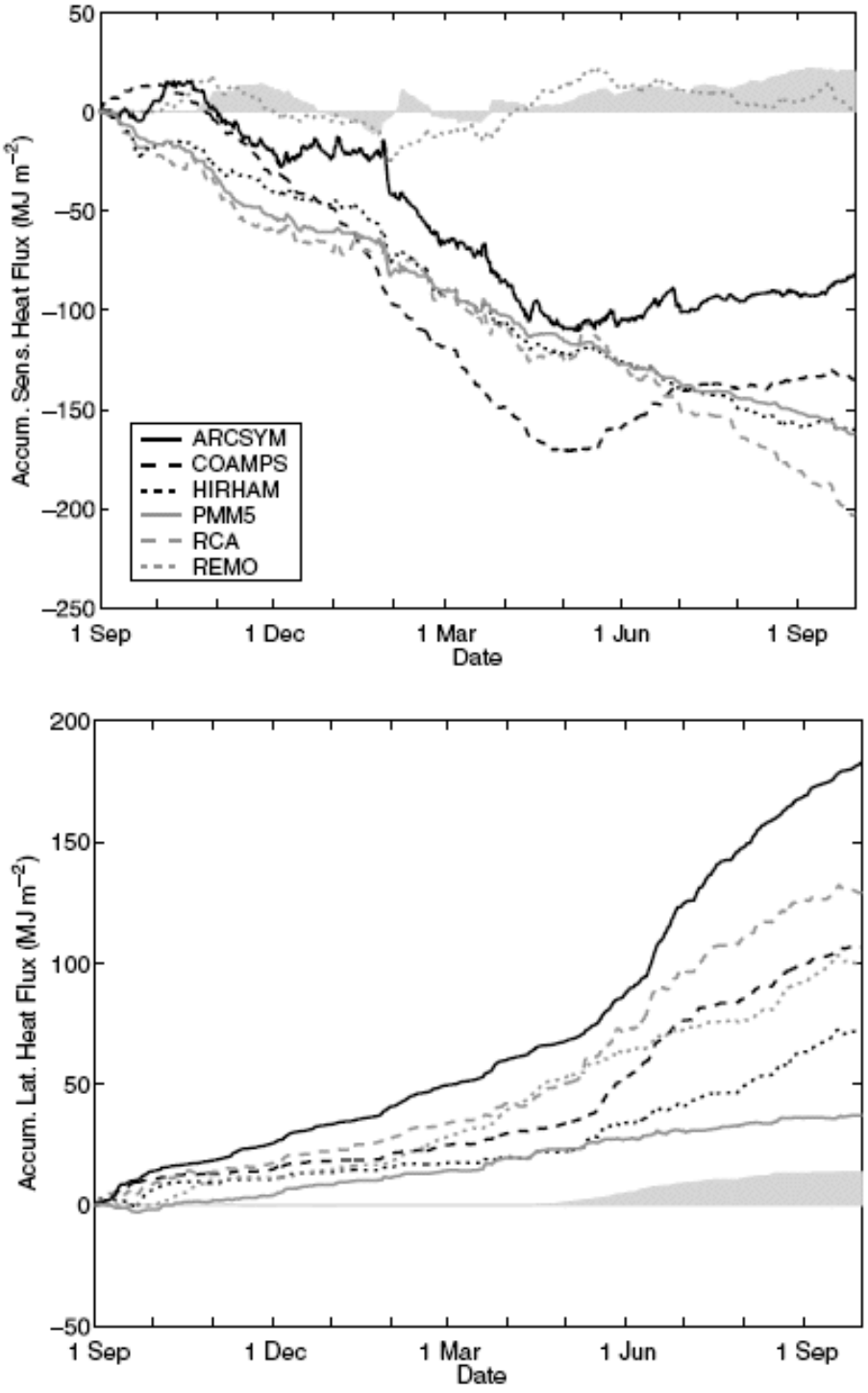

Fig. PA-1. Cumulative fluxes of surface sensible heat (top panel) and latent heat (bottom) at the SHEBA site from six models simulating a western Arctic domain for Sept. 1997 – Sept. 1998 for ARCMIP. SHEBA observations are the gray vertical bars; model

identifications are given by the key in the upper panel. Adapted from Tjernstrom et al. (2005).

:

Sea ice plays a critical role in the exchange of heat, mass, and momentum between the ocean and atmosphere and any errors in the sea-ice system will contribute to errors in the other components. Two recent papers [*Holland and Raphael* 2006 and *Parkinson et al.* 2006] quantify how the current models simulate the sea-ice process of the climate system. Very limited observations make any evaluation of sea ice difficult. The primary observation available is sea ice concentration. In some comparisons, sea ice extent (ice concentration greater than 15%), is used. Satellites have made it possible for a more complete data set of observations for the past few decades. Prior to satellite measurements becoming available, observations of ice extent were fewer. Other quantities that might be evaluated include ice thickness. Such comparisons are difficult because of the limited number of observations and will not be discussed.

Ice Concentration and extent: Both of these studies indicate that the seasonal pattern in ice growth and decay in the polar regions for all the models is reasonable [*Holland and Raphael* 2006] (**FIGURE XXX from Holland and Raphael**). However, there is a large amount of variability between the models in their representation of the sea ice extent in both the northern and southern hemispheres. Generally, the models do better in simulating the Arctic region than in their simulation of the Antarctic region as shown with **Figure XXX [*Parkinson et al.* 2006].** An example of the complex nature of reproducing the ice field is given in *Parkinson et al.* [2006]. They found that all the models showed an ice-free region in winter to the west of Norway, as seen in observational data, but all the models also produced too much ice north of Norway. They suggest that this is because the North Atlantic Current is not being simulated correctly. In a qualitative comparison, Hudson Bay is ice covered in winter in all the models correctly reproducing the observations. The set of models are not consistent in their "fidelity" between the Northern and Southern regions and maybe due, partly, to how the parameters are defined in the sea ice models.

Holland and Raphael [2006] examined the variability in the Southern Ocean sea ice extent extensively. As an indicator of the ice response to large scale atmospheric events, they compared a set of IPCC AR4 climate models sea ice response to the atmospheric index, the Southern Annular Mode (SAM) for the April-June (AMJ) period (Table 1). The models show that the ice variability does respond modestly to the large scale atmosphere forcing but less than limited observations show. Two of the models also exhibit the out-of-phase buildup of ice between the Atlantic and Pacific sectors (the Antarctic Dipole) to some degree.

MODIFIED FROM Table 1 *Holland and Raphael* [2006] Correlations of the leading mode of sea ice variability and the southern annular mode (SAM) for the observations and model simulations

	AMJ SAM and high-pass filtered fields	AMJ SAM and detrended fields
Observations	**0.47**	**0.47**
CCSM3	**0.40**	**0.44**
GFDL-CM2.1	**0.39**	0.19
GISS-ER	0.30	0.20

Bold values are significant at the 95% level accounting for the autocorrelation of the timeseries

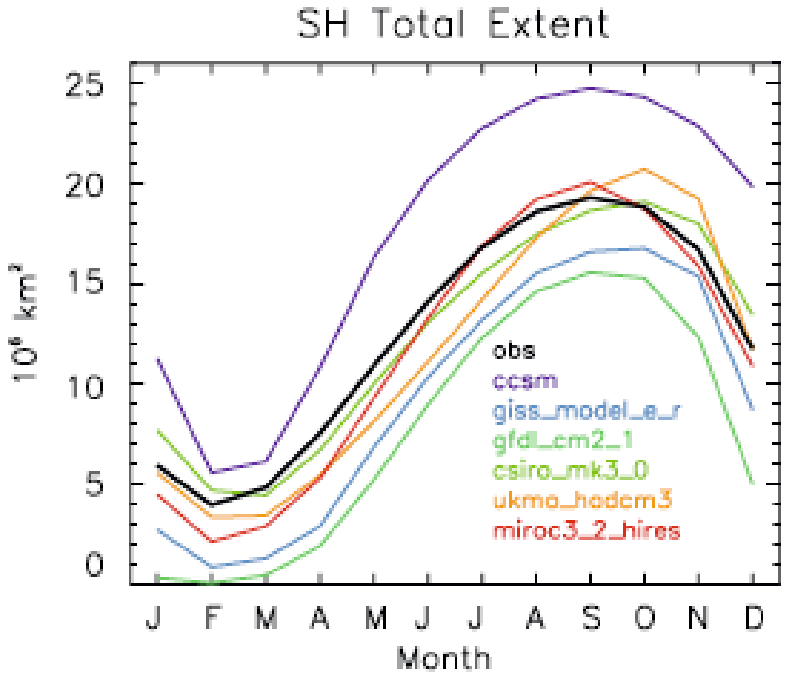

From *Holland and Raphael* 2006. Fig. 1 The annual cycle of southern hemisphere ice extent defined to be the area of ice with concentrations greater than 15%

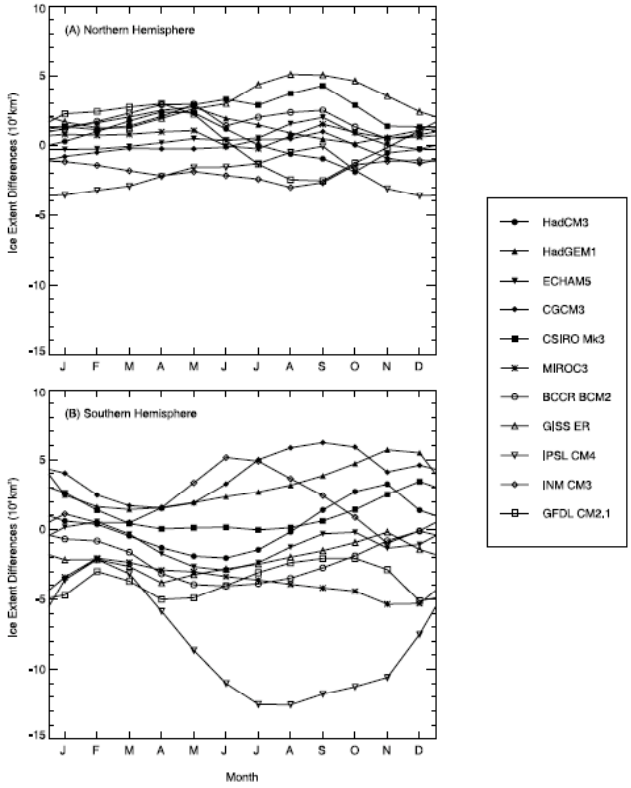

From Parkinson et al. 2006: Figure 4. Difference between the modeled 1979–2004 monthly average sea ice extents and the satellite-based observations (modeled minus

observed), for each of 11 major GCMs, for both the (a) Northern Hemisphere and (b) Southern Hemisphere.

Modes of variability

The Madden-Julian Oscillation: (MJO) is a characteristic pattern in the tropical atmosphere. It has taken on special prominence in research on simulating the tropical atmosphere. This phenomenon consists of large-scale eastward propagating patterns in humidity, temperature, and atmospheric circulation which strengthen and weaken tropical rainfall as they propagate around the Earth in roughly 30-60 days. This pattern often dominates intraseasonal (within season) variability of tropical precipitation on time scales longer than a few days, creating such phenomena as 1-2 week breaks in Asian monsoonal rainfall and weeks with enhanced hurricane activity in the Eastern North Pacific and the Gulf of Mexico. Inadequate prediction of the evolution of these propagating structures is considered one the main impediments to more useful extended-range weather forecasts in the tropics, and improved simulation of this phenomenon is considered by some a litmus test for the credibility of climate models in the tropics

Recent surveys of model performance indicate that simulations of the MJO remain inadequate. For example, Lin et al (2006), in a study of many of the models in the PCMDI/AR4 archive (Dave – we need a consistent terminology for the Archive), conclude that "… current GCMs still have significant problems and display a wide range of skill in simulating the tropical intraseasonal variability", while Zhang et al. (2005) in another multi-model comparison study, state that "… commendable progress has been made in MJO simulations in the past decade, but the models still suffer from severe deficiencies …" Nearly all models do capture the essential feature of the pattern, with large-scale eastward propagation and with roughly the correct vertical structure. But the propagation is often too rapid and the amplitudes too weak. As an example of recent work, Klein (2007?) studies whether two of the US IPCC models can maintain a pre-existing strong MJO pattern when initialized with observations (from the TOGA-COARE field experiment), with limited success. Controlled experiments have suggested that for

models to simulate MJO, the moist static energy in the lower troposphere must be accumulated to a certain amount before convections are triggered, and sufficient mesoscale statiform heating from convective systems should exist in the upper troposphere (Wang and Schlesinger 1999). These processes are however the least understood in current climate models.

The difficulty in simulation of the MJO is related to the multi-scale nature of the phenomenon: the propagating pattern is itself of large enough scale that it should be resolvable by climate models, but the convection and rainfall modulated by this pattern, and feeding back and energizing it, occur on much smaller, unresolved, scales. In addition to this dependence on the parameterization of tropical convection, a long list of other effects has been shown by models and/or observational studies to be important for the MJO. These include the pattern of evaporation generated as the MJO propagates through convecting regions, feedback from cloud-radiative interactions, intraseasonal ocean temperature changes, the diurnal cycle of convection over the ocean, as well as the vertical structure of the latent heating, including especially the proportion of shallow cumulus congestus clouds and deep convective cores in the different phases of the oscillation (Lin et al. 2004).

A picture seems to be emerging that the difficulty in simulation may not be due to a single model deficiency but a result of the complexity of the phenomenon, given this long list of factors thought to be significant. In several of the multi-model studies, such as Lin et al (2006) a few of the models do perform well, but without a clearer understanding of how these factors combine to generate the observed characteristics of the MJO, it is difficult to maintain a good simulation as the model is modified for other reasons, and it is difficult to transfer one model's successful simulation to other models. It also remains unclear whether the models with superior MJO simulations should be given extra weight in multi-model studies of climate change in the tropics.

The El Nino – Southern Oscillation (ENSO) El Nino was named originally in the nineteenth century by Peruvian sailors to note the early arrival of a warm current from equatorial latitudes (Philander 1990). Every few years, a northerly current arrives around Christmas, rather than the following spring (Yu and McPhaden 1999), bringing heavy rains to coastal Peru and a temporary decline in the anchovy harvest. By the mid twentieth century, scientists recognized that this local anomaly was in fact part of a disruption to the atmospheric circulation across the entire Pacific basin. During El Nino, atmospheric mass migrates west of the dateline as part of the Southern Oscillation, reducing surface pressure and drawing rainfall into the central and eastern Pacific (Rasmussen and Wallace 1983). Together, El Nino and the Southern Oscillation, often abbreviated in combination as ENSO, are the largest source of tropical variability during recent decades.

Changes along the equatorial Pacific have been linked to global disruptions of climate (Ropelewski and Halpert 1987). During an El Nino event, the Asian monsoon is typically weakened, along with rainfall over eastern Africa, while precipitation increases over the American southwest. El Nino raises the surface temperature as far as Canada, while changes in the North Pacific Ocean are linked to decadal variations in ENSO (Trenberth and Hurrell 1994). Clearly, accurate projections of climate change in the twenty-first century depend upon the accurate projection of changes to El Nino. Moreover, the demonstration that changes in ocean temperature within the eastern equatorial Pacific can alter climate across the globe indicates that even changes to the mean equatorial Pacific climate during the twenty-first century can influence climate far beyond the tropical ocean. For example, a long-term warming of the eastern equatorial Pacific relative to the surrounding ocean will favor a weaker Asian monsoon, even in the absence of changes to the size and frequency of El Nino events.

While incident sunlight is largest on the equator, in the eastern Pacific, the ocean is colder than at neighboring latitudes. Because of the Earth's rotation, easterly winds along the equator cool the surface by raising cold water from below, which offsets heating by the absorption of sunlight (e.g. Clement et al 1996). In contrast, warm water extends

deeper to the west so upwelling has little effect upon the surface temperature of the West Pacific, which exhibits warmer temperatures consistent with the strong, equatorial solar heating. The westward increase of temperature along the equator is associated with a decrease in atmospheric pressure, reinforcing the easterly Trade winds.

One projection of tropical Pacific climate during the twenty-first century is for the equatorial temperature contrast to increase, so that the average state more closely resembles La Nina, marked by unusually cold ocean temperatures and enhanced upwelling in the East Pacific, the opposite to El Nino (Clement et al 1996; Cane et al 1997). According to this argument, an increase in net radiation into the ocean surface resulting from an increase in greenhouse gas concentration is partially offset by the upwelling of cold water. This compensation is stronger in the east than in the west, where the surface layer of warm water extends to greater depth. There is evidence for an observed trend toward a La Nina state (Cane et al 1997), but the trend remains ambiguous because of the large decadal variations in the ENSO cycle. Upwelling water along the equator can be traced back to the surface at higher latitudes. Liu et al (1998) suggest that as the subtropics warm, the temperature of the upwelling water will increase, reducing its ability to offset radiative warming at the surface. Until recently, many coupled ocean-atmosphere models calculated a warming of the East Pacific and a drift of mean conditions toward an ENSO state. Below we summarize the most recent model comparisons, carried out as part of the IPCC AR4. We find that even among the models with the most realistic simulation of ENSO and seasonal variability, there is no consensus on the anticipated change in climate within the tropical Pacific. This introduces uncertainty in the projected climate response within regions throughout the globe influenced by El Nino.

In general, coupled models developed for the AR4 are far more realistic than those of a decade ago, when ENSO variability was comparatively weak, and some models lapsed into permanent El Nino states (Neelin et al 1992). Even compared to the models assessed more recently by ENSIP and CMIP2 (Latif et al 2001; AchutaRao and Sperber 2002), ENSO variability of ocean surface temperature is more realistic, although sea level

pressure and precipitation anomalies show little recent improvement (AchutaRao and Sperber 2006). Part of this progress is the result of increased resolution of the equatorial ocean circulation that has accompanied inevitable increases in computing speed. Table X shows the horizontal and vertical resolution of the seven American coupled models whose output was submitted to AR4.

Table X: Spacing of grid points in the American coupled models developed for AR4.

Model:	Longitude	Latitude	Vertical Levels
GFDL CM2.0	1	1/3	50
GFDL CM2.1	1	1/3	50
GISS AOM	5	4	13
GISS modelE-H	2	2	16
GISS modelE-R	5	4	13
NCAR CCSM3	1.125	0.27	27
NCAR PCM	0.94	0.5	32

.....

Along the equator, oceanic waves that adjust the equatorial temperature and currents to changes in wind are tightly confined to within a few degrees of latitude. To simulate this adjustment, the ocean state is calculated at points as closely spaced as 0.27 degrees of latitude in the NCAR CCSM3. NCAR PCM has half degree resolution, while both GFDL models have equatorial resolution of one-third of a degree. This degree of detail is a substantial improvement compared previous generations of models. In contrast, the GISS AOM and modelE-R calculate equatorial temperatures on a grid with four degree spacing. This is broad compared to the latitudinal extent of cold temperatures in the eastern Pacific, the `cold tongue' region. This means that changes to upwelling are diluted over the coarse grid spacing, which limits the amplitude of the resulting temperature fluctuations. In fact, both the GISS AOM and modelE-R models have unrealistic ENSO

variations that are much smaller than observed (Hansen et al 2007). This minimizes the influence of their simulated El Nino and La Nina events on climate outside the equatorial Pacific, and we will not discuss these models further in this section.

In comparison to previous generations of models, where ENSO variability was typically weak (Neelin et al 1992; AchutaRao and Sperber 2006), the AR4 coupled models generally simulate El Nino near the observed amplitude, or even above. The latter study compared sea surface temperature (SST) variability within the tropical Pacific calculated under pre-industrial conditions. Despite its comparatively low two-degree latitudinal grid spacing, the GISS modelE-H among the American models most closely matches observed SST variability since the mid-nineteenth century, according to the HadISST v1.1 data set (Rayner et al 2003). The NCAR PCM also exhibits El Nino warming close to the observed magnitude. This comparison is based upon spatial averages within three longitudinal bands, and GISS modelE-H along with the NCAR models exhibit their largest variability in the eastern band as observed. However, within twentieth century experiments, GISS modelE-H underestimates variability since 1950, when the NCAR CCSM3 is closest to observations (Joseph and Nigam 2006). While the fidelity of each model's ENSO variability depends upon the specific data set and period of comparison (c.f. Capotondi et al 2006; Merryfield 2006, van Oldenborgh et al 2005), the general consensus is that the GISS modelE-H, both NCAR models, and GFDL CM2.0 have roughly the correct amplitude, while variability is too large by roughly one-third in the GFDL CM2.1. While most models (including GISS modelE-H and both NCAR models, but excluding the GFDL models) exhibit the largest variability in the eastern band of longitude, none of the AR4 models have larger variability at the South American coast, where El Nino was originally identified (AchutaRao and Sperber 2006; Capotondi et al 2006). This is possibly because the longitudinal spacing of the model grids is too large to resolve coastal upwelling, and its interruption during El Nino (Philander and Pacanowski 1981). Biases in the atmospheric model, including underestimate of the persistent stratus cloud decks along the coast, may also contribute (Mechoso et al 1995).

El Nino occurs every few years, albeit irregularly. The spectrum of anomalous ocean

temperature shows a broad peak between two and seven years, and there are multi-decadal variations in event frequency and amplitude. Almost all of the AR4 models have spectral peaks within this range of time scales. Interannual power is broadly distributed within the American models, as observed, with the exception of the NCAR CCSM3 which exhibits strong biennial oscillations.

While the models generally simulate the observed magnitude and frequency of events, reproduction of their seasonality is more elusive. Anomalous warming typically peaks late in the calendar year, as originally noted by South American fisherman. Among American models, this seasonal dependence is simulated only by the NCAR CCSM3 (Joseph and Nigam 2006). Warming in the GFDL CM2.1 and GISS modelE-H are nearly uniform throughout the year, while warming in the NCAR PCM is largest in December but exhibits a secondary peak in early summer. The seasonal cycle along the equatorial Pacific also remains a challenge for the models. Each year, the east Pacific cold tongue is observed to warm during NH spring and cool again late in the calendar year. The GFDL CM2.1 and NCAR PCM1 have the weakest seasonal cycle among the American models, while GISS modelE-H, GFDL 2.0 and NCAR CCSM3 are closest to the observed amplitude (Guilyardi 2006). Among the AR4 models as a group, the amplitude of the seasonal cycle of equatorial ocean temperature generally varies inversely with the strength of the ENSO cycle.

Anticipation of twenty-first changes to El Nino remains uncertain, because of a lack of consensus among the models. Among fifteen models examined under carbon dioxide doubling, three exhibit statistically significant increases in amplitude, while five exhibit a decrease, compared to their variability under pre-industrial conditions (Merryfield, 2006). Even when only the most realistic models are surveyed (including the GFDL CM2.1), identified according to a detailed examination of their mechanisms of variability (described below), no consensus emerges. No significant change in event period is found either (Guilyardi 2006). Moreover, changes in the climate of the tropical Pacific (as opposed to trends in El Nino variability) are also inconsistent (van Oldenborgh et al 2006). These trends are inferred based upon the response to a doubling or quadrupling of

carbon dioxide, compared to a pre-industrial climate. This forcing is strong compared to forcing over the twentieth century in which one might hope to infer trends in El Nino from the observational record. The occurrence of the two largest El Nino events late in the twentieth century has been attributed to increasing greenhouse gas concentrations (Trenberth and Hoar 1997; Knutsen and Manabe 1998), although this remains unsettled because of large variations in the tropical Pacific within the multi-decadal instrument record (Rajagopalan et al 1997).

The lack of consensus among model projections for the twenty-first century may result from the combination of physical mechanisms contributing to observed variability, and the difficulty of simulating them individually along with their relative importance. There is evidence that the importance of certain mechanisms changed in the middle of the 1970's (Wang 1995), so it is unclear what the correct emphasis should be. In addition, positive feedbacks, inferred from the observations, may exacerbate unrealistic features in the models, contributing further to model error.

Several studies have assessed the mechanisms contributing to variability among the AR4 models. Confidence in the models' projection of climate within the tropical Pacific during the twenty-first century depends upon accurate simulation of mechanisms of variability observed at present. El Nino occurs when the upwelling of cold water to the surface is interrupted within the equatorial eastern Pacific and South American coast. This can occur because the rate of upwelling decreases, or alternatively because the temperature of the upwelling water increases. This subsurface temperature is related to the depth of the thermocline, within which the water temperature falls off sharply with depth. During El Nino, the thermocline deepens, so that upwelling water originating in the cold water below now begins its rise within the relatively warm layer above (Wyrtki 1975). In addition, the slowing of the easterly Trade winds reduces the rate of upwelling (Bjerknes 1969), which at the surface reduces the export of water from the cold tongue toward the West Pacific. Within the weaker surface current, water has more time to be warmed by the sun and overlying atmosphere. El Nino a coupled phenomenon because the winds that change the upwelling of cold water to the surface depend upon the surface temperature

itself. Because the easterlies are driven partly by the temperature contrast between the cold east Pacific and the warmer ocean west of the dateline, warming in the east reinforces the slackening of the easterly Trade winds.

The coupling between ocean temperature and equatorial winds is typically inferred by regressing wind stress upon temperature averaged within the ENSO domain. The observed wind anomaly is westerly and strongest slightly to the west of a warm ocean anomaly, as expected based upon simple theoretical models (Gill 1980; Lindzen and Nigam 1987, Yu and Neelin 1997). The model wind anomalies are typically displaced farther west than observed, and are excessively confined to the equator (Capotondi et al 1987). The NCAR PCM regression is roughly half the observed strength, while the NCAR CCSM3 and GFDL CM2.1 come closest to observations (Van Oldenborgh et al 2005). The GISS modelE-H exhibits reasonable coupling in the Central Pacific, but almost no coupling toward South America.

The converse response of SST to wind anomalies is diagnosed by evaluating various terms in the equation for the evolution of ocean temperature (van Oldenborgh 2005; Capotondi et al 2006). Changes in the temperature of upwelling water are observed to be important in the eastern Pacific (Capotondi et al 2006). This feedback is reproduced by the GFDL CM2.0 and NCAR CCSM3 models, although with somewhat low amplitude, possibly because the climatological upwelling is weak. (The model output necessary for this diagnosis was not available for the GFDL CM2.1, NCAR PCM, and GISS modelE-H.) While a decrease in the rate of upwelling is crucial to observed warming in the Central Pacific, this feedback is weak in the GFDL CM2.0, and absent in the NCAR CCSM3. The ocean feedback to wind anomalies is also diagnosed by regressing the evolution of ocean temperature upon various mechanisms represented within the ocean heat budget (van Oldenborgh et al 2005). The NCAR PCM has very strong feedbacks of upwelling rate and temperature in response to wind anomalies, which compensate for its weak wind response to anomalous SST. The GFDL CM2.1 generally reproduces the observed regression relations. In contrast, van Oldenborgh et al (2005) note that regression analysis of GISS modelE-H is noisy and difficult to interpret. It is not clear at

this point how GISS modelE-H compensates for its weak wind response to ocean temperature anomalies in order to create ENSO temperature variability near the observed magnitude and location. This lack of transparency calls its projection of future changes into question, at least for the present.

In general, GFDL2.1 is consistently ranked among the American models as the most realistic simulation of El Nino (van Oldenborgh et al 2005; Guilyardi 2006; Merryfield 2006). This is based not only upon its surface temperature variability (which in fact is slightly too high), but upon its faithful simulation of the observed relationship between ocean temperature and surface wind, along with the wind-driven ocean response. While SST in many models is consistently dominated either by anomalies of upwelling strength or else temperature, these processes alternate in importance over several decades within the GFDL CM2.1 (Guilyardi 2006). This alternation is also found in the observations. Since the 1970's, the upwelling temperature has been the predominant feedback (Wang 1995).

While GFDL CM2.1 predicts a reduced ENSO amplitude in response to increased greenhouse forcing, there is no consensus even among the most highly regarded models. Philip and Van Oldenborgh (2006) find that while both upwelling feedbacks amplify as the greenhouse gas concentration increases, damping processes (due to cloud radiation, for example) also become more effective. A robust prediction of future El Nino amplitudes requires both the upwelling feedback and damping along with their relative amplitude to be simulated consistently, which is not true at present.

El Nino events are related to climate anomalies throughout the globe. Models with more realistic ENSO variability generally exhibit an anti-correlation with the strength of the Asian summer monsoon (e.g. Annamalai et al 2006), while twenty-first century changes to Amazon rainfall have been shown to depend upon projected trends in the tropical Pacific (Li et al 2006). El Nino has a long-established relation to North American climate (Horel and Wallace 1981), assessed in the AR4 models by Joseph and Nigam (2006). This relation is strongest during NH winter, when the tropical anomalies are largest.

Anomalous circulations driven by rainfall over the warming equatorial Central Pacific radiate atmospheric disturbances into mid-latitudes that are amplified within the North Pacific storm track (Sardeshmukh and Hoskins 1988; Held et al 1989; Trenberth et al 1998). To simulate the influence of ENSO upon North America, the models must simulate realistic rainfall anomalies and in the correct season in order that the connection is amplified by the wintertime storm tracks. The connection between equatorial Pacific and North American climate is simulated most accurately by the NCAR PCM model (Joseph and Nigam 2006). In the GFDL CM2.1, North American anomalies are too large. However, this reflects the model's excessive El Nino variability within the equatorial Pacific. The connection between the two regions is quite realistic if the model's tropical amplitude is accounted for. In the GISS model, anomalous rainfall during ENSO is small, consistent with the weak wind stress cited above. The influence of El Nino over North America is nearly negligible in this model. The weak rainfall anomaly is presumably a result of unrealistic coupling between the atmospheric and ocean physics. When SST is instead prescribed in this model, rainfall calculated by the GISS modelE AGCM over the American southwest is significantly correlated with El Nino as observed.

Realistic simulation of El Nino, and its global influence, remains a challenge for coupled models, because of the myriad processes contributing and their changing importance in the observational record. Key aspects of the coupling between the ocean and atmosphere, the relation between SST and wind stress anomalies, for example, are the result of complicated interactions between the resolved model circulations, along with parameterizations of the ocean and atmospheric boundary layers and moist convection. Simple models identify parameters controlling the magnitude and frequency of El Nino, such as the wind anomaly resulting from a change in SST (e.g., Zebiak and Cane 1987; Fedorov and Philander 2000), offering guidance to improve the realism of fully coupled GCM's. However, in a GCM, the coupling strength is emergent rather than prescribed, and it is often unclear how to change the coupling a priori. Nonetheless, the improved simulations of the ENSO cycle compared to previous generations (AchutaRao and Sperber 2006) suggest that additional realism can be expected in the future. This optimism arises in part from the extensive and unprecedented model comparisons carried

out as part of the AR4, where the flaws identified in current models may point toward future solutions.

Extreme events

Flood-producing precipitation, drought, heat waves, and cold waves have severe impacts on North America. Flooding resulted in average annual losses of $3.7 billion during 1983-2003 (**http://www.flooddamagedata.org/**). Losses from the 1988 drought were estimated at $40 billion and the 2002 drought at $11 billion. The heat waves in 1995 resulted in 739 excess deaths in Chicago alone (Whitman et al. 1997). It is probable that a large component of the overall impacts of climate change will arise from changes in the intensity and frequency of extreme events.

The modeling of extreme events poses special challenges since they are, by definition, rare in nature. Although the intensity and frequency of occurrence of extreme events are modulated by the state of the ocean and land surface and by trends in the mean climate state, internal variability of the atmosphere plays a very large role and the most extreme events arise from the chance confluence of unlikely conditions. Their very rarity makes statistical evaluation of model performance less robust than for the mean climate. For example, if one wanted to evaluate the ability of a model to simulate heat waves as intense as the 1995 event in Chicago, there are only a few episodes in the entire 20th Century that approach or exceed that intensity (Kunkel et al. 1996). For such rare events, there is substantial uncertainty in the real risk, varying from once every 30 years to once every 100 years or more. Thus, a model that simulates such events at a frequency of once every 30 years may be performing adequately, but it cannot be distinguished in its performance from a model simulating such an event at a frequency of once every 100 years.

Although one might expect that a change in mean climate conditions will apply equally to changes in the extremes, this is not necessarily the case. Using as an example the 50 state record low temperatures, the decade with the largest number of records is the 1930s, yet winters during this decade averaged as the third warmest since 1890; in fact, there is no significant correlation between the number of records and U.S. wintertime

temperature (Vavrus et al. 2006). Thus, the severest cold air outbreaks in the past have not necessarily been coincident with cold winters. Another examination of model data showed that the future changes in extreme temperatures differed from changes in the mean temperature in many regions (Hegerl et al. 2004). This means that climate model output must be analyzed explicitly for extremes by examining daily (or even finer) resolution data, a resource-intensive effort.

The evaluation of model performance with respect to extremes is hampered by incomplete data on the historical frequency and severity of extremes. A study by Frich et al. (2002) described a set of indices suitable for performing global analyses of extremes and presented global results. However, many areas were missing due to lack of suitable station data, particularly in the tropics. It has become common to use some of these indices for comparisons between models and observations. Another challenge for model evaluation is the spatially-averaged nature of model data, representing an entire grid cell, while station data represent point observations. For some comparisons, it is necessary to average the station data over areas representing a grid cell.

There are several approaches toward the evaluation of model performance of simulation of extremes. One approach examines whether a model reproduces the magnitude of extremes. For example, a daily rainfall amount of 100 mm or more is expected to occur about once every year in Miami, once every 6 years in New York City, once every 13 years in Chicago, and once every 200 years in Phoenix. To what extent is a model able to reproduce the absolute magnitudes and spatial variations of such extremes? A second approach examines whether a model reproduces observed trends in extremes. Perhaps the most prominent observed trend in the U.S. is an increase in the frequency and intensity of heavy precipitation, particularly during the last 20-30 years of the 20th Century. Another notable observed trend is an increase in the length of the frost-free season.

In some key respects, it is likely that the model simulation of temperature extremes is less challenging than of precipitation extremes, in large part due to the scales of these phenomena. The typical heat wave or cold wave covers a relatively large region, of the order of several hundred miles or more, or a number of grid cells in a modern climate model. By contrast, heavy precipitation can be much more localized, often

extending over regions of much less than 150 km, or less than the size of a grid cell. Thus, the modern climate model can directly simulate the major processes causing temperature extremes while heavy precipitation is sensitive to the parameterization of subgrid scale processes, particularly convection (Emori et al. 2005; Iorio et al. 2004).

Droughts, particularly over N. America and Africa Recent analysis indicates that there has been a globally-averaged trend toward greater areal coverage of drought since 1972 (Dai et al. 2004). A simulation by the HadCM3 model reproduces this dry trend (Burke et al. 2006) only if anthropogenic forcing is included. A control simulation indicates that the observed drying trend is outside the range of natural variability. However, the model does not always correctly simulate the regional distributions of areas of increasing wetness and dryness.

The simulation of specific regional features remains a major challenge for models. Globally, one of the most significant observed changes is the shift to more frequent and more severe droughts in the Sahel region of Africa since about 1970. Lau et al. (2006) find that only eight CGCMs produce a reasonable Sahel drought signal, while seven CGCMs produce excessive rainfall over the Sahel during the observed drought period. Even the model with the highest prediction skill of the Sahel drought could only predict the increasing trend of severe drought events but not the beginning and duration of the events. Hoerling et al. (2006) also finds that the AR4 models fail to simulate the drying and furthermore uses the model results to suggest that the observed drying was not due to anthropogenic forcing. However, two GFDL models are successful in reproducing the drying and analysis of those models suggests that the drying is of anthropogenic origin (Held et al. 2005). Biasutti and Giannini (2006) interpret these results as an indication that the drying was a combination of decadal-scale internal variability superimposed on longer timescale changes associated with anthropogenic forcing. The differences between modeled and observed regional patterns may then be due to the randomness of natural variability, but may also result from inadequate representation of regional processes and feedbacks.

Excessive rainfall leading to floods Several different measures of excessive rainfall have been used in analyses of model simulations. A common one is the annual maximum 5-day precipitation amount, one of the Frich et al. (2002) indices. This has been analyzed in several recent studies (Kiktev et al. 2003; Hegerl et al. 2004; Tebaldi et al. 2006). Other analyses have examined thresholds of daily precipitation, either absolute (e.g. 50 mm per day in Dai 2006) or percentile (e.g. 4th largest precipitation event equivalent to 99th percentile as in Emori et al. 2005). Recent studies of model simulations produced for the IPCC AR4 provide information on the performance of the latest generation of models.

There is a general tendency for models to underestimate very heavy precipitation. This is shown in a comparison between satellite (TRMM) estimates of daily precipitation and model-simulated values within the 50S-50N latitude belt (Dai 2006). The TRMM observations derive 7% of the total precipitation from very heavy rainfall of 50 mm or more per day, in contrast to only 0-2% for the models. For the frequency of very heavy precipitation of 50 or more mm per day, the TRMM data show a frequency of 0.35% (about once every 300 days), whereas it is 0.02-0.11% (once every 900 to 5000 days) for the models. A global analysis of model simulations showed that the models produced too little precipitation in events exceeding 10 mm per day (Sun et al. 2006). Examining how many days it takes to accumulate 2/3's of the annual precipitation, the models generally show too many days compared to observations over North America, although a few models are close to reality. In contrast to the general finding of a tendency toward underestimation, a study (Hegerl et al. 2004) of two models (HadCM3 and CGCM2) indicates generally good agreement with the observed annual maximum 5-day precipitation amount over North America for HadCM3 and even somewhat of an overestimation for CGCM2.

This model tendency to produce rainfall events less intense than observed appears to be due in part to the low spatial resolution of global models. Experiments with individual models show that increasing the resolution improves the simulation of heavy events. For example, the 4th largest precipitation event in a model simulation with a resolution of approximately 300 km averaged 40 mm over the conterminous U.S.,

compared to an observed value of about 80 mm. When the resolution was increased to 75 km and 50 km, the 4th largest event was still smaller than observed, but by a much smaller amount (Iorio et al. 2004). A second factor that is important is the parameterization of convection. Thunderstorms are responsible for many intense events, but they occur at resolutions smaller than the size of model grids and thus must be indirectly represented in models. One experiment showed that changes to this representation improves model performance and, when combined with high resolution of about 1.1 deg latitude, can produce quite accurate simulations of the 4th largest precipitation event on a globally-averaged basis (Emori 2005). Another experiment found that the use of a cloud-resolving model imbedded in a global model eliminated the underestimation of heavy events (Iorio et al. 2004). A cloud-resolving model eliminates the need for a parameterization of convection, but is very expensive to run. These sets of experiments indicate that the problem of heavy event underestimation may be significantly reduced in the future as increases in the computer power allows simulations at higher spatial resolution and perhaps eventually the use of cloud-resolving models.

The improved model performance at higher spatial resolutions provide motivation for use of regional climate models when only a limited area is of interest, such as North America. The spatial resolution of these models is sufficient to resolve the major mountain chains; some of these models thus display considerable skill in areas where topography plays a major role in the spatial patterns. For example, they are able to reproduce rather well the spatial distribution of the magnitude of the 95th percentile of precipitation (Leung et al. 2003), the frequency of days with more than 50 mm and 100 mm (Kim and Lee 2003), the frequency of days over 25 mm (Bell et al. 2004), and the annual maximum daily precipitation amount (Bell et al. 2004) over the western U.S. Kunkel et al. (2002) found that an RCM's simulation of the magnitude of extreme events over the U.S. varied spatially and depended on the duration of the event being examined; there was a tendency for overestimation in the western U.S. and good agreement or underestimation in the central and eastern U.S.

Most studies of observed precipitation extremes suggest that such extremes have increased in frequency and intensity during the latter half of the 20th Century. A study by Tebaldi et al. (2006) indicates that models generally simulate a trend towards a world

characterized by intensified precipitation, with a greater frequency of heavy-precipitation and high-quantile events, although with substantial geographical variability. This is in agreement with observations. Wang and Lau (2006) find that the CGCMs simulate an increasing trend in heavy rain over the tropical ocean.

Heat and cold waves

Analysis of simulations produced for the IPCC AR4 by seven climate models indicates that they reproduce the primary features of cold air outbreaks (CAOs), with respect to location and magnitude (Vavrus et al. 2006). In their analysis, a CAO is an episode of at least 2 days duration during which the daily mean winter (December-January-February) surface temperature at a gridpoint is 2 standard deviations below the gridpoint's winter mean temperature. Maximum frequencies of about four CAO days/winter are simulated over western North America and Europe, while minimal occurrences of less than one day/winter exist over the Arctic, northern Africa, and parts of the North Pacific. The GCMs are generally accurate in their simulation of primary features, with a high pattern correlation with observations and the maximum number of days meeting the CAO criteria around 4 per winter. One favored region for CAOs is in western North America, extending from southern Alaska into the upper Midwest. Here, the models simulate a frequency of about 4 CAO days per year, in general agreement with the observed values of 3-4 days. The models underestimate the frequency in the southeastern United States: mean simulated values range from 0.5 to 2 days *versus* 2 to 2.5 days in observations. This regional bias occurs in all the models and reflects the inability of GCMs to penetrate Arctic air masses far enough southeastward over North America.

The IPCC AR4 model simulations show a positive trend for growing season, heat waves and warm nights and a negative trend for frost days and daily temperature range (maximum minus minimum) (Tebaldi et al. 2006). They indicate that this is in general agreement with observations, except that there is no observed trend in heat waves. The modeled spatial patterns have generally larger positive trends in western North America than in eastern sections. For the U.S., this is in qualitative agreement with observations which show that the decreases in frost-free season and frost days are largest in the western U.S. (Kunkel et al. 2004; Easterling et al. 2002).

Analysis of individual models provides a more detailed picture of model performance. In a simulation from the PCM (Meehl et al. 2004), the largest trends for decreasing frost days occurs in the western and southwestern USA (values greater than –2 days per decade), and trends near zero in the upper Midwest and northeastern USA, in good agreement with observations. The biggest discrepancy between model and observations is over parts of the southeastern USA where the model shows trends for decreasing frost days and the observations show slight increases. This is thought to be a partial consequence of the two large El Nino events in the observations during this time period (1982–83 and 1997–98) where anomalously cool and wet conditions occurred over the southeastern USA and contributed to slight increases of frost days. The ensemble mean from the model averages out effects from individual El Nino events, and thus the frost day trends reflect a more general response to the forcings that occurred during the latter part of the twentieth century. In a four-member ensemble of simulations from the HadCM3 (Christidis et al. 2005), the model shows a rather uniform pattern of increases in the warmest night for 1950-1999. The observations also show a global mean increase, but with considerable regional variations. In North America, the observed trends in the warmest night vary from negative in the south-central sections to strongly positive in Alaska and western Canada, compared to a rather uniform pattern in the model. However, this discrepancy might be expected, since the observations probably reflect a strong imprint of internal climate variability that is reduced by ensemble averaging of the model simulations.

An analysis of the magnitude of temperature extremes for California in a regional climate model simulation (Bell et al. 2004) show mixed results. The hottest maximum in model is 4°C less than observations, while coldest min is 2.3°C warmer. The number of days >32°C is 44 in the model compared to an observed value of 71. This could result from the lower diurnal temperature range in the model (15.4°C observed vs. 9.7°C simulated). While these results are better than the driving GCM, the RCM results are still somewhat deficient, perhaps reflecting the very complex topography of the region of study.

Models display some capability to simulate extreme temperature and precipitation events, but there are differences from observed characteristics. They typically produce global increases in extreme precipitation and severe drought, and decreases in extreme minimum temperatures and frost days, in general agreement with observations. There is a general, though not universal, tendency to underestimate the magnitude of heavy precipitation events. Regional trend features are not always captured. Since the causes of observed regional trend variations are not known in general and such trends could be due in part to stochastic variability of the climate system, it is difficult to assess the significance of these discrepancies.

Chapter VI – Future Model Development

Cloud-resolved models

Cloud resolving models (CRMs) have spatial resolutions of less than a few kilometers. CRMs can therefore explicitly calculate many atmospheric systems that are on sub-grid scales of AGCMs (Randall et al. 2005). These include the mesoscale organizations in squall lines, updrafts and downdrafts, and cirrus anvils. The CRMs also allow calculation of cloud properties and cloud amount with more realistic dynamical conditions, and thus their impact on radiative transfer. Because of improved resolution, CRMs can also better simulate the spatial distribution of precipitation and convective enhancement of the surface fluxes, which are important to describe the interaction of the atmosphere with the land and ocean surfaces.

CRMs are variations of models designed for mesoscale storm and cumulus convection simulations. At CRM scales, hydrostatic balance is no longer universally valid. CRMs are therefore formulated with non-hydrostatic primitive equations in which vertical accelerations are calculated. Tripoli (1992) contains a good review of the various model formulations used to simulate non-hydrostatic meteorological dynamics.

Similar to AGCMs, CRMs also contain empirical relationships to calculate the impact of sub-grid scale processes. These relationships however have different roles from those in AGCMs. First, because CRMs capture a large portion of the size spectrum of the meteorological systems, the impact of the empiricism is less important in CRMs. For example, cumulus parameterizations are no longer needed in CRMs. Second, since CRMs better resolve atmospheric dynamics, moist processes can be formulated based on more realistic physical conditions.

CRMs can therefore accommodate more sophisticated microphysical and precipitation processes than AGCMs. One-moment bulk microphysical schemes (mass concentration only) with two-class liquid (cloud water and rain) and three-class ice (cloud ice, snow

and graupel/hail) are commonly used in CRMs. This level of sophistication is however rare in AGCMs. Some CRMs have started to use explicit bin-microphysical schemes. These schemes solve the stochastic kinetic equations for the size distribution functions of water droplets (both cloud droplets and raindrops) and different ice particle habitats (i.e., columnar, plate-like, dendrites, snowflakes, graupel and frozen drops). Because of better size information, these schemes can more realistically calculate the nucleation or activation processes of clouds, along with more accurate calculation of conversion processes among different cloud habitats (Tao 2007).

Subgrid scale processes in CRMs are calculated by using turbulence models. The majority of CRMs use either simple first-order closure to diagnostically compute the turbulent diffusion strength, or the one-and-a-half order closure to prognostically calculate the turbulent kinetic energy which is then used to determine turbulent diffusion coefficients. Prognostic methods typically take into account the thermodynamic stability, deformation, shear stability, diffusion, dissipation, moist processes and transport of sub-grid energy (Klemp and Wilhelmson 1978). Other CRMs use higher order turbulence closures (Krueger 1988).

Radiative transfer in the atmosphere and surface fluxes of heat and moisture in CRMs are computed using algorithms similar those in AGCMs. Because of better spatial resolution atmospheric fields such as clouds and precipitation, CRMs calculate these parameters more accurately than AGCMs.

High resolution of CRMs, however, is at the expense of model domain size and integration length. Current computing infrastructure, with the exception of the Earth Simulator, only allows CRMs to simulate the atmosphere of less than a few thousand kilometers. Most previous CRM studies were carried out only for two-dimensional slices of the atmosphere, an assumption that somewhat compromises the fidelity of three-dimensional convective cloud simulations. Few CRM simulations are carried out for longer than a year. CRMs with explicit bin-microphysics or high order turbulence closures have been integrated only for a few days.

Research with CRM falls into two categories. In the first one, CRMs are used to investigate the time evolution of cloud systems by specifying realistic initial conditions. This type of study enables deterministic understanding of convection initiation, cold pools, surface fluxes and their direct comparison with aircraft and other high resolution observation. The simulations are however only valid for a few hours. In the second category, CRMs are used to study the properties of cloud ensembles by specifying external forcing fields. This approach allows statistical description of multiple cloud types with different life cycles (Tao 2007). CRMs have been used to study convective organizations (e.g., Nakazawa 1988; Grabowski et al. 1998), convective transport of heat, moisture and momentum (e.g., Trier et al. 1996; Tao et al. 2003). They have been also used to study diurnal variation of precipitation (e.g., Sui et al. 1998; and Liu and Moncrieff 1998), radiation-convection interaction (e.g., Held et al. 1993; Xu and Randall 1998; Tao et al. 1999; Tompkins and Craig 1998; Grabowski and Moncrieff 2001; Gao et al. 2006), aerosol-chemistry-precipitation interaction (e.g., Khain and Porovsky 2004; Fridlind et al. 2004; Khain et al. 2004, 2005; Wang et al. 2005; DeCaria et al. 2005; Lynn et al. 2005; Ott et al. 2006; Chen et al. 2006), intraseasonal oscillation (e.g., Grabowski 2003), and representation of moist processes in large-scale models (e.g., Xu and Randall 1998; Wu and Moncrieff 2001; Grabowski and Moncrieff 2001; Wu et al. 2003; Ghan et al., 2001; Xie et al. 2005; Xu et al. 2005; Wu et al. 2006; Chen and Xu 2006).

Although CRMs are advantageous over ACGMs in describing moist processes, they also face unique challenges. CRM results are often very sensitive to the specification of initial conditions and external forcing conditions. They are also sensitive to the physical algorithms in it. There are still large uncertainties in the CRM cloud microphysics, including prediction of ice particle concentrations, falling speed calculation of cloud habitats, initial broadening of cloud droplet spectra in warm clouds, details of hydrometeor spectra evolution, quantitative simulations of entrainment rates (Cotton 2003). The high sensitivity of model results makes it difficult to rigorously validate CRMs.

Several field programs, such as the DOE ARM program, have enabled collection of observational data that are essential to evaluate CRMs (Zhang et al. 2001; Tao et al. 2004). Results from these programs will facilitate the improvement of model physics. On the other hand, global CRM has been developed and has been integrated on the Earth Simulator with spatial resolution of 7 kilometers (Miura et al. 2005). Progresses on both fronts could guide where climate models should go in the future.

Biogeochemistry

The Carbon Cycle *Libes* [1992] defined biogeochemistry as "the science that studies the biological, chemical, and geological aspects of environmental processes". At present, three-dimensional climate models are usually limited to the physical climate system: atmosphere, land, ocean, and sea ice. However, the physical climate system and biogeochemical processes are tightly coupled. For example, changes in climate affect the exchange of atmospheric CO_2 with the land surface and ocean, and changes in CO_2 fluxes affect Earth's radiative forcing and thus the physical climate system. Some recently developed AOGCMs have included the carbon cycle and confirmed the potential for strong feedback between it and global climate (Cox et al., 2001; Friedlingstein et al., 2001; Govindasamy et al., 2005). The next generation of AOGCMs is expected to include the carbon cycle and possibly interactive atmospheric aerosols and chemistry. Such models would predict time-evolving atmospheric concentrations of CO_2, etc., using anthropogenic emissions rather than assumed concentrations as input.

Models that include the global carbon cycle must account for the processes shown in Figure 6.1. Boxes represent the carbon reservoirs and arrows show the direction and magnitude of the fluxes. The present-day atmosphere holds about 750 Petagrams of carbon atoms in the form of CO_2. ("Petagrams of carbon" is abbreviated PgC; note that 1 Petagram $=10^{15}$ grams $= 10^9$ metric tons.) A roughly equal amount of carbon is contained in land vegetation and about twice as much in soils. The ocean is by far the largest reservoir of carbon with about 40,000 PgC. The largest flows of carbon in the system are

photosynthetic uptake of ~120 PgC / year by terrestrial ecosystems (gross primary productivity or GPP), plant respiration which releases ~60 PgC / year back to the atmosphere (hence the remainder—net primary production or NPP—is ~60 PgC / year), and heterotrophic (soil) respiration which releases ~60 PgC / year. In the upper ocean, photosynthesis by marine organisms incorporates carbon at the rate of ~50 PgC / year, about 4/5 of which is reconverted to CO_2 and related inorganic carbon molecules by respiration. The remaining ~10 PgC / yr of organic matter sinks into deep ocean, a process sometimes called the "biological pump." This organic matter is oxidized and eventually returns to the surface ocean via a combination of both convective / turbulent mixing and the "solubility pump" (the latter so named because it involves sinking of cold water, with high levels of dissolved inorganic carbon, near the poles).

The present-day global carbon cycle is not in equilibrium because of fossil fuel burning and other anthropogenic carbon emissions. These must of course be included in models of climate change, but such a calculation is not easy because human-induced changes to the carbon cycle are small compared to the large natural fluxes discussed above. Fossil fuels are estimated to contain about 4,000 PgC. During the 1990s, fossil fuel emissions averaged ~6 PgC / year and carbon release from land cover change (e.g. deforestation) averaged ~2 PgC / year, providing a net anthropogenic source of ~8 PgC / year to the atmosphere. Terrestrial and ocean ecosystems together absorbed about half of this flux, i.e. ~4 PgC / year, with the net uptake of carbon by the terrestrial biosphere and the net flux of CO_2 into the ocean each estimated as ~2 PgC / year. The rest (~ 4 PgC/ year) accumulated in the atmosphere, appearing as an increasing concentration of atmospheric CO_2.

The globally averaged carbon reservoirs and fluxes shown in Figure 6.1 are consistent with estimates from a variety of sources, but substantial uncertainties attach to the numbers (e.g. often a factor > 2 uncertainty for fluxes; see Prentice et al. 2001). Additional uncertainty applies to regional, seasonal and interannual variations in the carbon cycle. Evaluation of climate-carbon cycle models is therefore problematic: for many aspects of a simulation it is not clear what the "right answer" is.

Recent three-dimensional climate-carbon modeling studies

The feedbacks between the physical climate system and the carbon cycle are represented plausibly, but with substantial differences, in different AOGCM / carbon-cycle models. Cox et al. (2000) obtained a very large positive feedback, with global warming reducing the fraction of anthropogenic carbon absorbed by the biosphere and thus boosting the model's simulated atmospheric CO_2; Friedlingstein et al. (2001) obtained a much weaker feedback. Thompson et al. (2004) demonstrated that making different assumptions about the land biosphere within a single model gave markedly different feedback values. Using the same model, Govindasamy et al. (2005) noted a positive correlation between the magnitude of carbon cycle feedback and the sensitivity (q.v.) of the physical climate system.

A recent study examined carbon cycle feedbacks in eleven coupled AOGCM / carbon-cycle models using the same forcing (Friedlingstein et al., 2006). There was unanimous agreement among the models that global warming will reduce the fraction of anthropogenic carbon absorbed by the biosphere, but the magnitude of this feedback varied widely among the models (Fig 6.2), leading to additional global warming (when the models included an interactive carbon cycle) ranging between 0.1 to 1.5 °C. Eight models attributed most of the feedback to the land biosphere, while three attributed it to the ocean.

These results demonstrate extreme sensitivity of climate model output to assumptions about carbon-cycle processes. To reduce the consequent uncertainties in model predictions of the future, it will be necessary to thoroughly compare model output with real-world observations for present day conditions. Studies that span a broad range of ecosystems and climate regimes, including both and global remote sensing by satellites and local in situ measurements, are beginning to be integrated with diagnosis and improvements of the models. For example, the CCSM Biogeochemistry Working Group

has recently begun intercomparison of three different biogeochemistry sub-models within the CCSM (climate.ornl.gov/bgcmip).

Other biogeochemical cycles Methane (CH_4) is a potent greenhouse gas and part of the carbon cycle. Also, CO_2-fertilized ecosystems are limited by the availability of nutrients such as nitrogen and phosphorous, so changes in their availability are important to the carbon cycle through changes in plant nutrient availability (Field et al. 1995; Schimel 1998; Nadelhoffer et al. 1999; Shaw et al. 2002; Hungate et al. 2003). Future climate-carbon models will probably represent these variables. The few models that do so now show less plant growth in response to increasing atmospheric CO_2 (Cramer et al. 2001, Oren et al. 2001, Nowak et al. 2004). Incorporation of other known limiting factors such as acclimation of soil microbiology to the higher temperatures (Kirschbaum, 2000; Tjoelker*, et al*., 2001), and other elemental cycles such as the sulfur cycle (which affects aerosol and cloud properties), will also be important in developing comprehensive Earth system models.

Land Cover and land management practice changes

Generally, climate-carbon models do not include the effects land cover and land management changes on natural ecosystems. Land cover change is often accounted for simply by prescribing estimates for the historical period (e.g., Houghton, 2003) and the IPCC SRES scenarios for the future. These estimates do not include practices such as crop irrigation and fertilization. Many models with "dynamic vegetation" do not actually simulate crops; they allow only natural vegetation to grow. Deforestation, land cultivation and related human activities will probably be included in at least some future AOGCMs, enabling assessment of total anthropogenic effects on the global climate and environment (Ramankutty et al. 2002, Root and Schneider 1993).

Ocean Biogeochemistry

With respect to the ocean, we are concerned with how global warming impacts the marine environment including changes in the carbon content of the ocean and feedbacks to the atmosphere. Also of importance are the effects of modified ocean temperature, salinity and circulation patterns on the ocean's biota. Implementation of ocean biogeochemistry processes into AOGCMs is still in the development stage (e.g. CCSM Biogeochemistry Working Group Meeting Report, Mar. 2006, and NOAA-GFDL Earth System Model, *http://gfdl.noaa.gov/~jpd/esmdt.html*) but is expected to proceed rapidly (*Doney et al.* 2004) to improve simulation of the ocean carbon cycle under various scenarios.

One challenge to this effort is the complexity of the ocean's ecosystems. Complexity is added with each organism that fixes nitrogen, denitrifies, calcifies, or silicifies because each adds additional parameterizations and variables to the system (*Hood et al*. 2006). There needs to be sufficient complexity in the biological models to capture the variability of the system as observed. In addition, models should include processes that are important over time periods substantially greater than a year (*Rothstein et al.* 2006) in addition to much shorter periods. However, Earth system models cannot be so complex that their computational cost precludes their actual use, and adding complexity to the biogeochemistry models may lead to a decrease in their predictive ability because the inability to constrain the model with the available data (*Hood et al*. 2006). Thus, as with other component models such as those simulating clouds and convection, the development of ocean (and land) BGC models for incorporation into physical climate models involves a trade-off between realism and tractability.

The current strategy of climate modeling groups to address ocean carbon and biogeochemistry includes systematic comparison of different models in the Ocean Carbon-Cycle Model Intercomparison Project (OCMIP) under auspices of the International Geosphere-Biosphere Programme (IGBP). The most recent phase of OCMIP involved 13 groups—including several from the USA—implementing a common biological model in their different ocean GCMs (*Najjar et al.* 2006). The common biological model includes five prognostic variables: inorganic phosphate (PO_4^{2-}),

dissolved organic phosphorus (DOP), dissolved oxygen (O_2), dissolved inorganic carbon (CO_2 + HCO_3^- + CO_3^{2-}) and total alkalinity (the acid / base buffering capacity of the system). Intercomparison of the models revealed significant differences in simulated biogeochemical fluxes and reservoirs. A biogeochemistry model's realism of any particular simulation is closely tied to the dynamics of the simulation's circulation model. The US climate modeling groups are building upon this community effort to incorporate biogeochemistry into the ocean component of the models.

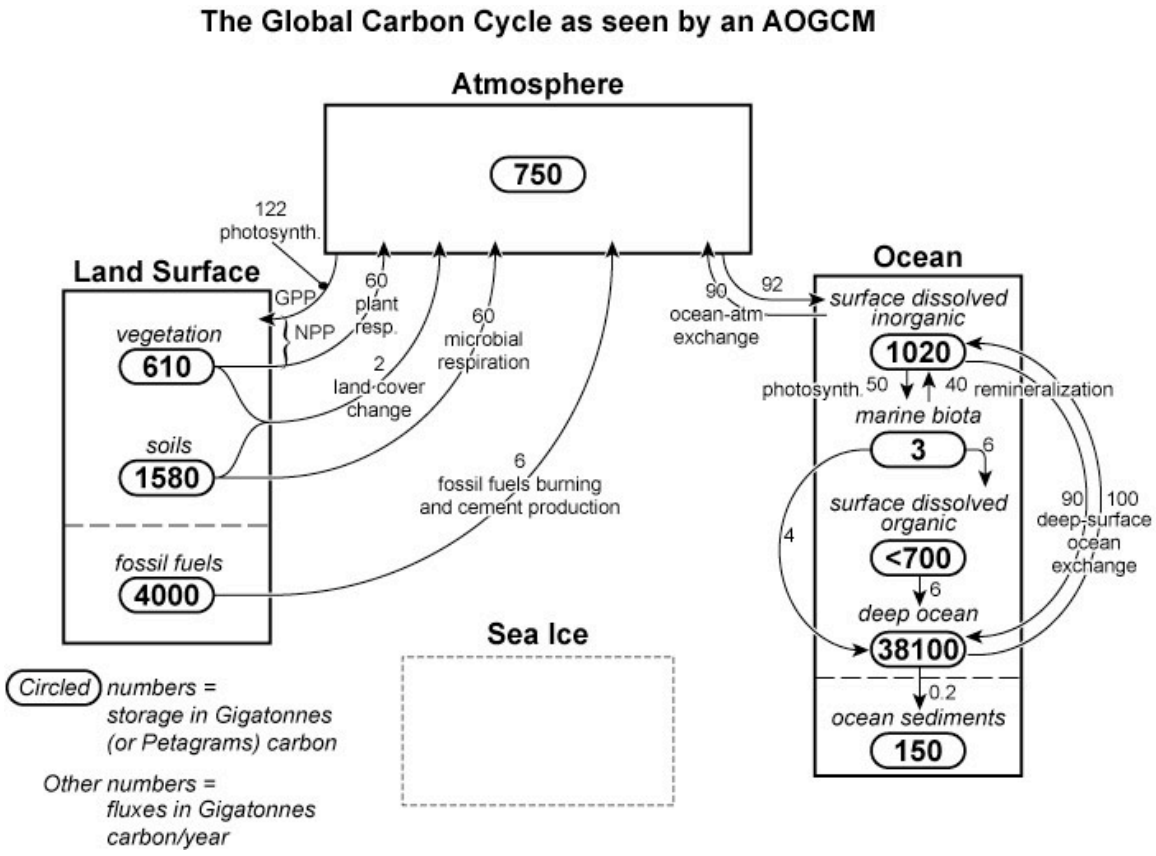

Figure 6.1: The global carbon cycle from the point of view of existing physical climate system models (coupled AOGCMs). The four boxes represent atmosphere, land-surface, ocean and sea-ice—the major components of AOGCMS. Earth System Models will evolve from AOGCMS by incorporating the relevant biogeochemical cycles into the four-box framework (with the sea-ice component not being a reservoir of carbon). Numbers shown are average values for the 1990s. Small (□1 PgC / year) fluxes such as carbon runoff from land to ocean and methane fluxes are not shown, except for burial of ~0.2 PgC / year in ocean bottom sediments. Burial in ocean sediments removes carbon from the AOGCM four-box domain;

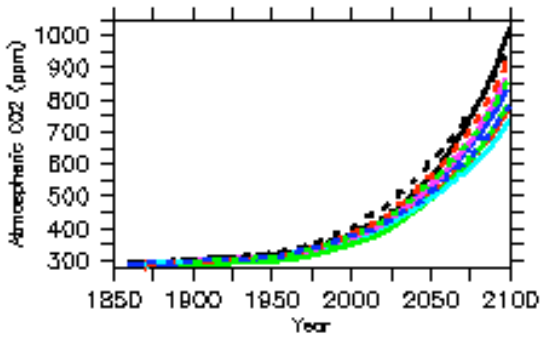

Figure 6.2: Time series of atmospheric CO_2 temperature from eleven different AOGCM / carbon cycle models (from Friedlingstein et al. 2006, Figure 1(a))

Chapter VII - Example Applications of Climate Model Results

Dryland Crop Yields

The effects of weather and climate on crops are complicated and not fully understood. Numerous models that simulate crop growth have been developed. These models parameterize many physiological processes. The present generation of state-of-the-art crop models typically steps through the growth process at a daily resolution and utilizes as input a number of meteorological variables that usually include maximum and minimum temperature, precipitation, solar radiation, and potential evapotranspiration. A key characteristic of these models is that they have been developed for application to a point location and have been validated based on point data, including meteorological inputs. Thus, the use of these models for assessment of climate change impacts on crop yields confronts a mismatch between the spatially-averaged climate model grid box data and the point data expected by the crop models. Also, biases in climate model data can have unknown effects on crop model results because the dependence of crop yields on meteorological variables is highly non-linear. The typical applications study circumvents these difficulties by avoiding the direct use of climate model output using some form of statistical downscaling. One approach developed during the early days of climate change assessments is still used today. In this approach, sometimes dubbed the “delta” method, the climate model output is used to determine the future change in climate with respect to the present-day climate, typically a difference for temperature and a percentage change for precipitation. Then, these change functions are applied to historical daily climate data for input to the crop model. In a second approach, the climate model data is used to adjust statistical characteristics of the observed data. Then, daily weather data for future periods are artificially produced using weather generators. In a recent study, Zhang (2005) used this approach to estimate Oklahoma wheat yields for a future simulation from HadCM3. These methods do not transmit certain climate model-simulated changes that do not affect basic statistical characteristics but might affect yields (a change to longer wet and dry spells without a change in total precipitation). Thus, additional uncertainty is introduced by such downscaling.

Small watershed flooding

This application faces many of the same issues as for dryland crop yields. For example, the models used for simulating runoff in small watersheds have been validated using point station data. In addition, runoff is a highly non-linear function of precipitation and the occurrence of flooding is particularly sensitive to the exact frequency and amount of precipitation for the most extreme events. As noted in Section V.H, climate models often under-estimate the magnitude of extremes. The ubiquitous "delta" method is also often used in such applications. Recently, Cameron (2006) determined percentage changes in precipitation from climate model simulations and applied these to a stochastic rainfall model to produce precipitation time series for input to a hydrologic model.

Urban heat waves

This estimation of changes in heat wave frequency and intensity can be accomplished using only near-surface temperature, a state variable. In addition, heat waves are large-scale phenomena and near-surface temperature is rather highly correlated over the scale of grid box size. Biases remain an issue, but that can be circumvented by using percentile-based definitions of heat waves. Meehl and Tebaldi (2004) used output from the National Center for Atmospheric Research/U.S. Department of Energy Parallel Climate Model (PCM) for 2080-2099 to calculate percentile-based measures of extreme heat; they found that heat waves will increase in intensity, frequency, and duration. If mortality estimates are desired, then biases are an issue because existing models (Kalkstein and Green 1997) used location-specific absolute magnitudes of temperature to estimate mortality. However, in this case, there are other factors that should be considered, such as adaptation (e.g. Davis et al. 2002).

REFERENCES:

AchutaRao, K.M., B.D. Santer, P.J. Gleckler, K.E. Taylor, D.W. Pierce, T.P. Barnett, and T.M.L. Wigley, 2006: Variability of ocean heat uptake: Reconciling observations and models. *Journal of Geophysical Research,* **111**, 10.1029/2005JC003136.

AchutaRao, Krishna and K.R. Sperber, 2006: ENSO simulation in coupled ocean-atmosphere models: Are the current models better? *Climate Dynamics*, 10.1007/s00382-006-0119-7.

Ackerman, A.S., M.P. Kirkpatrick, D.E. Stevens, and O.B. Toon, 2004: The impact of humidity above stratiform clouds on indirect aerosol climate forcing. *Nature,* **432**, 1014–1017.

Adams, R.M., B.A. McCarl, L.O. Mearns, 2003: The effects of spatial scale of climate scenarios on economic assessments: An example from U.S. agriculture. *Climate Change,* **60**, 131–148.

Albrecht, B.A., 1989: Aerosols, cloud microphysics, and fractional cloudiness. *Science,* **245**, 1227–1230.

Alley, R.B., R.U. Clark, P. Huybrechts, and I. Joughin, 2005: Ice-sheet and sea-level changes. *Science,* **310**, 456–460.

Ammann, C.M., G.A. Meehl, W.M. Washington, and C.S. Zender, 2003: A monthly and latitudinally varying volcanic forcing dataset in simulations of 20th century climate. *Geophysical Research Letters,* **30(12)**, **1657**.

Anderson, B.T., J.O. Roads, S.C. Chen, and H.M.H. Juang, 2001: Model dynamics of summertime low-level jets over northwestern Mexico. *Journal of Geophysical Research,* **106 (D4)**, 3401–3413.

Anderson, C.J., R.W. Arritt, E.S. Takle, Z. Pan, W.J. Gutowski, R. da Silva, and PIRCS modelers, 2003: Hydrologic processes in regional climate model simulations of the central United States flood of June–July 1993. *Journal of Hydrometeorology*, **4**, 584–598.

Anderson, C.J., R.W. Arritt, and J.S. Kain, 2007: An alternative mass flux profile in the Kain-Fritsch Convective Parameterization and its effects in seasonal precipitation. *Journal of Hydrometeorology* (accepted).

Anderson, T.L., R.J. Charlson, S. Schwartz, R. Knutti, O. Boucher, H. Rodhe, and J. Heintzenberg, 2003: Climate forcing by aerosols—a hazy picture. *Science*, **300**, 1103–1104.

Andersson, L., J.J. Wilk, M.C. Todd, D.A. Hughes, A. Earle, D. Kniverton, R. Layberry, and H.H.G. Savenije, 2006: Impact of climate change and development scenarios on flow patterns in the Okavango River. *Journal of Hydrology,* **331**, 43–57.

Annamalai, H., K. Hamilton, and K.R. Sperber, 2007: South Asian summer monsoon and its relationship with ENSO in the IPCC AR4 simulations. *Journal of Climate* (in press).

Antic, S., R. Laprise, B. Denis, and R. de Elia, 2006: Testing the downscaling ability of a one-way nested regional climate model in regions of complex topography. *Climate Dynamics,* **26**, 305–325.

Antonov, J.I., S. Levitus, and T.P. Boyer, 2005: Thermosteric sea level rise, 1955–2003. *Geophysical Research Letters,* **32**, L12602.

Arakawa, A. and W.H. Schubert, 1974: Interaction of a cumulus cloud ensemble with the large-scale environment. Part I. *Journal of Atmospheric Science,* **31**, 674–701.

Arendt, A.A., K.A. Echelmeyer, W.D. Harrison, C.S. Lingle, and V.B. Valentine, 2002: Rapid wastage of Alaska glaciers and their contribution to rising sea level. *Science,* **297**, 382–386.

Arora, V.K. and G.J. Boer, 2003: A representation of variable root distribution in dynamic vegetation models. *Earth Interactions,* **7**, 1–19.

Arzel, O., T. Fichefet and H. Goosse, 2006: Sea ice evolution over the 20th and 21st centuries as simulated by current AOGCMs. *Ocean Modelling*, **12**, 401–415.

Aurela, M., T. Laurila, and J.P. Tuovinen, 2004: The timing of snow melt controls the annual CO2 balance in a subarctic fen. *Geophysical Research Letters,* **31**, L16119.

Avissar, R.and R.A. Pielke, 1989: A parameterization of heterogeneous land-surface for atmospheric numerical models and its impact on regional meteorology. *Monthly Weather Review,* **117**, 2113–2136.

Baldocchi, D. and P. Harley, 1995: Scaling carbon dioxide and water vapour exchange from leaf to canopy in a deciduous forest. I. Leaf model parameterization. *Plant, Cell and Environment,* **18**, 1146–1156.

Barnett, T.P., D.W. Pierce, K.M. AchutaRao, P.J. Gleckler, B.D.Santer, J.M. Gregory, and W.M. Washington, 2005: Penetration of human-induced warming into the world's oceans. *Science*, 309, 284.

Beckman, A. and R. Doscher, 1997: A method for improved representation of dense water spreading over topography in geopotential-coordinate models, *Journal Physical Oceanography*, **27**, 581–591.

Bell, J.L., L.C. Sloan, and M.A. Snyder, 2004: Regional changes in extreme climatic events: a future climate scenario. *Journal of Climate*, **17**(**1**), 81–87.

Bellouin, N., O. Boucher, J. Haywood, and M.S. Reddy, 2005: Global estimate of aerosol direct radiative forcing from satellite measurements, *Nature*, **438**, 1138–1141.

Beringer, J., A.H. Lynch, F.S. Chapin, M. Mack, and G.B. Bonan, 2001: The representation of arctic soils in the land surface model: The importance of mosses. *Journal of Climate,* **14**, 3324–3335.

Biasutti, M.and A. Giannini, 2006: Robust Sahel drying in response to late 20th century forcings, *Geophysical Research Letters,* **33**, L11706.

Bierbaum, R.M., M.J. Prather, E.M. Rasmusson and A.J. Weaver, 2003: *Estimating Climate Sensitivity: Report of a Workshop.* National Academy of Sciences, Washington, D.C. (http://books.nap.edu/catalog/10787.html).

Bitz, C.M.and W.H. Lipscomb, 1999: An energy-conserving thermodynamic model of sea ice. *Journal of Geophysical Research,* **104**, 15 669–15 677.

Bjerknes, Jacob, 1969: Atmospheric teleconnections from the equatorial Pacific. *Monthly Weather Review,* **97**, 163172.

Bleck, R., 2002: An oceanic general circulation model framed in hybrid isopycnic-Cartesian coordinates. *Ocean Modelling*, **4**, 55–88.

Boisserie, M., D.W. Shin, T.E. Larow, and S. Cocke, 2006: Evaluation of soil moisture in the Florida State University climate model - National Center for Atmospheric Research community land model (FSU-CLM) using two reanalyses (R2 and ERA40) and *in situ* observations. *Journal of Geophysical Research,* **111** (**D8**), Art. No. D08103.

Bonan, G.B., 1995: Sensitivity of a GCM simulation to inclusion of inland water surfaces. *Journal of Climate,* **8**, 2691–2704.

Bony, S., R. Colman, V.M. Kattsov, R.P. Allan, C.S. Bretherton, J.-L. Dufresne, A. Hall, S. Hallegatte, M.M. Holland, W. Ingram, D.A. Randall, B.J. Soden, G.Tselioudis and M. J. Webb, 2006: How Well Do We Understand and Evaluate Climate Change Feedback Processes?, *Journal of Climate,* **19**, 3445–3482.

Bony, S., and J.-L. Dufresne, 2005: Marine boundary layer clouds at the heart of tropical cloud feedback uncertainties in climate models. *Geophysical Research Letters,* **32**, L20806.

Bony, S., J.-L. Dufresne, H. LeTreut, J.-J. Morcrette, and C. Senior, 2004: On dynamic and thermodynamic components of cloud changes. *Climate Dynamics*, **22**, 71–86.

Boone, A., V. Masson, T. Meyers, and J. Noilhan, 2000: The influence of the inclusion of soil freezing on simulations by a soil-vegetation-atmosphere transfer scheme. *Journal of Applied Meteorology,* **39**, 1544–1569.

Braithwaite, R.J. and S.C.B. Raper, 2002: Glaciers and their contribution to sea level change. *Physics and Chemistry of the Earth.,* **27**, 1445–1454.

Brankovic, T.and D. Gregory, 2001: Impact of horizontal resolution on seasonal integrations. *Climate Dynamics,* **18**, 123–143.

Breugem, W.-P., W. Hazeleger, and R.J. Haarsma, 2006: Multi-model study of tropical Atlantic variability and change. *Geophysical Research Letters* (submitted).

Briegleb, B.P., E.C. Hunke, C.M. Bitz, W.H. Lipscomb, and J.L. Schramm, 2002: *Description of the Community Climate System Model Version 2 Sea Ice Model*, 60 pp. (available at http://www.ccsm.ucar.edu/models/ccsm2.0/csim/).

Brinkop, S. and Roeckner, E., 1995: Sensitivity of a general circulation model to parameterizations of cloud-turbulence interactions in the atmospheric boundary layer. *Tellus*, **47A**, 197–220.

Bryan, F. O., G. Danabasoglu, P. R. Gent, K. Lindsay, 2006: Changes in ocean ventilation during the 21st Century in the CCSM3, *Ocean Modelling,* **15**, 141–156.

Bryan, K., 1969a: A numerical method for the study of the circulation of the world ocean, *Journal of Computational Physics,* **4**, 347–376.

Bryan, K., 1969b: Climate and the ocean circulation III: The ocean model, *Monthly Weather Review*, **97**, 806–824.

Bryan, K. and Cox, M. D., 1967: A numerical investigation of the oceanic general circulation, *Tellus,* **19**, 54–80.

Burke, E. J., S.J. Brown, and N. Christidis, 2006: Modelling the recent evolution of global drought and projections for the 21st century with the Hadley Centre climate model. *Journal of Hydrometeorology*, **7**, 1113–1125.

Byerle, L.A.and J. Paegle, 2003: Modulation of the Great Plains low-level jet and moisture transports by orography and large-scale circulations. *Journal of Geophysical Research,* **108 (D16)**, Art. No. 8611.

Cai, W.J., P.H. Whetton, and D.J. Karoly, 2003: The response of the Antarctic Oscillation to increasing and stabilitzed atmospheric CO_2. *Journal of Climate,* **16**, 1525–1538.

Callaghan, T.V. and Coauthors, 2004: Responses to projected changes in climate and UV-B at the species level. *Ambio,* **33**, 418–435.

Cameron, D., 2006: An application of the UKCIP02 climate change scenarios to flood estimation by continuous simulation for a gauged catchment in the northeast of Scotland, UK (with uncertainty). *Journal of Hydrology*, **328**, 212–226

Cane, M.A., A.C. Clement, A. Kaplan, Y. Kushnir, R. Murtugudde, D. Pozdnyakov, R. Seager, and S.E. Zebiak, 1997: Twentieth century sea surface temperature trends. *Science,* **275**, 957–960.

Capotondi, A., A. Wittenber, S. Masina, 2006: Spatial and temporal structure of ENSO in 20th century coupled simulations. *Ocean Modelling*, **15**, 274–298.

Carril, A.F., C.G. Menéndez, and A. Navarra, 2005: Climate response associated with the Southern Annular Mode in the surroundings of Antarctic Peninsula: A multimodel ensemble analysis. *Geophysical Research Letters,* **32**.

Cassano, J.J., P. Uotila, A.H. Lynch, and E.N. Cassano, 2007: Predicted changes in synoptic forcing of net precipitation in large Arctic river basins during the 21st century. *Journal of Geophysical Research* (in press).

Cassano, J.J., P. Uotilla, and A.H. Lynch, 2006: Changes in synoptic weather patterns in the polar regions in the 20th and 21st centuries, Part 1: Arctic. *International Journal of Climatology* (in press).

Cess, R.D., *et al.,* 1990: Intercomparison and interpretation of climate feedback processes in 19 atmospheric general circulation models. *Journal of Geophysical Research,* **95**, 16 601–16 615.

Charney, J.G., 1979: *Carbon Dioxide and Climate: A Scientific Assessment.* National Academy of Sciences, Washington, D.C., 22 pp.

Chen, F. and J. Dudhia, 2001: Coupling an advanced land surface–hydrology model with the Penn State–NCAR MM5 modeling system. Part I: Model implementation and sensitivity. *Monthly Weather Review,***129**, 569–585.

Cheng, A. and K.-M. Xu, 2006: Simulation of shallow cumuli and their transition to deep convective clouds by cloud-resolving models with different third-order turbulence closures. *Quarterly Journal of the Royal Meterological Society,* **132**, 359–382.

Cheng, Y., V.M. Canuto, and A.M. Howard, 2002: An improved model for the turbulent PBL, *Journal of Atmospheric Science,* **59**, 1550–1565.

Chiacchio, M., J. Francis, and P. Stackhouse, Jr., 2002: Evaluation of methods to estimate the surface downwelling longwave flux during Arctic winter. *Journal of Applied Meteorology,* **41**, 306–318.

Christensen, J.H., T. Carter, F. Giorgi, 2002: PRUDENCE employs new methods to assess European climate change. *Eos*, **83**, 147.

Christensen, O.B, 1999: Relaxation of soil variables in a regional climate model. *Tellus,* **51A**, 674–685.

Christidis, N., P.A. Stott, S. Brown, G.C. Hegerl, 2005: Detection of changes in temperature extremes during the second half of the 20th century. *Geophysical Research Letters,* **32**, L20716.

Chung, C.E., V. Ramanathan, D. Kim, and I. Podgorny, 2005: Global anthropogenic aerosol direct forcing derived from satellite and ground-based observations. *Journal of Geophysical Research,* **110**, D24207.

Church, J.A.and N.J. White, 2006: A 20th century acceleration in global sea-level rise. *Geophysical Research Letters,* **33**, L01602.

Choi, H.I., P. Kumar, and X.-Z. Liang, 2007: 3-D volume averaged soil-moisture transport model with a scalable parameterization of subgrid topographic variability. *Water Resources Research* (in press).

Clement, A.C., R. Seager, M.A. Cane, and S.E. Zebiak, 1996: An ocean dynamical thermostat. *Journal of Climate,* **9**, 2190–2196.

Clement, A.C. and B. Soden, 2005: The sensitivity of the tropical-mean radiation budget. *Journal of Climate,* **18**, 3189–3203.

Collins, M., B.B.B. Booth, G. Harris, J.M. Murphy, D.M.H. Sexton, M. Webb, 2006: Towards quantifying uncertainty in transient climate change. *Climate Dynamics* (in press)

Collins, W., *et al.,* 2004, Description of the NCAR Community Atmospheric Model (CAM3). *NCAR Technical Report* (in preparation).

Collins, W.D., C.M. Bitz, M.L. Blackmon, G.B. Bonan, C.S. Bretherton, J.A. Carton, P. Chang, S.C. Doney, J.J. Hack, T.B. Henderson, J.T. Kiehl, W.G. Large, D.S. McKenna, B.D. Santer, and R.D. Smith, 2006: The community climate system model: CCSM3. *Journal of Climate* (in press).

Collins, W.D., *et al.,* 2006: Radiative forcing by well-mixed greenhouse gases: Estimates from climate models in the Intergovernmental Panel on Climate Change (IPCC) Fourth Assessment Report (AR4), *Journal of Geophysical Research,* **111**, D14317.

Collins, W.D., C.M. Bitz, M.L. Blackmon, G.B. Bonan, C.S. Bretherton, J.A. Carton, P. Chang, S.C. Doney, J.J. Hack, T.B. Henderson, J.T. Kiehl, W.G. Large, D.S. McKenna, B.D. Santer, R.D. Smith, 2005: The Community Climate System Model: CCSM3. *Journal of Climate*, **18**.

Colman, R., 2003: A comparison of climate feedbacks in general circulation models. *Climate Dynamics*, **20**, 865–873.

Conkright, M.E., *et al.,* 2002: *World Ocean Atlas 2001:* Objective Analyses, Data Statistics, and Figures, CD-ROM documentation. NOAA, Silver Spring, Md. 17 pp.

Cook, K.H. and E.K. Vizy, 2006: Coupled model simulations of the West African monsoon system: 20th century simulations and 21st centurypredictions. *Journal of Climate*, **19**, 3681–3703.

Cotton, W.R., 2003: Cloud modeling from days of EML to the present—Have we made progress? AMS Meteorological Monographs—Symposium on Cloud Systems, Hurricanes and TRMM, 95–106.

Covey, C., L.C. Sloan, and M.I. Hoffert, 1996: Paleoclimate data constraints on climate sensitivity: The paleocalibration method. *Climatic Change,* **32**, 165–184.

Cox, P. M., R.A. Betts, C.D Jones, S.A. Spall, and I.J. Totterdell, 2000: Acceleration of global warming due to carbon-cycle feedbacks in a coupled model. *Nature*, **408**, 184–187.

Cramer, W., A. Bondeau, F.I. Woodward, and Coauthors, 2001: Global response of terrestrial ecosystem and function to CO_2 and climate change: Results from six dynamic global vegetation models. *Global Change Biology,* **7**, 357373.

Crane, R.G.and B.C. Hewitson, 1998: Doubled CO_2 precipitation changes for the Susquehanna basin: Down-scaling from the GENESIS general circulation model. *International Journal of Climatology,* **18**, 65–76.

Cubasch, U., G.A. Meehl, G.. Boer, R.J. Stouffer, M. Dix, A. Noda, C.A. Senior, S. Raper, and K.S. Yap, 2001: Projections of future climate change, pp. 525–582 in *Climate Change 2001: The Scientific Basis,* J.T. Houghton, Y. Ding, D.J. Griggs, M. Noguer, P.J. van der Linden, X. Dai, K. Maskell and C.A. Johnson (eds.), Cambridge University Press, 881 pp.

Curry, J.A. and A.H. Lynch, 2002: Comparing Arctic regional climate models. *Eos,* **83**, 87.

Curry, J.A., J. Schramm, and E.E. Ebert, 1995: On the sea ice albedo climate feedback mechanism. *Journal of Climate,* **8**, 240–247.

Curry, J.A., W.B. Rossow, D. Randall, and J.L. Schramm, 1996: Overview of Arctic cloud and radiation characteristics. *Journal of Climate,* **9**, 1731–1764.

Cusack, S., J.M. Edwards, and R. Kershaw, 1999: Estimating subgrid variance of saturation and its parametrization for use in a GCM cloud scheme. *Quarterly Journal of the Royal Meteorological Society,* **125**, 3057–3076.

Dai, A., 2006: Precipitation characteristics in eighteen coupled climate models. *Journal of Climate* (in press).

Dai, A., K.E. Trenberth, and T. Qian, 2004: A global data set of Palmer Drought Severity Index for 1870–2002: Relationship with soil moisture and effects of surface warming. *Journal of Hydrometeorology*, **5**, 1117–1130.

Danabasoglu, G., W.G. Large, J.J. Tribbia, P.R. Gent, and B.P. Briegleb, 2006: Diurnal ocean-atmosphere coupling. *Journal of Climate*, DOI: 10.1175/JCLI3739.1.

Davies, H.C., 1976: Lateral boundary formulation for multilevel prediction models. *Quarterly Journal of the Royal Meteorological Society,* **102**, 405–418.

Davies, H.C.and R.E. Turner, 1977: Updating prediction models by dynamical relaxation: An examination of the technique. *International Journal of Climatology,* **103**, 225–245.

Davis, R.E., P.C. Knappenberger, W.M. Novicoff, and P.J. Michaels, 2002: Decadal changes in heat-related human mortality in the eastern United States, *Climate Research*, **22**, 175–184.

Dehtloff, K. and Coauthors, 2006: A dynamical link between the Arctic and the global climate system. *Geophysical Research Letters,* **33**, L03703.

Del Genio, A.D. and M.-S. Yao, 1993: Efficient cumulus parameterization for long-term climate studies: The GISS scheme. *The Representation of Culumus Convection in Numeric Models. Meteoroogical Monograph,* No. 46, American Meteorological Society, 181–184.

Del Genio, A.D., W. Kovari, M.-S. Yao, and J. Jonas, 2004: Cumulus microphysics and climate sensitivity. *Journal of Climate* (journal).

Del Genio, A.D., A. Wolf, and M.-S. Yao, 2005b: Evaluation of regional cloud feedbacks using single-column models. *Journal of Geophysical Research*, **110**,

Del Genio, A.D., M.-S. Yao, W. Kovari, and K.-W. Lo, 1996: A prognostic cloud water parameterization for global climate models. *Journal of Climate,* **9**, 270–304.

Delworth, T.L., *et al.,* ????: GFDL's CM2 global coupled climate models—Part 1: Formulation and simulation characteristics. *Journal of Climate*, 19, 643–674, nested regional climate models: The big-brother experiments. *Climate Dynamics,* **18**, 627–646.

Denis, B., R. Laprise, and D. Caya, 2003: Sensitivity of a regional climate model to the resolution of the lateral boundary conditions. *Climate Dynamics,* **20**, 107–126.

Déqué, M.and J.P. Piedelievre, 1995: High-resolution climate simulation over Europe. *Climate Dynamics,* **11**, 321–339.

Déqué, M., R.G. Jones, M. Wild, F. Giorgi, J.H. Christensen, D.C. Hassell, P.L. Vidale, B. Rockel, D. Jacob, E. Kjellström, M. de Castro, F. Kucharski, and B. van den Hurk, 2005: Global high resolution versus Limited Area Model climate change projections over Europe: quantifying confidence level from PRUDENCE results. *Climate Dynamics,* **25**, 653–670.

Dickinson, R.E., A. Henderson-Sellers, and P.J. Kennedy, 1993: Biosphere-Atmosphere Transfer Scheme (BATS) version 1e as coupled to the NCAR Community Climate Model. NCAR Tech. Note, NCAR/TN-387+STR, National Center for Atmospheric Research, Boulder, CO, 72 pp.

Diffenbaugh, N.S., M.A. Snyder, L.C. Sloan, 2004: Could CO_2-induced land-cover feedbacks alter near-shore upwelling regimes? *Proceedings of the National Acadamy of Sciences,* **101**, 27–32.

Doney, S.C., R. Anderson, J. Bishop, K. Caldeira, C. Carlson, M..-E. Carr, R. Feely, M. Hood, C. Hopkinson, R. Jahnke, D. Karl, J. Kleypas, C. Lee, R. Letelier, C. McClain, C. Sabine, J. Sarmiento, B. Stephens, and R. Weller, 2004: *Ocean*

Carbon and Climate Change (OCCC): An implementation strategy for U.S. ocean carbon cycle science. UCAR, Boulder, CO, 108 pp.

Ducharne, A., C. Golaz, E. Leblois, K. Laval, J. Polcher, E. Ledoux, and G. de Marsily, 2003: Development of a high resolution runoff routing model, calibration and application to assess runoff from the LMD GCM. *Journal of Hydrology,* **280**, 207–228.

Duffy, P.B., B. Govindasamy, J.P. Iorio, J. Milovich, K.R. Sperber, K.E. Taylor, M.F. Wehner, and S.L. Thompson, 2003: High-resolution simulations of global climate, part 1: Present climate. *Climate Dynamics,* **21**, 371–390.

Duynkerke, P.G. and S.R. de Roode, 2001: Surface energy balance and turbulence characteristics observed at the SHEBA Ice Camp during FIRE III., *Journal of Geophysical Research,* **106**, 15 313–15 322.

DeCaria, A.J., K.E. Pickering, G.L. Stenchikov, and L.E. Ott, 2005: Lightning-generated NOx and its impact on tropospheric ozone production: A three-dimensional modeling study of a Stratosphere-Troposphere Experiment: Radiation, Aerosols and Ozone (STERAO-A) thunderstorm. *Journal of Geophysical Research,* **110**, D14303.

de Elía, R., R. Laprise, and B. Denis, 2002: Forcasting skill limits of nested, limited-area models: A perfect-model approach. *Monthly Weather Review,***130**, 2006–2023.

Easterling, D.R., 2002: Recent changes in frost days and the frost-free season in the United States. *Bulletin of the American Meteorological Society,* **83**, 1327–1332.

Ebert, E.E., J.L. Schramm, and J.A. Curry, 1995: Disposition of solar radiation in sea ice and the upper ocean. *Journal of Geophysical Research,* **100**, 15 965–15 975.

Emanuel, K.A., 1991: A scheme for representing cumulus convection in large-scale models. *Journal of Atmospheric Science,* **48**, 2313–2335.

Emanuel, K.A., 1994: *Atmospheric Convection*. Oxford University Press, Oxford, 580 pp.

Emori, S. and S.J. Brown, 2005: Dynamic and thermodynamic changes in mean and extreme precipitation under changed climate. *Geophysical Research Letters,* **32**, L17706.

Essery, R. and J. Pomeroy, 2004: Implications of spatial distributions of snow mass and melt rate for snow-cover depletion: theoretical considerations. *Annals of Glaciology,* **38**, 261–265.

Fedorov, A. and S.G. Philander. 2000. Is El Nino changing? *Science,* 288:1997–2002.

Field, C., R. Jackson, and H. Mooney, 1995: Stomatal responses to increased CO_2: Implications from the plant to the global scale. *Plant, Cell and Environment*, **18**, 1214–1225.

Fox-Rabinovitz, M.S. and R.S. Lindzen, 1993: Numerical experiments on consistent horizontal and vertical resolution for atmospheric models and observing systems. *Monthly Weather Review,* **121**, 264–271.

Fox-Rabinovitz, M.S., L. Takacs, R.C. Govindaraju, and M.J. Suarez, 2001: A variable-resolution stretched-grid general circulation model: Regional climate simulation. *Monthly Weather Review,***129**, 453–469.

Fox-Rabinovitz, M.S., L.L. Takacs, and R.C.Govindaraju, 2002: A variable-resolution stretched-grid general circulation model and data assimilation system with multiple areas of interest: Studying the anomalous regional climate events of 1998. *Journal of Geophysical Research,* **107(D24)**, Art. No. 4768.

Fox-Rabinovitz, M.S., J. Cote, B. Dugas, M. Deque, and J.L. McGregor, 2006: Variable resolution general circulation models: Stretched-grid model intercomparison project (SGMIP). *Journal of Geophysical Research,* **111**, (**D16)**, DI Art. No. D16104.

Frei, C., R. Schöll, S. Fukutome, J. Schmidli, and P.L. Vidale, 2006: Future change of precipitation extremes in Europe: An intercomparison of scenarios from regional climate models. *Journal of Geophysical Research,* **111** (**D6**), Art. No. D06105.

Frich, P., *et al.,* 2002: Observed coherent changes in climatic extremes during the second half of the twentieth century. *Climate Research,* **19**, 193–212.

Fridlind, A.M., *et al.,* 2004: Evidence for the predominance of mid-tropospheric aerosols as subtropical anvil cloud nuclei, *Science*, **304**, 718–722.

Friedlingstein, P., L. Bopp, P. Clais, and Coauthors, 2001: Positive feedback between future climate change and the carbon cycle. *Geophysical Research Letters,* **28**, 1543–1546.

Friedlingstein, P., P. Cox, R. Betts, and Coauthors, 2006: Climate-carbon cycle feedback analysis: Results from the C^4MIP model intercomparison, *Journal of Climate*, **19**, 3337–3353.

Foukal, P. and C. Fröhlich, H. Spruit and T.M.L. Wigley, 2006: Variations in solar luminosity and their effect on the Earth's climate. *Nature,* **443**, 161–166.

Fu, C B., S. Wang, Z. Xiong, W.J. Gutowski, D.-K. Lee, J.L. McGregor, Y. Sato, H. Kato, J.-W. Kim, and M.-S. Su, 2005: Regional Climate Model Intercomparison Project for Asia . *Bulletin of the American Meteorological Society,* **86**, 257–266.

Fyfe, J.C., G.J. Boer, and G.M. Flato, 1999: The Arctic and Antarctic Oscillations and their projected changes under global warming. *Geophysical Research Letters,* **11**, 1601–1604.

Ganachaud, A., 2003: Large-scale mass transports, water mass formation, and diffusivities estimated from World Ocean Circulation Experiment (WOCE) hydrographic data, *Journal of Geophysical Research,* **108**(**C7**), 3213.

Ganachaud, A. and C. Wunsch, 2000: Improved estimates of global ocean circulation, heat transport and mixing from hydrographic data, *Nature*, **408**, 453–457.

Gao, S., L. Ran, and X. Li, 2006: Impacts of ice microphysics on rainfall and thermodynamic processes in the tropical deep convective regime: A 2D cloud-resolving modeling study. *Monthly Weather Review* (in press).

Gates, W.L., A. Henderson-Sellers, G.J. Boer, C.K. Folland, A. Kitoh, B.J. McAvaney, F. Semazzi, N. Smith, A.J. Weaver and Q.-C. Zeng, 1996: Climate Models—Evaluation. In: *Climate Change 1995: The Science of Climate Change. Contribution of Working Group I to the Second Assessment Report of the Intergovernmental Panel on Climate Change* [Houghton, J.T., L.G. Meira Filho, B.A. Callander, N. Harris, A. Kattenberg, and K. Maskell (eds.)]. Cambridge University Press, Cambridge, United Kingdom, and New York, NY, USA, pp. 228–284.

Gent, P. and J.C. McWilliams, 1990: Isopycnal mixing in ocean circulation models. *Journal of Physical Oceanography,* **20**, 150–155.

GFDL Global Atmospheric Model Development Team (GAMDT), 2004: The new GFDL global atmosphere and land model AM2/LM2: evaluation with prescribed SST conditions. *Journal of Climate* (submitted).

Ghan, S. J., et al., 2000: An intercomparison of single column model simulations of summertime midlatitude continental convection, *Journal of Geophysical Research,* **105**, 2091–2124.

Giorgi, F. and X. Bi, 2000: A study of internal variability of a regional climate model. *Journal of Geophysical Research,* **105,** 29503–29521.

Giorgi, F., B. Hewitson, J. Christensen, M. Hulme, H. Von Storch, P. Whetton, R. Jones, L. Mearns, and C. Fu, 2001: Chapter 10. Regional climate change information—Evaluation and projections. In: *Climate Change 2001: The Scientific Basis*. [Houghton, J.T., Y. Ding, D.J. Griggs, M. Noguer, P.J. vad der Linden, X. Dai, K. Maskell, and C.A. Johnson (eds.)]. Cambridge University Press, Cambridge, United Kingdom, pp. 583–638.

Giorgi, F., M. R. Marinucci, and G. T. Bates, 1993: Development of a second-generation regional climate model (RegCM2). Part II: Convective processes and assimilation of lateral boundary conditions. *Monthly Weather Review,* **121,** 2814–2832.

Giorgi, F. and L.O. Mearns, 1991: Approaches to the simulation of regional climate change—A review. *Review of Geophysics,* **29**, 191–216

Giorgi, F. and L.O. Mearns, 1999: Introduction to special section: Regional climate modeling revisited. *Journal of Geophysical Research,* **104(D6),** 6335–6352.

Giorgi, F. and L.O. Mearns, 2003: Probability of regional climate change based on the Reliability Ensemble Averaging (REA) method. *Geophysical Research Letters,* **30**, Art. No. 1629.

Giorgi, F., L.O. Mearns, C. Shields, and L. Mayer, 1996: A regional model study of the importance of local versus remote controls of the 1988 drought and the 1993 flood over the central United States. *Journal of Climate*, **9**, 1150–1162.

Gleckler, P.J., K.R. Sperber, and K. AchutaRao, 2006: Annual cycle of global ocean heat content: Observed and simulated, *Journal of Geophysical Research,* **111**, C06008.

Gnanadesikan, A., K.W. Dixon, S.M. Griffies, V. Balaji, M. Barreiro, J.A. Beesley, W.F. Cooke, T.L. Delworth, R. Gerdes, M.J. Harrison, I.M. Held, W.J. Hurlin,

H.-C. Lee, Z. Liang, G. Nong, R.C. Pacanowski, A. Rosati, J. Russell, B.L. Samuels, Q. Song, M.J. Spelman, R.J. Stouffer, C.O. Sweeney, G. Vecchi, M. Winton, A.T. Wittenberg, F. Zeng, R. Zhang, and J.P. Dunne, 2006: GFDL's CM2 global coupled climate models. Part II: The baseline ocean simulation. *Journal of Climate,* **19**, 675–697.

Gorham, E., 1991: Northern peatlands—role in the carbon-cycle and probable responses to climatic warming. *Ecological Applications,* **1**, 182–195.

Govindasamy, B., S. Thompson, A. Mirin, M. Wickett, K. Caldeira, and C. Delire, 2005: Increase of carbon cycle feedback with climate sensitivity: Results from a coupled climate and carbon cycle model. *Tellus*, **57B**, 153–163.

Grabowski, W.W. and M. W. Moncrieff, 2001: Large-scale organization of tropical convection in two-dimensional explicit numerical simulations. *International Journal of Climatology,***127**, 445–468.

Grabowski, W.W., 2003: MJO-like coherent structures: Sensitivity simulations using the cloud-resolving convection parameterization (CRCP). *Journal of Atmospheric Science,* **60**, 847–864.

Gregory, D. and S. Allen, 1991: The effect of convective scale downdrafts upon NWP and climate simulations. *9th Conference Numerical Weather Prediction*. American Meteorological Society, Denver, Colorado, pp. 122–123.

Gregory, D. and P.R. Rowntree,1990: A mass flux convection scheme with representation of cloud ensemble characteristics and stability dependent closure. *Monthly Weather Review,* **118**, 1483–1506.

Gregory, J.M., 1999: Representation of the radiative effect of convective anvils. *Hadley Centre Technical Note 7*, Hadley Centre for Climate Prediction and Research, Met Office, Fitzroy Road, Exeter, EX1 3BP, United Kingdom.

Gregory, J.M., H.T. Banks, P.A. Stott, J.A. Lowe, and M.D. Palmer, 2004: Simulated and observed decadal variability in ocean heat content. *Geophysical Research Letters*, **31(15),** L15312, doi:10.1029/2004GL020258.

Gregory, J.M., J.A. Lowe, and S.F.B. Tett, 2006: simulated global-mean sea level changes over the last half-millennium. *Journal of Climate,* **19,** 4576–4592.

Grell, G.A., 1993: Prognostic evaluation of assumptions used by cumulus parameterizations. *Monthly Weather Review,* **121**, 764–787.

Grell, G.A., H. Dudhia, and D. S. Stanfler, 1994: A description of the fifth generation Penn State–NCAR Mesoscale Model (MM5). *NCAR Technical Note.* NCAR/TN-3981STR, 122 pp. [Available from National Center for Atmospheric Research, P.O. Box 3000, Boulder, CO 80305.]

Grell, G.A., L. Schade, R. Knoche, A. Pfeiffer, and J. Egger, 2000: Nonhydrostatic climate simulations of precipitation over complex terrain. *Journal of Geophysical Research,* **105 (D24),** 29595–29608.

Griffies, S.M., 1998: The Gent-McWilliams skew-flux. *Journal of Physical Oceanography,* **28**, 831–841.

Griffies, S.M., A. Gnanadesikan, K.W. Dixon, J.P. Dunne1, R. Gerdes, M.J. Harrison, A. Rosati1, J. L. Russell, B.L. Samuels, M.J. Spelman, M. Winton, and R. Zhang, 2005: Formulation of an ocean model for global climate simulations, *Ocean Science,* **1,** 45–79.

Griffies, S. M., Pacanowski, R. Schmidt, and V. Balaji, 2001: Tracer conservation with an explicit free surface method for z coordinate ocean models. *Monthly Weather Review,* **129**, 1081–1098.

Gu, L., H. Shugart, J. Fuentes, T. Black, and S. Shewchuk, 1999: Micrometeorology, biophysical exchanges and NEE decomposition in a two-storey boreal forest–development and test of an integrated model. *Agricultural and Forest Meteorology,* **94**, 123–148.

Guilyardi, E., 2006: El Niño—mean state—seasonal cycle interactions in a multi–model ensemble. *Climate Dynamics*, **26**, 329–348.

Guo, Z., D.H. Bromwich, and J.J. Cassano, 2003: Evaluation of polar MM5 simulations of Antarctic atmospheric circulation. *Monthly Weather Review,* **131**, 384–411.

Gutowski, W.J., S.G. Decker, R.A. Donavon, Z. Pan, R.W. Arritt and E.S. Takle, 2003: Temporal-spatial scales of observed and simulated precipitation in central U.S. climate. *Journal of Climate*, **16**, 3841–3847.

Gutowski, W.J., K.A. Kozak, R.W. Arritt, J.H. Christensen, J. Patton, and S. Takle, 2007: A possible constraint on regional precipitation intensity changes under global warming. *Journal of Hydrometeorology*, submitted.

Gutowski, W.J., Z. Ötles, and Y. Chen, 1998: Effect of ocean-surface heterogeneity on climate simulation. *Monthly Weather Review,* **126**, 1419–1429.

Gutowski, W., C. Vörösmarty, M. Person, Z. Ötles, B. Fekete, and J. York, 2002: A Coupled Land–Atmosphere Simulation Program (CLASP). *Journal of Geophysical Research,* **107(D16),** 4283,10.1029/2001JD000392.

Gutowski, W.J., H. Wei, C.J. Vörösmarty, and B.M. Fekete, 2007: Influence of Arctic wetlands on Arctic atmospheric circulation. *Journal of Climate* (accepted).

Hack, J. J., 1994: Parameterization of moist convection in the National Center for Atmospheric Research Community Climate Model (CCM2). *Journal of Geophysical Research,* **99**, 5551–5568.

Hagemann, S. and L. Dümenil, 1998: A parameterization of the lateral water flow for the global scale. *Climate Dynamics*, **14**, 17–31.

Hall, A., 2004: The role of surface albedo feedback in climate. *Journal of Climate,* **17**, 1550–1568.

Han, J. and J.O. Roads, 2004: U.S. climate sensitivity simulated with the NCEP regional spectral model. *Climate Change,* **62**, 115–154.

Hansen, J., *et al.,* 1984: Climate sensitivity: analysis of feedback mechanisms. In: *Climate Processes and Climate Sensitivity,* Maurice Ewing Series, 5 [Hansen, J.E. and T. Takahashi (eds.)]. American Geophysical Union, Washington, DC, USA, pp. 130–163.

Hansen, J., D. Johnson, A. Lacis, S. Lebedeff, P. Lee, D. Rind, and G. Russell, 1981: Climate impact of increasing atmospheric carbon dioxide, *Science*, **213**, 957–966.

Hansen, J., A. Lacis, R. Ruedy, M. Sato, and W. Wilson, 1993: How sensitive is the world's climate? *National Geographic Research and Exploration*, 9: 42–158.

Hansen, J., L. Nazarenko, R. Ruedy, M. Sato, J. Willis, A. Del Genio, D. Koch, A. Lacis, K. Lo, S. Menon, T. Novakov, J. Perlwitz, G. Russell, G. A. Schmidt, and N. Tausnev, 2005: Earth's energy imbalance: Confirmation and implications. *Science,* **308,** 1431–1435.

Hansen, J., M. Sato, R. Ruedy, P. Kharecha, A. Lacis, R. Miller, L. Nazarenko, K. Lo, G.A. Schmidt, G. Russell, I. Aleinov, S. Bauer, E. Baum, B. Cairns, V. Canuto, M. Chandler, Y. Cheng, A. Cohen, A. Del Genio, G. Faluvegi, E. Fleming, A. Friend, T. Hall, C. Jackman, J. Jonas, M. Kelley, N.Y. Kiang, D. Koch, G. Labow, J. Lerner, S. Menon, T. Novakov, V. Oinas, Ja. Perlwitz, Ju. Perlwitz, D. Rind, A. Romanou, R. Schmunk, D. Shindell, P. Stone, S. Sun, D. Streets, N. Tausnev, D. Thresher, N. Unger, M. Yao, and S. Zhang, 2006: Climate simulations for 1880–2003 with GISS modelE. http://arxiv.org/abs/physics/0610109; also submitted to *Climate Dynamics*.

Hansen, J., M. Sato, R. Ruedy, L. Nazarenko, A. Lacis, G.A. Schmidt, G. Russell, I. Aleinov, M. Bauer, S. Bauer, N. Bell, B. Cairns, V. Canuto, M. Chandler, Y. Cheng, A. Del Genio, G. Faluvegi, E. Fleming, A. Friend, T. Hall, C. Jackman, M. Kelley, N.Y. Kiang, D. Koch, J. Lean, J. Lerner, K. Lo, S. Menon, R.L. Miller, P. Minnis, T. Novakov, V. Oinas, Ja. Perlwitz, Ju. Perlwitz, D. Rind, A. Romanou, D. Shindell, P. Stone, S. Sun, N. Tausnev, D. Thresher, B. Wielicki, T. Wong, M. Yao, and S. Zhang, 2005: Efficacy of climate forcings. *Journal of Geophysical Research*, **110**, D18104, doi:10.1029/2005JD005776.

Harries, J.E., H.E. Brindley, P.J. Sagoo, and R.J. Bantges, 2001: Increases in greenhouse forcing inferred from the outgoing longwave radiation spectra of the Earth in 1970 and 1997. *Nature,* **410**, 355–357.

?**Hartmann**, D.L. and M.L. Michelsen, 2002: No evidence for iris. *Bulletin of the American Meteorological Society,* **83**: ???-???

Hay, L.E., M.P. Clark, M. Pagowski, G.H. Leavesley, G.A. Grell, and W.J. Gutowski, Jr., 2006: One-way coupling of an atmospheric and a hydrologic model in Colorado. *Journal of Hydrometeorology*, 7, 569–589.

Haylock, M.R., G.C. Cawley, C. Harpham, R.L. Wilby, and C.M. Goodess, 2006: Downscaling heavy precipitation over the United Kingdom: A comparison of dynamical and statistical methods and their future scenarios. *International Journal of Climatology,* **26**, 1397–1415.

Hegerl, G.C., T.J. Crowley, W.T. Hyde and D.J. Frame, 2006: Climate sensitivity constrained by temperature reconstructions over the past seven centuries. *Nature,* **440**, 1029–1032.

Hegerl, G.C., F.W. Zwiers, P.A. Stott, and V.V. Kharin, 2004: Detectability of anthropogenic changes in annual temperature and precipitation extremes. *Journal of Climate*, **17(19)**, 3683–3700.

?**Held,** ????? and M.J. Suarez, 1994: A proposal for the intercomparison of the dynamical cores of atmospheric general circulation models. *Bulletin of the American Meteorological Society,* **75(10)**, 1825–1830, 1994.

Held, I.M. and B.J. Soden, 2006: Robust Responses of the Hydrological Cycle to Global Warming. *Journal of Climate*, **19**, 5686–5699.

Held, I.M., S.W. Lyons, and S. Nigam, 1989: Transients and the extratropical response to El Nino. *Journal of the Atmospheric Sciences,* **46(1)**, 163–174.

Held, I.M., R.S. Hemler, and V. Ramaswamy, 1993: Radiative-convective equilibrium with explicit two-dimensional moist convection. *Journal of the Atmospheric Sciences,* **50**, 3909–3927.

?**Held**, I.M., T.L. Delworth, J. Lu, K.L. Findell, and T.R. Knutson, 2005: *Simulation of Sahel drought in the 20th and 21st centuries.* Proceedings of the National Academy of Sciences. ?????USA, **102**, 17,891–17,896.

Helfand, H.M. and J.C. Labraga, 1988: Design of a non-singular level 2.5 second order closure model for the prediction of atmospheric turbulence. *Journal of the Atmospheric Sciences,* **45,** 113–132.

Hellstrom, C., D.L. Chen, C. Achberger, and J. Raisanen, 2001: Comparison of climate change scenarios for Sweden based on statistical and dynamical downscaling of monthly precipitation. *Climate Research,* **19**, 45–55.

Henderson-Sellers, A., 2006: Improving land-surface parameterization schemes using stable water isotopes: Introducing the "iPILPS" initiative. *Global and Planetary Change,* **51**, 3–24.

Henderson-Sellers, A., P. Irannejad, K. McGuffie, and A.J. Pitman, 2003: Predicting land-surface climates—Better skill or moving targets? *Geophysical Research Letters,* **30**, 1777.

Henderson-Sellers, A., A.J. Pitman, P.K. Love, P. Irannejad, and T.H. Chen, 1995: The project for Intercomparison of Land-Surface Parameterization Schemes (PILPS) —Phase-2 and Phase-3. *Bulletin of the American Meteorological Society,* **76**, 489–503.

Hewitson, B.C. and R.G. Crane, 1996: Climate downscaling: Techniques and application. *Climate Research*, **7**, 85–95.

Hewitt, C.D and D.J. Griggs, 2004: Ensembles-based predictions of climate changes and their impacts. *Eos,* **85**, 566.

Heyen, H., H. Fock, and W. Greve, 1998: Detecting relationships between the interannual variability in ecological time series and climate using a multivariate statistical approach—A case study on Helgoland Roads zooplankton. *Climate Research,* **10**, 179–191.

Hibler, W.D., 1979: A dynamic thermodynamic sea ice model. *Journal of Physical Oceanography,* **9**, 815–846.

Hines, K.M., R.W. Grumbine, D.H. Bromwich, and R.I. Cullather, 1999: Surface energy balance of the NCEP MRF and NCEP-NCAR reanalysis in Antarctic latitudes during FROST. *Weather Forecasting,* **14**, 851–866.

Hirano, A., R. Welch, and H. Lang, 2003: Mapping from ASTER stereo image data: DEM validation and accuracy assessment. *ISPRS J. Photogram. Rem. Sens.,* **57**, 356–370.

Hoerling, M., J. Hurrell, J. Eischeid, and A. Phillips, 2006: Detection and attribution of 20th century northern and southern African rainfall change. *Journal of Climate*, **19**, 3989–4008.

Hoffert, M.I. and C. Covey, 1992: Deriving global climate sensitivity from paleoclimate reconstructions. *Nature,* **360**, 573–576.

Holland, M.M. and C.M. Bitz, 2003: Polar amplification of climate change in coupled models. *Climate Dynamics,* **21**, 221–232.

Holland, M.M. and M.N. Raphael, 2006: Twentieth century simulation of the southern hemisphere climate in coupled models. Part II: Sea ice conditions and variability. *Climate Dynamics*, **26**, 229–245.

Holtslag, A.A.M. and B.A. Boville, 1993: Local versus nonlocal boundary-layer diffusion in a global climate model, *Journal of Climate*, **6,** 1825–1842.

Hong, S.-Y. and H.-M.H. Juang, 1998: Orography blending in the lateral boundary of a regional model. *Monthly Weather Review,* **126**, 1714–1718.

Hoogenboom, G., J.W. Jones, and K.J. Boote, 1992: Modeling growth, development, and yield of grain legumes using SOYGRO, PNUTGRO, and BEANGRO—A Review. *Trans. ASAE,* **35**, 2043–2056.

Hood, R.R., E.A. Laws, R.A. Armstrong, N.R. Bates, C.W. Brown, C.A. Carlson, F. Chai, S.C. Doney, P.G. Falkowski, R.A. Feely, M.A.M. Friedrichs, M.R. Landry, J.K. Moore, D.M. Nelson, T. Richardson, B. Salihoglu, M. Schartau, D.A. Toole, and J.D. Wiggert, 2006: Pelagic functional group modeling: Progress, challenges and prospects. *Deep-Sea Research II,* **53***,* 459–512.

Hope, P.K., N. Nicholls, and J.L. McGregor, 2004: The rainfall response to permanent inland water in Australia. *Australian Meteorological Magazine,* **53**, 251–262.

Horel, J.D. and J.M. Wallace, 1981: Planetary-scale atmospheric phenomena associated with the Southern Oscillation. *Monthly Weather Review,* **109**, 813–829.

Hori, M.E. and H. Ueda, 2006: Impact of global warming on the East Asian winter monsoon as revealed by nine coupled atmosphere–ocean GCMs. *Geophysical Research Letters,* **33**, doi:10.1029/2005GL024961.

Horowitz, L. W., et al. (2003), A global simulation of tropospheric ozone and related tracers: Description and evaluation of MOZART, version 2, J. Geophys. Res., 108(D24), 4784, doi:10.1029/2002JD002853.

Houghton, R., 2003: Revised estimates of the annual net flux of carbon to the atmosphere from changes in land use and land management 1850–2000. *Tellus*, **55B**, 378–390.

Hungate, B.A., J.S. Dukes, M.R. Shaw, Y. Luo, and C.B. Field, 2003: Nitrogen and climate change. *Science*, **302**, 1512–1513.

Hunke, E.C. and J.K. Dukowicz, 1997: An elastic-viscous-plastic model for sea ice dynamics. *Journal of Physical Oceanography,* **27**, 1849–1867.

Hunke, E.C. and Y. Zhang, 1999: A comparison of sea ice dynamics models at high resolution. *Monthly Weather Review*, **127**, 396–408.

Hurrell, J.W., 1995: Decadal trends in the North Atlantic oscillation: Regional temperature and precipitation. *Science,* **269**, 676–679.

Iorio, J.P., P.B. Duffy, B. Govindasamy, S.L. Thompson, M. Khairoutdinov, and D. Randall, 2004: Effects of model resolution and subgrid-scale physics on the simulation of precipitation in the continental United States. *Climate Dynamics,* **23**, 243–258.

Irannejad, P., A. Henderson-Sellers, and S. Sharmeen, 2003: Importance of land-surface parameterization for latent heat simulation. *Geophysical Research Letters,* **30**, 1904.

Jakob, C. and G. Tselioudis, 2003: Objective identification of cloud regimes in the tropical western Pacific. *Geophysical Research Letters,* **30**, 2082.

Jones, C.A. and J.R. Kiniry, 1986: *CERES-Maize: A simulation model of maize growth and development*. Texas A&M University Press, College Station, Texas, USA.

Jones, R.G., J.M. Murphy, and M. Noguer, 1995: Simulation of climate change over Europe using a nested regional climate model. I: Assessment of control climate, including sensitivity to location of lateral boundaries. *International Journal of Climatology,* **121**, 1413–1449.

Joseph, R. and S. Nigam, 2006: ENSO evolution and teleconnections in IPCC's 20th century climate simulations: Realistic representation? *Journal of Climate*. Accepted.

Kain, J.S. and J. M. Fritsch, 1993: Convective parameterization in mesoscale models: The Kain-Fritsch scheme. In: *The Representation of Cumulus Convection in Numerical Models*, *Meteorological Monographs,* American Meteorological Society, **46**, 165–170.

Kalkstein, L.S. and J.S. Greene, 1997: An evaluation of climate/mortality relationships in larger U.S. cities and the possible impacts of a climate change, *Environmental Health Perspectives,* **105**, 84–93.

Kanamitsu, M., W. Ebisuzaki, J. Woollen, S.-K. Yang, J.J. Hnilo, M. Fiorino, and G.L. Potter, 2002: NCEP-DEO AMIP-II Reanalysis (R-2). *Bulletin of the American Meteorological Society,* **83**, 1631–1643.

?**Kattenberg**, A., F. Giorgi, H. Grassl, G A. Meehl, J.F.B. Mitchell, R.J. Stouffer, ???? Tokioka, A.J. Weaver, T.M.L. Wigley, 1996: Chapter 6. Climate Models Projections of Future Climate. In: *Climate Change 1995–The Science of Climate Change.* [Houghton, J.T., L.G. Miera Filho, B.A. Chandler, N. Harris, A. Kattenberg, and K. Maskell (eds.)]. Cambridge University Press, Cambridge, United Kingdom, pp. 285–358.

Kattsov, V.M., J.E. Walsh, A. Rinke, K. Dethloff, 2000: Atmospheric climate models: simulation of the Arctic Ocean fresh water budget components. In: *The Freshwater Budget of the Arctic Ocean.* [Lewis, E.L. (ed.)]. Kluwer Academic Publishers, Dordrecht, The Netherlands, pp. 209–247.

Kattsov, V. and E. Källén, 2005: Future changes of climate: Modelling and scenarios for the Arctic Region. In: *Arctic Climate Impact Assessment (ACIA).* Cambridge University Press, Cambridge, United Kingdom, 1042 pp.

Khain, A. and A. Pokrovsky, 2004: Simulation of effects of atmospheric aerosols on deep turbulent convective clouds using a spectral microphysics mixed-phase cumulus cloud model. Part II: Sensitivity study. *Journal of Atmospheric Science,* **61**, 2963–2982.

Kidson, J.W. and C.S. Thompson, 1998: Comparison of statistical and model-based downscaling techniques for estimating local climate variations. *Journal of Climate,* **11**, 35–753.

Kiehl, J.T., J. Hack, G. Bonan, B. Boville, B. Briegleb, D. Williamson, and P. Rasch, 1996: *Description of the NCAR Community Climate Model (CCM3).* Technical Report NCAR/TN-420+STR, National Center for Atmospheric Research, Boulder, Colorado, 152 pp.

Kiehl, J.T., C.A. Shields, J.J. Hack, and W.D. Collins, 2006: The climate sensitivity of the Community Climate System Model Version 3 (CCSM3). *Journal of Climate,***19**, 2584–2596.

Kiktev, D., D.M.H. Sexton, L. Alexander, and C.K. Folland, 2003: Comparison of modeled and observed trends in indices of daily climate extremes. *Journal of Climate,* **16**, 3560–3571.

Kim, J., J. Kim, J.D. Farrara, and J.O. Roads, 2005: The effects of the Gulf of California SSTs on warm-season rainfall in the southwestern United States and northwestern Mexico: A regional model study. *Journal of Climate,* **18**, 4970–4992.

Kim, J. and J.E. Lee, 2003: A multiyear regional climate hindcast for the western United States using the mesoscale atmospheric simulation model. *Journal of Hydrometeorology*, **4(5),** 878–890.

Kimoto, M., 2005: Simulated change of the east Asian circulation under global warming scenario. *Geophysical Research Letters,* **32**, L16701, doi:10.1029/2005GL023383.

King, J.C. and J. Turner, 1997: *Antarctic Meteorology and Climatology.* Cambridge University Press, Cambridge, United Kingdom, 256 pp.

Kirschbaum, M.U.F., 2000: Will changes in soil organic carbon act as a positive or negative feedback on global warming? *Biogeochemistry*, **48**, 21–51.

Kitoh, A. and T. Uchiyama, 2006: Changes in onset and withdrawal of the East Asian summer rainy season by multi-model global warming experiments. *Journal of the Meteorological Society of Japan,* **84**, 247–258.

Kleidon, A., 2004: Global datasets of rooting zone depth inferred from inverse methods. *Journal of Climate,* **17**, 2714–2722.

Klein, S.A. and C. Jakob, 1999: Validation and sensitivities of frontal clouds simulated by the ECMWF model. *Monthly Weather Review*, **127**, 2514–2531.

Klemp, J.B. and R. Wilhelmson, 1978: The simulation of three-dimensional convective storm dynamics. *Journal of Atmospheric Science,* **35**, 1070–1096.

Knutson, T.R., T.L. Delworth, K.W. Dixon, I M. Held, J. Lu, V. Ramaswamy, M.D. Schwarzkopf, G. Stenchikov, and R J. Stouffer, 2006: Assessment of twentieth-century regional surface temperature trends using the GFDL CM2 coupled models. *Journal of Climate,* **19(9),** 1624–1651.

Knutson, T. and S. Manabe, 1998: Model assessment of decadal variability and trends in the tropical Pacific Ocean. *Journal of Climate,* **11**, 2273– 2296.

Knutti, R., G.A. Meehl, M.R. Allen, and D.A. Stainforth, 2006: Constraining climate sensitivity from the seasonal cycle in surface temperature. *Journal of Climate.* in press.

Koren, V., J. Schaake, K. Mitchell, Q.Y. Duan, F. Chen, and J.M. Baker, 1999: A parameterization of snowpack and frozen ground intended for NCEP weather and climate models. *Journal of Geophysical Research,* **104(D16),** 19569–19585.

Kraus, E. B. and J. S. Turner, 1967: A one-dimensional model of the seasonal thermocline. II, The general theory and its consequences. *Tellus*, **19**, 98–105.

Krinner, G., 2003: Impact of lakes and wetlands on boreal climate. *Journal of Geophysical Research,* **108(D16),** 4520.

Kripalani, R.H., J.H. Oh, and H.S. Chaudhari, 2007: Response of the East Asian summer monsoon to doubled atmospheric CO2: Coupled climate models simulations and projections under IPCC AR4. *Theoretical and Applied Climatology,* **87**, 1–28.

Kripalani, R.H., J.H. Oh, Ashwini Kulkarni, S.S. Sabade, and H.S. Chaudhari, 2006: South Asian summer monsoon precipitation variability: Coupled climate simulations and projections under IPCC AR4. *Theoretical and Applied Climatology*. In press.

Krueger, S.K., 1988: Numerical simulation of tropical cumulus clouds and their interaction with the subcloud layer. *Journal of Atmospheric Science,* **45**, 2221–2250.

Kunkel, K.E., K. Andsager, X.-Z. Liang, R.W. Arritt, E.S. Takle, W.J. Gutowski, Jr., and Z. Pan, 2002: Observations and regional climate model simulations of heavy precipitation events and seasonal anomalies: A comparison. *Journal of Hydrometeorology*, **3**, 322–334.

Kunkel, K.E., S.A. Changnon, B.C. Reinke, and R.W. Arritt, 1996: The July 1995 heat wave in the Midwest: A climatic perspective and critical weather factors. *Bulletin of the American Meteorological Society,* **77**, 1507–1518.

Kunkel, K.E., D.R. Easterling, K. Hubbard, and K. Redmond, 2004: Temporal variations in frost-free season in the United States: 1895–2000. *Geophysical Research Letters,* **31**, L03201, doi:10.1029/2003GL018624.

Kuo, H.L., 1974: Further studies of the parameterization of the influence of cumulus convection on large-scale flow. *Journal of Atmospheric Science,* **31**, 1232–1240.

Laprise, R., 2003: Resolved scales and nonlinear interactions in limited-area models. *Journal of Atmospheric Science,* **60**, 768–779.

Large, W., J.C. McWilliams, and S.C. Doney, 1994: Oceanic vertical mixing: A review and a model with a nonlocal boundary mixing parameterization. *Reviews of Geophysics,* **32**, 363–403.

Latif, M. and Coauthors, 2001: ENSIP: The El Nino simulation intercomparison project. *Climate Dynamics,* **18**, 255–272.

Lau, K.-M., S. Shen, K.-M. Kim, and H. Wang, 2006: A multi-model study of the 20th century simulations of Sahel drought from the 1970s to 1990s. *Journal of Geophysical Research,* **111(D0711),** doi:10.1029/2005JD006281.

Lawrence, D.M. and A.G. Slater, 2005: A projection of severe near-surface permafrost degradation during the 21st century. *Geophysical Research Letters,* **32**, L24401, doi:10.1029/2005GL025080.

Le Treut, H. and Z.X. Li, 1991: Sensitivity of an atmospheric general circulation model to prescribed SST changes: Feedback effects associated with the simulation of cloud optical properties. *Climate Dynamics*, **5**, 175–187.

Le Treut, H., Z.X. Li, and M. Forichon, 1994: Sensitivity of the LMD general circulation model to greenhouse forcing associated with two different cloud water parametrizations. *Journal of Climate,* 7, 1827–1841.

Leaman, K., R. Molinari, and P. Vertes, 1987: Structure and variability of the Florida Current at 27N: April 1982–July 1984. *Journal of Physical Oceanography*, **17**, 565–583.

Lean, J., J. Beer, and R. Bradley, 1995: Reconstruction of solar irradiance since 1610: Implications for climate change. *Geophysical Research Letters,* **22**, 3195–3198.

Lee, H.-C., A. Rosati, M. Spelman, and T. Delworth, 2006: Barotropic tidal mixing effects in a coupled climate model: Ocean conditions in the northern Atlantic. *Ocean Modelling*, **11**, 464–477.

Leung, L.R. and Y. Qian, 2003: The sensitivity of precipitation and snowpack

simulations to model resolution via nesting in regions of complex terrain. *Journal of Hydrometeorology*, **4**, 1025–1043.

Leung, L.R., Y. Qian, and X. Bian, 2003: Hydroclimate of the western United States based on observations and regional climate simulation of 1981–2000. Part I: seasonal statistics. *Journal of Climate*, **16(12),** 1892–1911.

Leung, L.R., Y. Qian, X. Bian, W.M. Washington, J. Han, and J.O. Roads, 2004: Mid-century ensemble regional climate change scenarios for the western United States. *Climate Change,* **62**, 75–113.

Leung L.R. and M.S. Wigmosta, 1999: Potential climate chance impacts on mountain watersheds in the Pacific Northwest. *Journal of the American Water Resources Association,* **35**, 1463–1471.

Levitus, S., J.I. Antonov, J. Wang, T.L. Delworth, K.W. Dixon, and A J. Broccoli, 2001: Anthropogenic warming of Earth's climate system. *Science,* **292**, 267–270.

Li, K.Y., R. De Jong, M.T. Coe, and N. Ramankutty, 2006: Root-water-uptake based upon a new water stress reduction and an asymptotic root distribution function. *Earth Interactions,* **10**, Art. No. 14.

Li, W., R. Fu, and R.E. Dickinson, 2006: Rainfall and its seasonality over the Amazon in the 21st century as assessed by the coupled models for the IPCC AR4. *Journal of Geophysical Research,* **11**, D02111, doi:10.1029/2005JD006355.

Li, X., Y. Chao, J. McWilliams, and L-L. Fu, 2001: A comparison of two vertical-mixing schemes in a Pacific Ocean General Circulation Model. *Journal of Climate*, **14**, 1377–1398.

Li, X. and T. Koike, 2003: Frozen soil parameterization in SiB2 and its validation with GAME-Tibet observations. *Cold Regions Science and Technology,* **36**, 165–182.

Li, Z.X., 1999: Ensemble atmospheric GCM simulation of climate interannual variability from 1979 to 1994. *Journal of Climate*, **12**, 986–1001.

Liang, X.-Z., K.E. Kunkel, and A.N. Samel, 2001: Development of a regional climate model for U.S. Midwest applications. Part 1: Sensitivity to buffer zone treatment. *Journal of Climate*, **14**, 4363–4378.

Liang, X.-Z., L. Li, A. Dai, and K.E. Kunkel, 2004: Regional climate model simulation

of summer precipitation diurnal cycle over the United States. *Geophysical Research Letters,* **31**, L24208, doi:10.1029/2004GL021054.

Liang, X.-Z., J. Pan, J. Zhu, K.E. Kunkel, J.X.L. Wang, and A. Dai, 2006: Regional climate model downscaling of the U.S. summer climate and future change. *Journal of Geophysical Research*, **111**, D10108, doi:101029/2005JD006685.

Liang, X., Z. Xie, and M. Huang, 2003: A new parameterization for surface and groundwater interactions and its impact on water budgets with the variable infiltration capacity (VIC) land surface model. *Journal of Geophysical Research,* **108**, 8613.

Libes, S.M., 1992: *An Introduction to Marine Biogeochemistry.* Wiley, New York, New York, USA, 734 pp.

Lin, J.L., B. Mapes, M.H. Zhang, and M. Newman, 2004: Stratiform precipitation, vertical heating profiles, and the Madden–Julian Oscillation. *Journal of the Atmospheric Sciences,* **61**, 296–309.

Lin, J.L., G.N. Kiladis, B.E. Mapes, K.M. Weickmann, K.R. Sperber, W.Y. Lin, M. Wheeler, S.D. Schubert, A. Del Genio, L.J. Donner, S. Emori, J.-F. Gueremy, F. Hourdin, P.J. Rasch, E. Roeckner, and J.F. Scinocca, 2006: Tropical intraseasonal variability in 14 IPCC AR4 climate models. Part I: Convective signals. *Journal of Climate*. In press.

Lin SJ, Rood RB (1996) Multidimensional Flux-Form Semi-Lagrangian Transport Schemes. Monthly Weather Review: Vol. 124, No. 9 pp. 2046–2070

Lin, W.Y. and M.H. Zhang, 2004: Evaluation of clouds and their radiative effects simulated by the NCAR Community Atmospheric Model CAM2 against satellite observations. *Journal of Climate*, **17**, 3302–3318.

Lindzen, R.S., M.-D. Chou, and A. Y. Hou, 2001: Does Earth have an adaptive infrared iris? *Bulletin of the American Meteorological Society,* **82**, 417–432.

Lindzen R.S. and M.S. Fox-Rabinovitz, 1989: Consistent vertical and horizontal resolution. *Monthly Weather Review,* **117**, 2575–2583.

Liston, G.E., 2004: Representing subgrid snow cover heterogeneities in regional and global models. *Journal of Climate,* **17**, 1381–1397.

Liu, Z., 1998: On the role of ocean in the transient response of tropical climatology to global warming. *Journal of Climate*, **11**, 864–875.

Lock, A., 1998: The parametrization of entrainment in cloudy boundary layers. *Quarterly Journal of the Royal Meterological Society,* **124**, 2729–2753.

Lock, A.P., A.R. Brown, M.R. Bush, G.M. Martin, and R.N.B. Smith, 2000: A new boundary layer mixing scheme. Part I: Scheme description and single-column model tests. *Monthly Weather Review,***128**, 3187–3199.

Lofgren, B.M., 2004: A model for simulation of the climate and hydrology of the Great Lakes basin. *Journal of Geophysical Research,* **109(D18),** Art. No. D18108.

Lohmann, U. and E. Roeckner, 1996: Design and performance of a new cloud microphysics scheme developed for the ECHAM4 general circulation model. *Climate Dynamics*, **12**, 557–572.

Lumpkin, R. and K. Speer, 2003: Large-scale vertical and horizontal circulation in the North Atlantic Ocean. *Journal of Physical Oceanography*, **33**, 1902–1920.

Luo, L.F. and Coauthors, 2003: Effects of frozen soil on soil temperature, spring infiltration, and runoff: Results from the PILPS 2(d) experiment at Valdai, Russia. *Journal of Hydrometeorology*, **4**, 334-351.

Lynch, A.H., W.L. Chapman, J.E. Walsh, and G. Weller, 1995: Development of a regional climate model of the western Arctic. *Journal of Climate,* **8,** 1555–1570.

Lynch, A.H., J.A. Maslanik, and W.L. Wu, 2001: Mechanisms in the development of anomalous sea ice extent in the western Arctic: A case study. *Journal of Geophysical Research,* **106(D22),** 28097-28105.

Lynn, B.H., A. Khain, J. Dudhia, D. Rosenfeld, A. Pokrovsky, and A. Seifert, 2005: Spectral (bin) microphysics coupled with a mesoscale model (MM5). Part II: Simulation of a CaPE rain event with a squall line. *Monthly Weather Review,* **133**, 59-71.

Maak, K. and H. von Storch, 1997: Statistical downscaling of monthly mean temperature to the beginning of flowering of *Galanthus nivalis L.* in Northern Germany. *International Journal of Biometeor*ology, **41**, 5–12.

Malevsky–Malevich, S.P., E.D. Nadyozhina, V.V. Simonov, O.B. Shklyarevich, and E.K. Molkentin, 1999: The evaluation of climate change influence on the permafrost season soil thawing regime. *Contemporary Investigation at Main Geophysical Observatory,* **1**, 33–50 (in Russian).

Manabe, S., 1969: Climate and the ocean circulation. The atmospheric circulation and hydrology of the Earth's surface. *Monthly Weather Review,* **97**, 739–774.

Manabe, S., J. Smagorinsky, and R. F. Strickler, 1965: Simulated climatology of a general circulation model with a hydrological cycle. *Monthly Weather Review,* **93**, 769–798.

Manabe, S., R J. Stouffer, M.J. Spelman, and K. Bryan, 1991: Transient responses of a coupled ocean-atmosphere model to gradual changes of atmospheric CO2. Part I: Annual mean response. *Journal of Climate*, **4**, 785–818.

Martin, G.M., M.R. Bush, A.R. Brown, A.P. Lock, and R.N.B. Smith, 2000: A new boundary layer mixing scheme. Part II: Tests in climate and mesoscale models. *Monthly Weather Review,* **128**, 3200–3217.

Maxwell, R.M. and N.L. Miller, 2005: Development of a coupled land surface and groundwater model. *Journal of Hydrometeorology*, **6**, 233–247.

McCreary, J. and P. Lu, 1994: Interaction between the subtropical and equatorial ocean circulation—the subtropical cell. *Journal of Physical Oceanography,* **24**, 466–497.

McGregor, J.L., 1997: Regional climate modelling. *Meteorology and Atmospheric Physics,* **63**, 105–117.

McGregor, J.L., 1999: Regional modelling at CAR: Recent developments. In *Parallel Computing in Meteorology and Oceanography*, BMRC Research Report No. 75, Bureau of Meteorology, Melbourne, Australia, pp. 43–48.

McPhaden, M.J., A.J. Busalacchi, R. Cheney, J.R. Donguy, K.S. Gage, D. Halpern, M. Ji, P. Julian, G. Meyers, G.T. Mitchum, P.P. Niiler, J. Picaut, R.W. Reynolds, N. Smith, and K. Takeuchi, 1998: The Tropical Ocean Global Atmosphere (TOGA) observing system: A decade of progress. *Journal of Geophysical Research,* **103**, 14 169–14 240.

Mearns, L.O., 2003: Issues in the impacts of climate variability and change on agriculture—Applications to the southeastern United States. *Climate Change,* **60**, 1–6.

Mearns, L.O., I. Bogardi, F. Giorgi, I. Matayasovszky, and M. Palecki, 1999: Comparison of climate change scenarios generated daily temperature and precipitation from regional climate model experiments and statistical downscaling. *Journal of Geophysical Research,* **104**, 6603–6621.

Mearns, L.O., F. Giorgi, L. McDaniel, and C. Shields, 2003: Climate scenarios for the southeastern US based on GCM and regional model simulations. *Climate Change,* **60**, 7–35.

Mechoso, C.R., A.W. Robertson, N. Barth, M.K. Davey, P. Delecluse, P.R. Gent, S. Ineson, B. Kirtman, M. Latif, H. Le Treut, T. Nagai, J.D. Neelin, S.G.H. Philander, J. Polcher, P.S. Schopf, T. Stockdale, M.J. Suarez, L. Terray, O. Thual, and J J. Tribbia, 1995: The seasonal cycle over the tropical Pacific in coupled ocean-atmosphere general circulation models. *Monthly Weather Review,* **123**, 2825–2838.

Meehl, G. and C. Tebaldi, 2004: More intense, more frequent, and longer lasting heat waves in the 21st Century. *Science*, **305**, 994–997.

Meehl, G.A., C. Tebaldi, and D. Nychka, 2004: Changes in frost days in simulations of twenty-first century climate. *Climate Dynamics,* **23**, 495–511.

Meehl, G.A., W.M. Washington, B.D. Santer, W.D. Collins, J.M. Arblaster, A. Hu, D.M. Lawrence, H. Teng, L.E. Buja, and W.G. Strand, 2006: Climate change projections for the twenty-first century and climate change commitment in the CCSM3. *Journal of Climate*, **19**, 2597–2616.

Mellor, G.L. and T. Yamada, 1974: A hierarchy of turbulent closure models for planetary boundary layers. *Journal of Atmospheric Science,* **31**, 1791–1806.

Mellor, G.L. and T. Yamada, 1982: Development of a tubulence closure model for geophysical fluid problems. *Reviews of Geophysics and Space Physics*, **20**, 851–875.

Merryfield, W.J., 2006: Changes to ENSO under CO2 doubling in a multi-model ensemble. *Journal of Climate,* **19**, 4009–4027.

Miguez-Macho, G., G.L. Stenchikov, and A. Robock, 2005: Regional climate simulations over North America: Interaction of local processes with improved large-scale flow. *Journal of Climate,* **18**, 1227–1246.

Miller, D.A., and R.A. White, 1998: A conterminous United States multilayer soil characteristics dataset for regional climate and hydrology modeling. *Earth Interactions*, **2**, 1–26.

Miller, R.L., G.A. Schmidt, and D.T. Shindell, 2006: Forced variations of annular modes in the 20th century IPCC AR4 simulations. *Journal of Geophysical Research.* In press.

Mirocha, J.D., B. Kosovic, and J.A. Curry, 2005: Vertical heat transfer in the lower atmosphere over the Arctic Ocean during clear-sky periods. *Boundary-Layer Meterology,* **117**, 37–71.

Mitchell, J. F. B., C.A. Senior, and W. J. Ingram, 1989: CO2 and climate: A missing feedback? *Nature,* **341**, 132–134.

Miura, H., H. Tomita, T. Nasuno, S. Iga, M. Satoh, and T. Matsuno, 2005: A climate sensitivity test using a global cloud resolving model under an aqua planet condition. *Geophysical Research Letters,* **32**, L19717, doi:10.1029/2005GL023672.

Mo, K.C., J.E. Schemm, H.M.H. Juang, R.W. Higgins, and Y. Song, 2005: Impact of model resolution on the prediction of summer precipitation over the United States and Mexico. *Journal of Climate*, **18**, 3910–3927.

Moorthi, S. and M.J. Suarez, 1992: Relaxed Arakawa-Schubert: a parameterization of moist convection for general circulation models. *Monthly Weather Review,* **120**, 978–1002.

Morel, A. and D. Antoine, 1994: Heating rate within the upper ocean in relation to its bio-optical state. *Journal of Physical Oceanography,* **24**, 1652–1665.

Morrison, H. and J.O. Pinto, 2005: Mesoscale modeling of springtime Arctic mixed-phase stratiform clouds using two-moment bulk microphysics scheme. *Journal of Atmospheric Science*, **62**, 3683–3704.

Murray, R.J., 1996: Explicit generation of orthogonal grids for ocean models. *Journal of Computational Physics,* **126**, 251–273.

?NARCCAP, cited as 2007: http://www.narccap.ucar.edu.

Nadelhoffer, K. J., B.A. Emmett, P. Gundersen, and Coauthors, 1999: Nitrogen makes a minor contribution to carbon sequestration in temperate forests. *Nature*, **398**, 145–148.

Najjar, R.G., X. Jin, F. Louanchi, O. Aumont, K. Caldeira, S.C. Doney, J.-C. Dutay, M. Follows, N. Gruber, F. Joos, K. Lindsay, E. Maier-Reimer, R.J. Matear, K. Matsumoto, A. Mouchet, J.C. Orr, G.-K. Plattner, J.L. Sarmiento, R. Schlitzer, M.F. Weirig, Y. Yamanaka, and A. Yool, 2006: Impact of circulation on export production, dissolved organic matter and dissolved oxygen in the ocean: Results from OCMIP-2. *Global Biogeochemistry Cycles*. Submitted.

Neelin, J.D., M. Latif, M.A.F. Allaart, M.A. Cane, U. Cubasch, W.L. Gates, P.R. Gent, M. Ghil, C. Gordon, N.C. Lau, C.R. Mechoso, G.A. Meehl, J.M. Oberhuber, S.G.H. Philander, P.S. Schopf, K.R. Sperber, A. Sterl, T. Tokioka, J. Tribbia, and S.E. Zebiak, 1992: Tropical air-sea interaction in general circulation models. *Climate Dynamics,* **7**, 73–104.

Niu, G.Y., and Z.L. Yang, 2006: Effects of frozen soil on snowmelt runoff and soil water storage at a continental scale. *Journal of Hydrometeorology*, **7**, 937–952.

Nordeng, T.E., 1994: Extended versions of the convective parameterization scheme at ECMWF and their impact on the mean and transient activity of the model in the tropics. *Technical Memorandum 206, ECMWF*, Reading, United Kingdom.

Norris, J. and C.P. Weaver, 2001: Improved techniques for evaluating GCM cloudiness applied to the NCAR CCM3. *Journal of Climate*, **14**, 2540–2550.

Nowak, R.S., D.S. Ellsworth, and S.D. Smith, 2004: Tansley ˆreview: Functional responses of plants to elevated atmospheric CO_2—Do photosynthetic and productivity data from FACE experiments support early predictions? *New Phytologist*, **162**, 253–280.

Ohlmann, J.C., 2003: Ocean radiant heating in climate models. *Journal of Climate*, **16**, 1337–1351.

Oleson, K.W., Y. Dai, G. Bonan, M. Bosilovich, R. Dickinson, P. Dirmeyer, F. Hoffman, P. Houser, S. Levis, G.-Y. Niu, P. Thornton, M. Vertenstein, Z.-L. Yang, and X. Zeng, 2004: *Technical description of the Community Land Model (CLM)*. *NCAR*

Technical Note. NCAR/TN-461+STR, National Center for Atmospheric Research, Boulder, Colorado, USA, 173 pp. [Available from National Center for Atmospheric Research, P.O. Box 3000, Boulder, CO 80305.]

Oren, R. and Coauthors, 2001: Soil fertility limits carbon sequestration by forest ecosystems in a CO_2-enriched atmosphere. *Nature*, **411**, 469–477.

Ott, L.E., K.E. Pickering, G.L. Stenchikov, and H. Huntrieser, 2006: The effects of lightning NOx production during the July 21 EULINOX storm studied with a 3-D cloud-scale chemical transport mode. *Journal of Geophysical Research.* Submitted.

Overgaard, J., D. Rosbjerg, and M.B. Butts, 2006: Land-surface modelling in hydrological perspective–A review. *Biogeosciences,* **3**, 229–241.

Pacanowski, R.C. and S.G.H. Philander, 1981: Parametrization of vertical mixing in numerical models of tropical oceans. *Journal of Physical Oceanography*, **11**, 1443–1451.

Paegle, J., K.C. Mo., and J. Nogués-Paegle, 1996: Dependence of simulated precipitation on surface evaporation during the 1993 United States summer floods. *Monthly Weather Review,* **124**, 345–361.

Pan, Z., J.H. Christensen, R.W. Arritt, W.J. Gutowski, Jr., E.S. Takle, and F. Otieno, 2001: Evaluation of uncertainties in regional climate change simulations. *Journal of Geophysical Research*, **106**, 17,735–17,752.

Parkinson, C.L., K.Y. Vinnikov, and D.J. Cavalieri, 2006: Evaluation of the Simulation of the Annual Cycle of Arctic and Antarctic. *Journal of Geophysical Research,* **111**, C07012, doi:10.1029/2005JC003408. (Evaluates the ability of models to simulate the sea ice distribution for the Arctic and Antarctic for 1974-2004. Each of the models is simulating annual cycles that are phased at least approximately correctly in both hemispheres. Several models do noticeably better in the Northern Hemisphere than in the Southern Hemisphere)

Paulson, C.A. and J.J. Simpson, 1977: Irradiance measurements in the upper ocean. *Journal of Applied Oceanography,* **7**, 952–956.

Pavolonis, M., J.R. Key, and J.J. Cassano, 2004: Study of the Antarctic surface energy budget using a polar regional atmospheric model forced with satellite-derived

cloud properties. *Monthly Weather Review,* **132**, 654–661.

Peltier, W.R., 2004: Global glacial isostasy and the surface of the ice-age earth: The ice-5G (VM2) model and GRACE. *Annual Review of Earth Planetary Science,* **32**, 111–149.

Philander, S.G.H., 1990: *El Nino, La Nina, and the Southern Oscillation*. Academic Press, San Diego, California, USA, 293 pp.

Philander, S.G.H. and R.C. Pacanowski, 1981: The oceanic response to cross-equatorial winds (with application to coastal upwelling in low latitudes). *Tellus,* **33**, 201–210.

Philip, S.Y. and G.J. Van Oldenborgh, 2006: Shifts in ENSO coupling processes under global warming. GRL, **33**, L11704, doi:10.1029/2006GL026196.

Piani, C., D.J. Frame, D.A. Stainforth, and M.R. Allen, 2005: Constraints on climate change from a multi-thousand member ensemble of simulations. *Geophysical Research Letters,* **32**, L23825, doi:10.1029/2005GL024452.

Pincus, R., H.W. Barker, and J.J. Morcrette, : A fast, flexible, approximate technique for computing radiative transfer in inhomogeneous cloud fields. *Journal of Geophysical Research*, doi:10.1209/2002JD003322,2003.

Pinto, J.O., J.A. Curry, and J.M. Intrieri, 2001: Cloud-aerosol interactions during autumn over Beaufort Sea. *Journal of Geophysical Research.* **106**, 15,077–15097.

Pierce, D. W, T. P. Barnett, E. J. Fetzer, P. J. Gleckler, 2006: Three-dimensional **tropospheric water vapor in coupled climate models compared with observations from the AIRS satellite system**, Geophys Res Lett 33, no. 21, L21701

Pitman, A.J., A.G. Slater, C.E. Desborough, and M. Zhao, 1999: Uncertainty in the simulation of runoff due to the parameterization of frozen soil moisture using the GSWP methodology. *Journal of Geophysical Research,* **104**, 16879–16888.

Plummer, D.A., D. Caya, A. Frigon, H. Côté, M. Giguère, D. Paquin, S. Biner, R. Harvey, and R. de Elía, 2006: Climate and climate change over North America as simulated by the Canadian Regional Climate Model. *Journal of Climate,* **19**, 3112–3132.

Pope, V.D., M. Gallani, P.R. Rowntree, and R.A. Stratton, 2000: The impact of new physical parametrizations in the Hadley Centre climate model—HadAM3. *Climate Dynamics,* **16**, 123–146.

?Prentice, I.C., *et al.,* 2001: [IPCC 3rd Assessment Report, Working Group I, Chapter 3]?????

Qian, J., F. Giorgi, and M.S. Fox–Rabinovitz, 1999: Regional stretched grid generation and its application to the NCAR RegCM. *Journal of Geophysical Research,* **104(D6),** 6501–6514.

Qian, J.H., W.K. Tao, and K.M. Lau, 2004: Mechanisms for torrential rain associated with the mei-yu development during SCSMEX 1998. *Monthly Weather Review,* **132**, 3–27.

Raisanen, J. and T.N. Palmer, 2001: A probability and decision-model analysis of a multimodel ensemble of climate change simulations. *Journal of Climate,* **14**, 3212–3226.

Rajagopalan, B., U. Lall, and M.A. Cane, 1997: Anomalous ENSO occurrences: An alternate view. *Journal of Climate,* **10(9),** 2351–2357.

Ramankutty, N., J.A. Foley, J. Norman, and K. McSweeney, 2002: The global distribution of cultivable lands: current patterns and sensitivity to possible climate change. *Global Ecology and Biogeography*, **11**, 377–392.

Ramaswamy, V., D. Boucher, J. Haigh, D. Hauglustaine, J. Haywood, G. Myhre, T. Nakajima, G.Y. Shi, and S. Solomon, 2001: Radiative forcing of climate change. In: *Climate Change 2001: The Scientific Basis,* [Houghton, J.T., Y. Ding, D.J. Griggs, M. Noguer, P.J. van der Linden, X. Dai, K. Maskell, and C.A. Johnson (eds.)]. Cambridge University Press, Cambridge, United Kingdom, pp. 349–416.

Randall, D., M. Khairoutdinov, A. Arakawa, and W. Grabowski, 2003: Breaking the cloud parameterization deadlock. *Bulletin of the American Meteorological Society,* **84**, 1547–1564.

Randall, D.A., M.E. Schlesinger, V. Galin, V. Meleshko, J.-J. Morcrette, and R. Wetherald, 2000: Cloud feedbacks. In: *Frontiers in the Science of Climate*

Modeling [Kiehl, J.T. and V. Ramanathan (eds.)]. Proceedings of a symposium in honor of Professor Robert D. Cess.

Raphael, M.N. and M.M. Holland, 2006: Twentieth century simulation of the Southern Hemisphere climate in coupled models. Part 1: Large scale circulation variability. *Climate Dynamics,* **26**, 217–228.

Rasch, P.J. and J.E. Kristjánsson, 1998: A comparison of the CCM3 model climate using diagnosed and predicted condensate parameterizations. *Journal of Climate*, **11**, 1587–1614.

Rasmussen, E.M. and J.M. Wallace, 1983: Meteorological aspects of the El Nino/Southern Oscillation. *Science*, **222**, 1195–2002.

Rawlins, M.A., R.B. Lammers, S. Frolking, B.M. Fekete, and C.J. Vorosmarty, 2003: Simulating pan-Arctic runoff with a macro-scale terrestrial water balance model. *Hydrodrology Proceedings,* **17**, 2521–2539.

Rayner, N.A., D.E. Parker, E.B. Horton, C.K. Folland, L.V. Alexander, D.P. Rowell, E.C. Kent, and A. Kaplan, 2003: Global analyses of sea surface temperature, sea ice, and night marine air temperature since the late nineteenth century. *Journal of Geophysical Research,* **108(D14),** 4407.

Ringer, M.A. and R.P. Allan, 2004: Evaluating climate model simulations of tropical clouds. *Tellus,* **56A,** 308–327.

Rinke, A., K. Dethloff, J. Cassano, J.H. Christensen, J.A. Curry, P. Du, E. Girard, J.-E. Haugen, D. Jacob, C.G. Jones, M. Koltzow, R. Laprise, A.H. Lynch, S. Pfeifer, M.C. Serreze, M.J. Shaw, M. Tjernstrom, K. Wyser, and M. Zagar, 2006: Evaluation of an ensemble of Arctic regional climate models: Spatiotemporal fields during the SHEBA year. *Climate Dynamics.* DOI 10.1007/s00382-005-0095-3.

Roads, J.O., S.-C. Chen, M. Kanamitsu, and H. Juang, 1999: Surface water characteristics in the NCEP Global Spectral Model and reanalysis. *Journal of Geophysical Research,* **4(D16),** 19307–19327.

Roads, J., S.C. Chen, and M. Kanamitsu, 2003: U.S. regional climate simulations and seasonal forecasts. *Journal of Geophysical Research,* **108(D16),** Art. No. 8606.

Roberts, M.J. and R. Wood, 1997: Topographic sensitivity studies with a Bryan-Cox-type ocean model. *Journal of Physical Oceanography*, **27**, 823–836.

Roeckner E., R. Brokopf, M. Esch, M. Giorgetta, S. Hagemann, L. Kornblueh, E. Manzini, U. Schlese, and U. Schulzweida, 2006: Sensitivity of simulated climate to horizontal and vertical resolution in the ECHAM5 atmosphere model. *Journal of Climate,* **19**, 3771–3791.

Roeckner, E., *et al.,* 1987: Cloud optical depth feedbacks and climate modelling. *Nature*, **329**, 138–140.

Roeckner, E. *et al.*, 1996: The atmospheric general circulation model ECHAM-4: Model description and simulation of present-day climate. Report 128, Max-Planck-Institut für Meteorologie, Hamburg, Germany.

Root, T.L. and S.H. Schneider, 1993: Can large scale climatic models be linked with multiscale ecological studies? *Conservation Biology*, **7(2),** 256–270.

Ropelewski, C.F. and M.S. Halpert, 1987: Global and regional scale precipitation patterns associated with the El Nino Southern Oscillation. *Monthly Weather Review,* **115**, 1606–1626.

Rothstein, L.M., J.J. Cullen, M. Abbott, E.P.Chassignet, K. Denman, S.C. Doney, H. Ducklow, K. Fennel, M. Follows, D. Haidvogel, E. Hoffman, D.M. Karl, J. Kindle, I. Lima, M. Maltrud, C. McClain, D. McGillicuddy, M.J. Olascoaga, Y. Spitz, J. Wiggert, and J. Yoder, 2006: Modeling ocean ecosystems: The PARADIGM Program. *Oceanography,* **19**, 22–51.

Rotstayn, L.D., 1997: A physically based scheme for the treatment of stratiform clouds and precipitation in large-scale models. I: Description and evaluation of microphysical processes. *Quarterly Journal of the Royal Meterological Society,* **123**, 1227–1282.

Ruiz-Barradas, A. and S. Nigam, 2006: IPCC's twentieth-century climate simulations: Varied representations of North American hydroclimate variability. *Journal of Climate*, **19**, 4041–4058.

Rummukainen M., S. Bergstrom, G. Persson, J. Rodhe, and M. Tjernstrom, 2004: The Swedish Regional Climate Modelling Programme, SWECLIM: A review. *Ambio,* **33**, 176–182.

Russell G.L., J.R. Miller, and D. Rind, 1995. A coupled atmosphere-ocean model for transient climate change studies. *Atmosphere-Ocean*, **33(4),** 683–730.

Russell, G.L., J.R. Miller, L.-C. Tsang, R.A. Ruedy, G.A. Schmidt, and S. Sheth, 2000: Comparison of model and observed regional temperature changes during the past 40 years. *Journal of Geophysical Research,* **105**, 14 891–14 898.

Russell, J.L., R.J. Stouffer, and Keith W. Dixon, 2006: Intercomparison of the southern ocean circulations control simulations. *Journal of Climate*, **19**, 4560–4575.

Ryan, B.F., J.J. Katzfey, D.J. Abbs, C. Jakob, U. Lohmann, B. Rockel, L.D. Rotstayn, R.E. Stewart, K.K. Szeto, G. Tselioudis, and M.K. Yau, 2000: Simulations of a cold front by cloud-resolving, limited-area, and large-scale models, and a model evaluation using *in situ* and satellite observations. *Monthly Weather Review,* **128,** 3218–3235.

Saji, N.H., S.-P. Xie, and T. Yamagata, 2005: Tropical Indian Ocean variability in the IPCC 20th-century climate simulations. *Journal of Climate*. In press.

Saraf, A.K., B.P. Mishra, S. Choudhury, and P. Ghosh, 2005: Digital Elevation Model (DEM) generation from NOAA-AVHRR night-time data and its comparison with USGS-DEM. *International Journal of Remote Sensing,* **26**, 3879–3887.

Sardeshmukh, P.D. and B.J. Hoskins, 1988: The generation of global rotational flow by steady idealized tropical divergence. *Journal of Atmospheric Science*, **45**, 1228–1251.

Sato, M., J. Hansen, M.P. McCormick, and J. Pollack, 1993: Stratospheric aerosol optical depth, 1850–1990. *Journal of Geophysical Research,* **98**, 22987–2299

Sausen, R., S. Schubert, and L. Dumenil, 1994: A model of the river-runoff for use in coupled atmosphere-ocean models. *Journal of Hydrology,* **155**, 337352.

Schimel, D.S., 1998: The carbon equation. *Nature*, **393**, 208–209.

?Schmidt, G.A., R. Ruedy, J.E. Hansen, I. Aleinov, N. Bell, M. Bauer, S. Bauer, B. Cairns, V. Canuto, Y. Cheng, A. Del Genio, G. Faluvegi, A.D. Friend, T.M. Hall, Y. Hu, M. Kelley, N.Y. Kiang, D. Koch, A.A. Lacis, J. Lerner, K.K. Lo, R.L. Miller, L. Nazarenko, V. Oinas, J. Perlwitz, D. Rind, A. Romanou, G.L. Russell, M. Sato, D.T. Shindell, P.H. Stone, S. Sun, N. Tausnev, D. Thresher, M.S. Yao,

2006: Present day atmospheric simulations using GISS ModelE: Comparison to *in-situ,* satellite and reanalysis data. **19**, 153–192, doi:10.1175/JCLI3612.1.

Schmittner, A., M. Latif, and B. Schneider, 2005: Model projections of the North Atlantic thermohaline circulation for the 21st century assessed by observations. *Geophysical Research Letters,* **32**, doi:10.1029/2005GL024368.

Schneider, S.H. and C. Mass, 1975: Volcanic dust, sunspots, and temperature trends. *Science,* **190**, 741–746

Schneider, S.H. and S.L. Thompson, 1981: Atmospheric CO2 and climate: Importance of the transient response. *Journal of Geophysical Research,* **86**, 3135–3147.

?Schopf, P., M. Gregg, R. Ferrari, D. Haidvogel, R. Hallberg, W. Large, J. Ledwell, J. Marshall, J. McWilliams, R. Schmitt, E. Skyllingstad, K. Speer, K. Winters, 2003: *Coupling Process and Model Studies of Ocean Mixing to Improve Climate Models—A Pilot Climate Process Modeling and Science Team*.

Schramm, J.L., J.A. Curry, M.M. Holland, and E.E. Ebert, 1997: Modeling the thermodynamics of a sea ice thickness distribution. 1. Sensitivity to ice thickness resolution. *Journal of Geophysical Research,* **102**, 23 079–23 091.

?Schweitzer, L., 2006: Environmental justice and hazmat transport: A spatial analysis in southern California. *Transp. Res. Part D–Transp. Environ.,* **11**, 408–421.

Segal, M. and R.W. Arritt, 1992: Nonclassical mesoscale circulations caused by surface sensible heat-flux gradients. *Bulletin of the American Meteorological Society,* **73**, 1593–1604.

Segal, M., M. Leuthold, R.W. Arritt, C. Anderson, and J. Shen, 1997: Small lake daytime breezes: Some observational and conceptual evaluations. *Bulletin of the American Meteorological Society,* **78**, 1135–1147.

Sellers, P.J., Y. Mintz, Y.C. Sud, and A. Dalcher, 1986: A Simple Biosphere Model (SiB) for use within general-circulation models. *Journal of Atmospheric Science,* **43**, 503–531.

Sellers, P.J., D.A. Randall, C.J. Collatz, J.A. Berry, C.B. Field, D.A. Dazlich, C. Zhang, G. Collelo, and L. Bounoua, 1996: A revised landsurface parameterization (SiB2) for atmospheric GCMs. Part 1: Model formulation. *Journal of Climate*, **9**, 676–705.

Semtner, A.J., 1976: A model for the thermodynamic growth of sea ice in numerical investigations of climate. *Journal of Physical Oceanography*, **6**, 27–37.

Seneviratne, S.I., D. Lüthi, M. Litschi, and C. Schär, 2006: Land-atmosphere coupling and climate change in Europe. *Nature*, **443**, 205–209.

Senior, C.A. and J.F.B. Mitchell, 1993: Carbon dioxide and climate: the impact of cloud parameterization. *Journal of Climate*, **6**, 5–21.

Senior, C.A. and J.F.B. Mitchell, 1996: Cloud feedbacks in the unified UKMO GCM. In: *Climate Sensitivity to Radiative Perturbations, Physical Mechanism and Their Validation.* [Le Treut, H. (ed.)]., Springer, 331pp.

Shaw, M.R. and Coauthors, 2002: Grassland responses to global environmental changes suppressed by elevated CO_2. *Science*, **298**, 1987–1990.

Shindell, D.T., R.L. Miller, G.A. Schmidt, and L. Pandolfo, 1999: Simulation of recent northern winter climate trends by greenhouse-gas forcing. *Nature,* **399**, 452–455.

Skamarock, W.C., J.B. Klemp, J. Dudhia, D.O. Gill, D.M. Barker, W. Wang, and J.G. Powers, 2005: A description of the advanced research WRF Version 2. *NCAR Technical Note.* NCAR/TN–468+STR, 88 pp. [Available from National Center for Atmospheric Research, P.O. Box 3000, Boulder, CO 80305.]

Slater, A.G. and Coauthors, 2001: The representation of snow in land surface schemes: Results from PILPS 2(d). *Journal of Hydrometeorology*, **2**, 7–25.

Smethie, W.M., Jr., and R.A. Fine, 2001: Rates of North Atlantic Deep Water formation calculated from chlorofluorocarbon inventories, Deep Sea Res., Part I, **48**, 189–215.

Smith, R.D. and P.R. Gent, 2002: *Reference manual for the Parallel Ocean Program (POP), ocean component of the Community Climate System Model (CCSM2.0 and 3.0)*. Technical Report LA-UR-02-2484. Los Alamos National Laboratory, Los Alamos, NM. Available online at http://www.ccsm.ucar.edu/models/ccsm3.0/pop.

Smith, R.N.B., 1990: A scheme for predicting layer clouds and their water content in a general circulation model. *Quarterly Journal of the Royal Meterological Society,* **116**, 435–460.

Soden, B.J., A.J. Broccoli, and R.S. Hemler, 2004: On the use of cloud forcing to estimate cloud feedback. *Journal of Climate*, **17**, 3661–3665.

Soden, B.J. and I.M. Held, 2006: An assessment of climate feedbacks in coupled ocean–atmosphere models. *Journal of Climate*, **19**, 3354–3360.

Solman, S.A., M.N. Nunez, and P.R. Rowntree, 2003: On the evaluation of the representation of mid-latitude transients in the Southern Hemisphere by HadAM2B GCM and the impact of horizontal resolution. *Atmosfera,* **16**, 245–272.

Somerville, R.C.J. and L.A. Remer, 1984: Cloud optical thickness feedbacks in the CO2 climate problem. *Journal of Geophysical Research,* **89**, 9668–9672.

Stephens, G.L., 2005: Cloud feedbacks in the climate system: a critical review. *Journal of Climate,* **18**, 237–273.

Stouffer, R.J., A.J. Broccoli, T.L. Delworth, K.W. Dixon, R. Gudgel, I. Held, R. Hemler, T. Knutson, Hyun-Chul Lee, M.D. Schwarzkopf, B. Soden, M.J. Spelman, M. Winton, and Fanrong Zeng, 2006: GFDL's CM2 global coupled climate models. Part IV: Idealized climate response. *Journal of Climate,* **19**, 723–740.

Stratton, R.A., 1999: A high resolution AMIP integration using the Hadley Centre model HadAM2b. *Climate Dynamics,* **15**, 9–28.

Sud, Y.C. and G.K. Walker, 1999: Microphysics of clouds with the Relaxed Arakawa–Schubert Scheme (McRAS). Part II: Implementation and Performance in GEOS II GCM. *Journal of Atmospheric Science,* **56(18)**, 3221–3240.

Sui, C.-H., X. Li, and K.-M. Lau, 1998: Radiative-convective processes in simulated diurnal variations of tropical oceanic convection. *Journal of Atmospheric Science,* **55**, 2345–2359.

Sun, S. and R. Bleck, 2001: Atlantic thermohaline circulation and its response to increasing CO2 in a coupled atmosphere-ocean model. *Geophysical Research Letters,* **28**, 4223–4226.

Sun, S. and J. Hansen, 2003: Climate simulations for 1951–2050 with a coupled atmosphere-ocean model. *Journal of Climate*, **16**, 2807–2826.

Sun, Y., S. Solomon, A. Dai, and R.W. Portmann, 2006: How often does it rain? *Journal of Climate*, **19**, 916–934.

Takle, E.S., W.J. Gutowski, R.A. Arritt, Z. Pan, C.J. Anderson, R.R. da Silva, D.

Caya, S.-C. Chen, J.H. Christensen, S.-Y. Hong, H.-M.H. Juang, J. Katzfey, W.M. Lapenta, R. Laprise, P. Lopez, J. McGregor, and J.O. Roads, 1999: Project to Intercompare Regional Climate Simulations (PIRCS): Description and initial results. *Journal of Geophysical Research,* **104**, 19,443–19,461.

Talley, L.D., J.L. Raid, and P.E. Robbins, 2003: Data-based meridional overturning streamfunctions for the global ocean. *Journal of Climate*, **16**, 3213–3226.

Tao, W., 2007: Cloud-resolving modeling. 125th Anniversary Special Issue of the *Journal of the Meteorological Society of Japan.* Submitted.

Tao, W.-K, 2003: Goddard Cumulus Ensemble (GCE) model: Application for understanding precipitation processes. Cloud systems, hurricanes, and the Tropical Rainfall Measuring Mission (TRMM): A Tribute to Dr. Joanne Simpson, Meteorological Monograph. *American Meteorological Society,* **51**, 107–138.

Tao, W.-K., D. Johnson, C.-L. Shie, and J. Simpson, 2004: Atmospheric energy budget and large-scale precipitation efficiency of convective systems during TOGA COARE, GATE, SCSMEX and ARM: Cloud-resolving model simulations. *Journal of Atmospheric Science,* **61**, 2405–2423.

Tao, W.-K., J. Simpson, C.-H. Sui, C.-L. Shie, B. Zhou, K. M. Lau, and M. Moncrieff, 1999: On equilibrium states simulated by Cloud-Resolving Models. *Journal of Atmospheric Science,* **56**, 3128–3139.

Tebaldi, C., K. Hayhoe, J.M. Arblaster, and G.A. Meehl, 2006: Going to the extremes; An intercomparison of model-simulated historical and futre changes in extreme events. *Climate Change*. In press.

Tebaldi C., R.L. Smith, D. Nychka, and L.O. Mearns, 2005: Quantifying uncertainty in projections of regional climate change: A Bayesian approach to the analysis of multimodel ensembles. *Journal of Climate,* **18**, 1524–1540.

Tenhunen, J.D., R. Geyer, R. Valentini, W. Mauser, and A. Cernusca, 1999: Eco-system studies, land-use and resource management. In: *Integrating Hydrology, Ecosystems Dynamics and Biochemistry in Complex Landscapes*. [Tenhunen, J. D. and P. Kabat (eds.)]. Wiley, Chichester, pp. 1–19.

Thompson, D.W.J. and J.M. Wallace, 1998: The Arctic Oscillation signature in the

wintertime geopotential height and temperature fields. *Geophysical Research Letters,* **25**, 1297–1300.

Thompson, D.W.J. and J.M. Wallace, 2000: Annual modes in the extratopical circulation. Part I: Month-to-month variability. *Journal of Climate,* **13**, 1000–1016.

Thompson, S., B. Govindasamy, A. Mirin, K. Caldeira, C. Delire, J. Milovich, M. Wickett, and D. Erickson, 2004: Quantifying the effects of CO_2-fertilized vegetation on future global climate and carbon dynamics. *Geophysical Research Letters,* **31(23),** L23211.

Tiedtke, M., 1989: A comprehensive mass flux scheme for cumulus parameterization in large scale models. *Monthly Weather Review,* **117**, 1779–1800.

Tiedtke, M., 1993: Representation of clouds in large-scale models. *Monthly Weather Review,* **121**, 3040–3061.

Tjernström, M., M. Zagar, and G. Svensson, 2004: Model simulations of the Arctic atmospheric boundary layer from the SHEBA year. *Ambio,* **33**, 221–227.

Tjernstrom, M., M. Zagar, G. Svensson, J.J. Cassano, S. Pfeifer, A. Rinke, K. Wyser, K. Dethloff, C. Jones, T. Semmler, and M. Shaw, 2005: Modelling the Arctic boundary layer: An evaluation of six ARCMIP regional-scale models with data from the SHEBA project. *Boundary-Layer Meteorology,* **117**, 337–381.

Tjoelker, M.G., J. Oleksyn, and P.B. Reich, 2001: Modelling respiration of vegetation: evidence for a general temperature-dependent Q(10). *Global Change Biology*, **7**, 223–230.

Tompkins, A., 2002: A prognostic parameterization for the subgrid-scale variability of water vapor and clouds in large-scale models and its use to diagnose cloud cover. *Journal of Atmospheric Science,* **59,** 1917–1942.

Trenberth, K.E. and J. Hurrell, 1994: Decadal atmosphere-ocean variations in the Pacific. *Climate Dynamics,* **9**, 303–319.

Trenberth K. E. and T. J. Hoar, 1997: El Nino and climate change. *Geophysical Research Letters*, **24**, 3057–3060.

Trenberth, K. E., G. W. Branstator, D. Karoly, A. Kumar, N-C. Lau, and C. Ropelewski, 1998: Progress during TOGA in understanding and modeling global

teleconnections associated with tropical sea surface temperatures. *Journal of Geophysical Research,* **103** (special TOGA issue), 14291–14324.

Trenberth, K. E., J. Fasullo and L. Smith, 2005 *Climate Dynamics,* **DOI** 10.1007/s00382-005-0017-4.

Trier, S. B., W.C. Skamarock, M.A. LeMone, and D.B. Parsons, 1996: Structure and evolution of the 22 February 1993 TOGA COARE squall line: Numerical simulations. *Journal of Atmospheric Science,* **53**, 2861–2886.

Tripoli, G.J., 1992: A Nonhydrostatic Mesoscale Model Designed to Simulate Scale Interaction. *Monthly Weather Review*: Vol. 120, No. 7 pp. 1342–1359

Tripoli, G.J. and W.R. Cotton, 1989: Numerical study of an observed orogenic mesoscale convective system. Part 2: Analysis of governing dynamics. *Monthly Weather Review,* **117**, 305–328.

Tselioudis, G. and C. Jakob, 2002: Evaluation of midlatitude cloud properties in a weather and a climate model: Dependence on dynamic regime and spatial resolution. *Journal of Geophysical Research,* **107**, 4781.

Tsushima, Y., A. Abe-Ouchi, and S. Manabe, 2005: Radiative damping of annual variation in global mean surface temperature: Comparison between observed and simulated feedback. *Climate Dynamics,* **24**, 591–597.

Twomey, S., 1977: The influence of pollution on the short wave albedo of clouds. *Journal of Atmospheric Science,* **34**, 1149–1152.

Ueda, H., A. Iwai, K. Kuwako, and M.E. Hori, 2006: Impact of anthropogenic forcing on the Asian summer monsoon as simulated by 8 GCMs. *Geophysical Research Letters*, **33**, doi:10.1029/2005GL025336.

Uotila, P., A.H. Lynch, J.J. Cassano, and R.I. Cullather, 2007: Changes in Antarctic net precipitation in the 21st century based on IPCC model scenarios. *Journal of Geophysical Research.* Acepted pending revisions.

Uppala, S.M. and Coauthors, 2005: The ERA-40 re-analysis. *International Journal of Climatology,* **131**, 2961–3012.

van Oldenborgh, G.J., S.Y. Philip, and M. Collins, 2005: El Nino in a changing climate: A multi-model study. *Ocean Science*, **1**, 81–95.

Vavrus, S., J.E. Walsh, W.L. Chapman, and D. Portis, 2006: The behavior of extreme cold air outbreaks under greenhouse warming. *International Journal of Climatology,* **26**, 1133–1147.

Vidale, P.L., D. Lüthi, C. Frei, S.I. Seneviratne, and C. Schär, 2003: Predictability and uncertainty in a regional climate model. *Journal of Geophysical Research,* **108(D18),** 4586.

Vinnikov, K.Y., D.J. Cavalieri, and C.L. Parkinson, 2006: A model assessment of satellite observed trends in polar sea ice extents. *Geophysical Research Letters*, **33**, L05704, doi:10.1029/2005GL025282.

Von Storch, H., E. Zorita, and U. Cubasch, 1993: Downscaling of global climate change estimates to regional scales: An application to Iberian rainfall in wintertime. *Journal of Climate,* **6**, 1161–1171.

Wang, B., 1995: Interdecadal changes in El Nino onset in the last four decades. *Journal of Climate*, **8**, 267–284.

Wang, C., 2005: A model study of the response of tropical deep convection to the increase of CCN concentration. 1. Dynamics and microphysics. *Journal of Geophysical Research,* **110**, D21211, doi:10.1029/2004JD005720

Wang, H. and K.-M. Lau, 2006: Atmospheric hydrological cycle in the tropics in twentieth century coupled climate simulations. *Journal of Climate,* **26**, 655–678.

Wang, M., J.E. Overland, V. Kattsov, J.E. Walsh, X. Zhang, and T. Pavlova, 2006: Intrinsic versus forced variation in coupled climate model simulations over the Arctic during the 20th Century. *Journal of Climate.* Submitted.

Wang, W. and M.E. Schlesinger, 1999: The dependence on convection parameterization of the tropical intraseasonal oscillation simulated by the UIUC 11-Layer Atmospheric GCM. *Journal of Climate*, **12(5),** 1423–1457.

Warrach, K., H.T. Mengelkamp, and E. Raschke, 2001: Treatment of frozen soil and snow cover in the land surface model SEWAB. *Theoretical and Applied Climatology,* **69**, 23–37.

Webb, M., C. Senior, S. Bony, and J.J. Morcrette, 2001: Combining ERBE and ISCCP data to assess clouds in the Hadley Centre, ECMWF and LMD atmospheric climate models. *Climate Dynamics,* **17**, 905–922.

Wei, H., W.J. Gutowski Jr., C.J. Vorosmarty, and B.M. Fekete, 2002: Calibration and validation of a regional climate model for pan-Arctic hydrologic simulation. *Journal of Climate*, **15**, 3222–3236.

Wetherald, R.T. and S. Manabe, 1988: Cloud feedback processes in general circulation models. *Journal of Atmospheric Science,* **45**, 1397–1415.

Whitman, S., G. Good, E.R. Donoghue, N. Benbow, W. Shou, and S. Mou, 1997: Mortality in Chicago attributed to the July 1995 heat wave. *American Journal of Public Health*, **87**, 1515–1518.

Wilby, R.L., L.E. Hay, W.J. Gutowski, Jr., R.W. Arritt, E.S. Takle, G.H. Leavesley, and M. Clark, 2000: Hydrological responses to dynamically and statistically downscaled general circulation model output. *Geophysical Research Letters,* **27**, 1199–1202.

Wilby, R.L., S.P. Charles, E. Zorita, B. Timbal, P. Whetton, and L.O. Mearns, 2004: *Guidelines for Use of Climate Scenarios Developed from Statistical Downscaling Methods.* The IPCC Data Distribution Centre, University of East Anglia, United Kingdom, 27 pp. [Available online at http://ipcc-ddc.cru.uea.ac.uk/guidelines.]

Williams, K.D., M.A. Ringer, and C.A. Senior, 2003: Evaluating the cloud response to climate change and current climate variability. *Climate Dynamics*, **20**, 705–721.

Williams, K.D. and Coauthors, 2006: Evaluation of a component of the cloud response to climate change in an intercomparison of climate models. *Climate Dynamics,* **145**, 145–165.

Wilks, D.S. and R.L. Wilby, 1999: The weather generation game: A review of stochastic weather models. *Progress in Physical Georaphy,* **23**, 329–357.

Wilson, M.F., A. Henderson-Sellers, R.E. Dickinson, and P.J. Kennedy, 1987: Sensitivity of the Biosphere Atmosphere Transfer Scheme (BATS) to the inclusion of variable soil characteristics. *Journal of Climate and Applied Meteorology,* **26**, 341–362.

Wilson, T. B., J.M. Norman, W.L. Bland, and C.J. Kucharik, 2003: Evaluation of the importance of Lagrangian canopy turbulence formulations in a soil-plant-atmosphere model. *Agricultural and Forest Meteorology,* **115**, 51–69.

Wilson, D.R. and S.P. Ballard, 1999: A microphysical based precipitation scheme for the UK Meteorological Office Numerical Weather Prediction Model. *International Journal of Climatology,* **125,** 1607–1636.

Winton, M., 2000: A reformulated three-layer sea ice model. *Journal of Atmospheric and Oceanic Technology*, **17**, 525 531.

Wittenberg, A.T., A. Rosati, N.-C. Lau, and J.J. Ploshay, 2006: GFDL's CM2 Global Coupled Climate Models, Part III: Tropical Pacific Climate and ENSO. *Journal of Climate,* **19**, 698–722.

Wood, A.W., L.R. Leung, V. Sridhar, and D.P. Lettenmaier, 2004: Hydrological implications of dynamical and statistical approaches to downscaling climate model outputs. *Climate Change,* **62**, 189–216.

Wu, X. and M.W. Moncrieff, 2001: Long-term behavior of cloud systems in TOGA COARE and their interactions with radiative and surface processes. Part III: Effects on the energy budget and SST. *Journal of Atmospheric Science,* **58**, 1155–1168.

Wu, X., L. Deng, X. Song, and G.-J. Zhang, 2006: Coupling of convective momentum transport with convective heating in global climate simulations. *Journal of Atmospheric Science.* In press.

Wyant, M.C., C.S. Bretherton, J.T. Bacmeister, J.T. Kiehl, I.M. Held, M.Z. Zhao, S.A. Klein, and B J. Soden, 2006: A comparison of tropical cloud properties and responses in GCMs using mid-tropospheric vertical velocity. *Climate Dynamics,* **27**, 261–279.

Wyant, M.C., M. Khairoutdinov, and C.S. Bretherton, 2006: Climate sensitivity and cloud response of a GCM with a superparameterization, *Geophysical Research Letters,* **33**, L06714, doi:10.1029/2005GL025464.

Wyrtki, K., 1975: El Nino—The dynamic response of the equatorial Pacific Ocean to atmospheric forcing. *Journal of Physical Oceanography,* **5**, 572–584.

Xie and Arkin, 1997: Global precipitation: A 17-year monthly analysis based on gauge observations, satellite estimates, and numerical model outputs. *Bulletin of the American Meteorological Society,* **78**, 2539–2558.

Xie, S.C., *et al.,* 2005: Simulations of midlatitude frontal clouds by single-column and cloud-resolving models during the Atmospheric Radiation Measurement March 2000 cloud intensive operational period. *Journal of Geophysical Research,* **110**, D15S03, doi:10.1029/2004JD005119.

Xu, K.-M. and D.A. Randall, 1998: Influence of large-scale advective cooling and moistening effects on the quasi-equilibrium behavior of explicitly simulated cumulus ensembles. *Journal of Atmospheric Science,* **55**, 896–909.

Xu, K., M.H. Zhang, *et al.,* 2005: Modeling springtime shallow frontal clouds with cloud-resolving and single-column models. *Journal of Geophysical Research,* **110**, D15S04, doi:10.1029/2004JD005153.

?Xue, Y., F.J. Zeng, K.E. Mitchell, Z. Janjic, and E. Rogers, 2001: The impact of land surface processes on simulations of the U.S. hydrological cycle: A case study of the 1993 flood using the SSiB land surface model in the NCEP ETA regional model.

Yamaguchi, K., A. Noda, and A. Kitoh, 2005: The changes in permafrost induced by greenhouse warming: A numerical study applying multiple-layer ground model. *Journal of the Meteorological Society of Japan,* **83**, 799–815.

Yang Z.W. and R. W. Arritt, 2002: Tests of a perturbed physics ensemble approach for regional climate modeling. *Journal of Climate,* **15**, 2881–2896.

Yao, M.-S. and A.D. Del Genio, 2002: Effects of cloud parameterization on the simulation of climate changes in the GISS GCM. Part II: Sea surface temperature and cloud feedbacks. *Journal of Climate*, **15**, 2491–2503.

Yeh, P.J.-F. and E.A.B. Eltahir, 2005: Representation of water table dynamics in a land surface scheme. Part 1: Model development. *Journal of Climate,* 18, 1861–1880.

Yokohata, T., S. Emori, T. Nozawa, Y. Tsushima, T. Ogura, and M. Kimoto, 2005: Climate response to volcanic forcing: Validation of climate sensitivity of a coupled atmosphere-ocean general circulation model. *Geophysical Research Letters,* **32**, L21710.

York, J.P., M. Person, W.J. Gutowski, and T.C. Winter, 2002: Putting aquifers into atmospheric simulation models: An example from the Mill Creek Watershed, northeastern Kansas. *Advances in Water Resources,* **25**, 221–238.

Yu, H., Y.J. Kaufman, M. Chin, G. Feingold, L.A. Remer, T.L. Anderson, Y. Balkanski, N. Bellouin, O. Boucher, S. Christopher, P. DeCola, R. Kahn, D. Koch, N. Loeb, M.S. Reddy, M. Schulz, T. Takemura, and M. Zhou, 2006: A review of measurement-based assessment of aerosol direct radiative effect and forcing. *Atmospheric Chemistry and Physics,* **6**, 613–666.

Yu, X. and M.J. McPhaden, 1999: Seasonal variability in the equatorial Pacific. *Journal of Physical Oceanography*, **29**, 925–947.

Zebiak, S.E. and M.A. Cane, 1987: A model El Nino-Southern Oscillation. *Monthly Weather Review,* **115**, 2262–2278.

?Zhang, C., M. Dong, H.H. Hendon, E.D. Maloney, and A. Marshall, 2006: Simulations of the Madden-Julian Oscillation by Global Weather Forecast and Climate Models. *Climate Dynamics*.

Zhang, D. and M.J. McPhaden, 2006: Decadal variability of the shallow Pacific meridional overturning circulation: Relation to tropical sea surface temperatures in observations and climate change models. *Ocean Modelling,* **15**, 250–273.

Zhang, G.J. and N.A. McFarlane, 1995: Sensitivity of climate simulations to the Parameterization of cumulus convection in the Canadian Climate Centre general circulation model. *Atmos.-Ocean*, **33**, 407–446.

Zhang, J. and D. Rothrock, 2000: Modeling Arctic sea ice with an efficient plastic solution, *Journal of Geophysical Research,* **105**, 3325–3338.

Zhang, M.H., J.J. Hack, J.T. Kiehl, and R.D. Cess, 1994: Diagnostic study of climate feedback processes in atmospheric general circulation models. *Journal of Geophysical Research,* **99**, 5525–5537.

Zhang, M., 2004: Cloud-climate feedback: How much do we know? In: *Observation, Theory, and Modeling of Atmospheric Variability. World Scientific Series on Meteorology of East Asia*, Vol. 3 [Zhu, *et al.* (eds.)]. World Scientific Publishing Co., Singapore, 632 pp.

Zhang, M.H., *et al.,* 2005: Comparing clouds and their seasonal variations in 10 atmospheric general circulation models with satellite measurements. *Journal of Geophysical Research,* **110**, D15S02, doi:10.1029/2004JD005021.

Zhang, M.H., J.L. Lin, R.T. Cederwall, J.J. Yio, and S.C. Xie, 2001: Objective analysis of the ARM IOP data: method and sensitivity. *Monthly Weather Review*, **129**, 295–311.

Zhang, X. and J.E. Walsh, 2006: Toward a seasonally ice-covered Arctic Ocean: Scenarios from the IPCC AR4 model simulations. *Journal of Climate*, **19**, 1730–1747.

Zhang, X.-C., 2005: Spatial downscaling of global climate model output for site-specific assessment of crop production and soil erosion. *Agricultural and Forest Meteorology*, **135**, 215–229.

Zhang, Y.C., A.N. Huang, and X.S. Zhu, 2006: Parameterization of the thermal impacts of sub-grid orography on numerical modeling of the surface energy budget over East Asia. *Theoretical and Applied Climatology,* **86**, 201–214.

Zhu, J. and X.-Z. Liang, 2007: Regional climate model simulations of U.S. precipitation and surface air temperature during 1982–2002: Interannual variation. *Journal of Climate.* In press.